

Water Research Laboratory

Assessment of the Effects of Air-Sea-Land Interaction Processes on the Intensity and Impact of Modelled and Observed Coastal Extratropical Cyclones

WRL Research Report 244
September 2011

Approved for public release; distribution unlimited

by
W L Peirson, T D Shand, J E Ruprecht, J Evans and R J Cox



UNSW
THE UNIVERSITY OF NEW SOUTH WALES

Report Documentation Page				Form Approved OMB No. 0704-0188	
Public reporting burden for the collection of information is estimated to average 1 hour per response, including the time for reviewing instructions, searching existing data sources, gathering and maintaining the data needed, and completing and reviewing the collection of information. Send comments regarding this burden estimate or any other aspect of this collection of information, including suggestions for reducing this burden, to Washington Headquarters Services, Directorate for Information Operations and Reports, 1215 Jefferson Davis Highway, Suite 1204, Arlington VA 22202-4302. Respondents should be aware that notwithstanding any other provision of law, no person shall be subject to a penalty for failing to comply with a collection of information if it does not display a currently valid OMB control number.					
1. REPORT DATE AUG 2011		2. REPORT TYPE		3. DATES COVERED 00-00-2011 to 00-00-2011	
4. TITLE AND SUBTITLE Assessment of the Effects of Air-Sea-Land Interaction Processes on the Intensity and Impact of Modelled and Observed Coastal Extratropical Cyclones				5a. CONTRACT NUMBER	
				5b. GRANT NUMBER	
				5c. PROGRAM ELEMENT NUMBER	
6. AUTHOR(S)				5d. PROJECT NUMBER	
				5e. TASK NUMBER	
				5f. WORK UNIT NUMBER	
7. PERFORMING ORGANIZATION NAME(S) AND ADDRESS(ES) Water Research Laboratory, University of New South Wales, 110 King Street, Manly Vale, NSW, 2093, Australia,				8. PERFORMING ORGANIZATION REPORT NUMBER	
9. SPONSORING/MONITORING AGENCY NAME(S) AND ADDRESS(ES)				10. SPONSOR/MONITOR'S ACRONYM(S)	
				11. SPONSOR/MONITOR'S REPORT NUMBER(S)	
12. DISTRIBUTION/AVAILABILITY STATEMENT Approved for public release; distribution unlimited					
13. SUPPLEMENTARY NOTES					
14. ABSTRACT					
15. SUBJECT TERMS					
16. SECURITY CLASSIFICATION OF:			17. LIMITATION OF ABSTRACT Same as Report (SAR)	18. NUMBER OF PAGES 108	19a. NAME OF RESPONSIBLE PERSON
a. REPORT unclassified	b. ABSTRACT unclassified	c. THIS PAGE unclassified			

Water Research Laboratory
University of New South Wales
School of Civil and Environmental Engineering

**Assessment of the Effects of Air-Sea-Land Interaction Processes
on the Intensity and Impact of Modelled and Observed Coastal
Extratropical Cyclones**

WRL Research Report 244
August 2011

by
W L Peirson, T D Shand, J E Ruprecht, J Evans and R J Cox

Bibliographic Data Sheet

Report Title	Assessment of the Effects of Air-Sea-Land Interaction Processes on the Intensity and Impact of Modelled and Observed Coastal Extratropical Cyclones
Report Author(s)	W L Peirson, T D Shand, J E Ruprecht, J Evans and R J Cox
Report No.	244
Report Status	Final
Report Date	September 2011
ISBN	0-85824-086-6
Number of Pages	108
Distribution Statement	
Price	
Sponsoring Organisation	ERDC-IRO US ARMY RDECOM ACQ CTR W911NF
Keywords	

Document Status

Version	Reviewed By	Approved By	Date Issued
DRAFT v2.0	W L Peirson	WLP	30 August 2011
FINAL	W L Peirson	WLP	8 September 2011

Water Research Laboratory

110 King Street, Manly Vale, NSW, 2093, Australia

Tel: +61 (2) 8071 9800 Fax: +61 (2) 9949 4188

ABN: 57 195 873 179

www.wrl.unsw.edu.au

Quality System certified to AS/NZS ISO 9001:2008

Expertise, research and training for industry and government since 1959

Abstract

This investigation compares observed values with global circulation model (GCM) predictions of those atmospheric forcing variables relevant to coastal flooding prediction. Both reanalysis and predictive GCMs models are investigated.

While the limitations of these models in representing tropical storms are well established, in this investigation we have completed an assessment of their performance in more temperate regions as a function of latitude along the eastern United States and Australian coasts.

The models represent the probabilities and extreme values of atmospheric pressure very well. Their performance in relation to wind and rainfall is less impressive but the modelled values are of similar magnitude to those observed.

The models do simulate large-scale extreme events with mean surface pressures, winds and rainfalls that are of similar magnitude to those observed. Consequently, when combined with appropriate downscaling techniques, these models yield a direct method of defining the joint probability of the combinations of extreme low surface pressures, winds and rainfall in a way that has not previously been possible.

GCM data provide a unique new means of determining the joint probability of those atmospheric variables primarily responsible for coastal inundation and storm damage in highly-populated temperate regions.

Contents

1. Introduction	1
1.1 Background	1
1.2 Study Aims	2
1.3 Report Structure	2
2. Data Sources	3
2.1 Observational Data	4
2.1.1 United States of America	4
2.1.2 Australia	4
2.1.3 Observation data processing	4
2.2 Global Circulation Models	5
2.2.1 NCEP-NCAR 20 th Century Reanalysis V2	6
2.2.2 ECMWF ERA-40	6
2.2.3 AR-4 Models	6
3. Methodology	11
3.1 Mean skill	11
3.2 PDF skill	11
3.3 Extreme value skill	11
3.4 Processing and comparison	12
4. Results and Discussion	23
4.1 Precipitation	24
4.2 Mean Sea Level Pressure	26
4.3 Sea Level Pressure Gradient	29
4.4 Wind	30
5. Conclusions and Recommendations	34
6. Acknowledgements	36
References	37
Appendix A	Global Circulation Model Documentation
Appendix B	GCM Data Extraction Locations
Appendix C	20th Century Results
Appendix D	21st Century A2 Scenario Results

List of Tables

Table 2-1	List of Selected Observation Stations along the United States East Coast used in Present Assessment	3
Table 2-2	List of Selected Observation Stations along the Australian East Coast used in Present Assessment	4
Table 2-3	Extracted variables	5
Table 2-4	List of GCMs to be Used in Present Assessment	7
Table 2-5	Number of GCM datasets compared to each observation station used in present assessment	8
Table 4-1	Figure references in Appendix C for comparison of different GCM characterisations of recent climate with observed data	23
Table 4-2	Figure references in Appendix D for comparison of different GCM characterisations of future climate with observed data.	23
Table 4-4	Changes in Ensemble-averaged GCM Precipitation for the 21 st Century A2 Scenario from the 20 th Century 20Cm3 Scenario	26
Table 4-5	Comparison of Observed Mean Sea Level Pressure with Ensemble-averaged 20 th Century GCM results	27
Table 4-6	Changes in Ensemble-averaged GCM Mean Sea Level Pressure for the 21 st Century A2 Scenario from the 20 th Century 20Cm3 Scenario	28
Table 4-7	Comparison of Observed MSLP Gradient with Ensemble-averaged 20 th Century GCM results	29
Table 4-8	Changes in Ensemble-averaged GCM MSLP Gradient for the 21 st Century A2 Scenario from the 20 th Century 20Cm3 Scenario	30
Table 4-9	Comparison of Observed Wind with Ensemble-averaged 20 th Century GCM results	32
Table 4-10	Changes in Ensemble-averaged GCM Wind Speed for the 21 st Century A2 Scenario from the 20 th Century 20Cm3 Scenario	33

List of Figures

Figure 2-2	Locations of Selected Australian East Coast Observation Stations	10
Figure 3-1	Schematic diagram of the methods used to evaluate GCM performance compared to Observation (adapted from Perkins et al., 2007)	13
Figure 3-2	Example of an Observed Mean Sea Level Pressure time series at United States East Coast Latitude 36.90 (Norfolk Intl. Airport: WBAN 13750) compared to the GFDL-CM2.0 GCM: Scenario 20c3m, Run1.	14
Figure 3-3	Example probability distribution function and extreme value distribution comparison for observed Mean Sea Level Pressure at United States East Coast Latitude 36.90	15
Figure 3-4	Example probability distribution function and extreme value distribution comparison for observed Precipitation at United States East Coast Latitude 36.90	16
Figure 3-5	Example probability distribution function and extreme value distribution comparison for observed Absolute Wind Speed at United States East Coast Latitude 36.90	17
Figure 3-6	Example of an Observed Mean Sea Level Pressure time series at Australian East Coast Latitude -33.95 (Sydney Airport AMO BoM Station No. 066037) compared to the CSIRO-3.0 GCM: Scenario 20c3m, Run2.	18
Figure 3-7	Example probability distribution function and extreme value distribution comparison for observed Mean Sea Level Pressure at Australian East Coast Latitude -33.95	19

Figure 3-8 Example probability distribution function and extreme value distribution comparison for observed Precipitation at Australian East Coast Latitude -33.95	20
Figure 3-9 Example probability distribution function and extreme value distribution comparison for observed Westward (-u) wind at Australian East Coast Latitude -33.95	21
Figure 3-10 Example comparison of observed precipitation at Australian East Coast Latitude -33.95 with the GISS-ER 20c3m model output.	22

1. Introduction

1.1 Background

Coastal flooding and storm damage have potentially both maritime and inland contributions. Determining the conjunctive probability of the relative contributions of rainfall runoff and coastal extreme water levels and storm wave attack remains a longstanding and difficult problem.

In 2003 more than 50% of the US population (excluding Alaska) lived within 80km of the coast (National Ocean Service, NOAA). As of 2008, the total insured value of US coastal properties was estimated at US \$53.5 billion (AIR, 2008).

Correspondingly, around 85 per cent of the Australian population now live in the coastal region and it is of immense economic, social and environmental importance to the nation. All Australian state capital cities are located within the coastal zone. Up to \$63 billion of existing residential buildings are potentially at risk of inundation from projected sea-level rise in 2100. New South Wales with the bulk of its major cities and commercial centres in the coastal strip is particularly vulnerable.

Present concerns regarding sea level rise and other climate change effects has made development of suitable methods of resolving the issue of the conjunctive probability of inland and marine contributions to coastal inundation a priority.

The development of global climate and other general circulation models (GCMs) has provided potential tools to assist in resolving this issue. However, shortcomings in their ability to depict tropical cyclonic formation and intensification are well established (Emmanuel et al., 2008). In addition, such models exhibit different skill levels for critical primary state variables (e.g. central pressure, maximum pressure gradient, precipitation, wind speed (see Lambert & Fyfe, 2006; Bengtsson et al., 2007; Caron & Jones, 2008). It is anticipated that GCM performance will steadily improve over coming decades.

Whilst Emmanuel et al. (2008) have developed a technique to address issues associated with tropical cyclone formation (note that these are extremely computationally intensive), many highly populated areas (particularly the east coasts of the United States and Australia) are primarily impacted by larger-scale extratropical systems (NSWPWD, 1985). Extratropical cyclones are of sufficiently large scale to be resolved by GCMs, particularly those based on reanalysis data sets (NCAR-NCEP and ERA-40, Sinclair and Watterson, 1999; Wernli and Schwerz, 2006).

The techniques for determining coastal flooding and storm damage are reasonably well established (e.g. CERC, 1984 Chapter 3) but adequate assessment is fundamentally dependent on reliable data (NCCOE, 1993). A major concern associated with GCM application is the degree to which storm intensity is attenuated by the limited spatial resolution and the computational economy in key storm intensification processes within the GCMs.

A variety of downscaling techniques have been proposed (Wilby & Wigley, 1997; Mearns et al., 1999). In general, these are computationally intensive and all inherit weaknesses of the utilized GCM estimates, as these estimates all required source data for the downscaling process.

1.2 Study Aims

This investigation is the first stage of a larger five-stage programme to determine the present performance of Global Circulation Models (GCMs) as a function of latitude across the selected temperate zones for the purpose of resolving the conjunctive probability of the maritime and land-based contributions to flooding and coastal inundation.

This investigation has been planned as follows:

1. Identify variables of interest which affect large-scale coastal flooding and storm damage;
2. Select observation sites on the Australian and US East Coasts which encompass the range of latitudes and variables of interest;
3. Select GCMs and scenarios to be used in assessment and obtain the appropriate data;
4. Compare mean and extreme trends of observation data with concurrent GCM outputs (i.e. 20th Century Dataset) using established techniques (i.e. Kharin et al., 2007; Perkins et al., 2007) and assess model skill as a function of latitude;
5. Compare GCM future scenarios with both observation and 20th century GCM results;
6. Report on methodologies and findings within a WRL Research Report.

Future stages of this project will determine how best to incorporate GCM data into coastal engineering practice.

This study has been undertaken with reference to three types of GCM:

- Climatology obtained from re-analysis data sets (e.g. ECMWF ERA-40 and NCEP/NCAR). Use of the re-analysis data will provide a benchmark of model performance for subsequent lower resolution predictive models.
- Climate model simulations of past climate (using "Climate of the 20th century" simulations performed for the IPCC 4th assessment report). The simulations of past climate will enable the statistical distribution of storms between the re-analysis and unconstrained models to be assessed.

Climate model simulations of future climate (using SRES A2 emission scenario simulations performed for the IPCC 4th assessment report). The simulations of future climate will enable the statistical distribution of storms between predicted future conditions and past conditions to be assessed. Note that the SRES A2 is the highest emission scenario usually modelled by most GCMs. Since 2000, the actual emissions have grown faster than any SRES scenario considered so even the highest scenario is already too low to be representative of the current situation.

1.3 Report Structure

This report begins by describing the data sources used within the present study within Section 2. This includes description of the location of observed data sources and description of the GCM models used. Section 3 describes the methodology used within the present study and processing techniques. Section 4 presents study results and discussion with conclusions and recommendations presented within Section 5.

2. Data Sources

Observational data has been sourced from several long-term stations along both the Australian and United States East coasts covering a range of latitudes ($\pm 25^\circ$ to 45°). Environmental variables have been selected for analysis based on their contribution to coastal flooding and storm damage. Rainfall contributes to catchment flows and may result in coastal flooding, especially when combined with elevated water levels caused by storm surge induced by both onshore easterly winds (also termed westward or in a –u direction) and low pressure, possibly caused by the same weather system. The variables of interest therefore selected include:

- Rainfall,
- Wind Speed,
- Surface Pressure.

Comparable daily data has been sourced from several Global Circulation Models (GCMs) including two 20th Century reanalysis type models and seven climate models used within the Intergovernmental Panel on Climate Change (IPCC) 4th Assessment Report (AR-4).

Table 2-1 List of Selected Observation Stations along the United States East Coast used in Present Assessment

COOP/ WBAN ID	Latitude	Longitude	Location	State	Dates	Pressure	Rainfall	Wind
177255	44.10	290.88	Rockland	ME	1960-2002		✓	
14764	43.65	289.70	Portland INTL AP	ME	1948-2010	✓		✓
060806	41.16	286.87	Bridgeport Sikorsky AP	CT	1960-2002		✓	
94702	41.16	286.87	Bridgeport Sikorsky AP	CT	1943-2010	✓		✓
14732	40.78	286.12	New York La Guardia AP	NY	1949-2010	✓		✓
305811	40.78	286.12	New York La Guardia AP	NY	1960-2002		✓	
446139	36.90	283.81	Norfolk INTL AP	VA	1960-2002		✓	
13750	36.90	283.81	Norfolk INTL AP	VA	1945-2010	✓		✓
315830	34.73	283.27	Morehead City	WNW	1960-2002		✓	
93727	34.70	282.62	New River Marine Corps Air Station	NC	1955-2010	✓		✓
097847	32.13	278.79	Savannah INTL AP	GA	1960-2002		✓	
03822	32.13	278.79	Savannah INTL AP	GA	1948-2010	✓		✓
084358	30.40	278.58	Mayport Pilot Stn	FL	1960-2002		✓	
12843	27.65	279.76	Vero Beach INTL AP	FL	1973-2010	✓		✓
12844	26.68	279.90	West Palm Beach INTL AP	FL	1943-2010	✓		✓
080845	26.37	279.89	Boca Raton	FL	1960-2002		✓	
084570	24.56	278.25	Key West INTL AP	FL	1960-2002		✓	
12850	24.56	278.25	Key West INTL AP	FL	1945-2010	✓		✓

2.1 Observational Data

2.1.1 United States of America

Observation stations along the United States East Coast between 24.5 and 44°N have been identified on the basis of record length and data quality. Between these stations (shown within Table 2-1 and Figure 2-1), long-term records of all variables of interest are extracted between 1960 and 2000 to correspond with the 20th Century GCM simulation.

2.1.2 Australia

Observation stations along the Australian East Coast between 27 and 43°S have been similarly identified on the basis of record length and data quality. Between these stations (shown within Table 2-2 and Figure 2-2), long-term records of all variables of interest are provided at approximately 2° resolution.

Table 2-2 List of Selected Observation Stations along the Australian East Coast used in Present Assessment

Station	Latitude	Longitude	Location	State	Dates	Pressure	Rainfall	Wind
040043	-27.03	153.47	Cape Moreton Lighthouse	QLD	1957-2010	✓	✓	✓
058012	-29.43	153.36	Yamba Pilot Station	NSW	1944-2010	✓	✓	✓
059030	-30.92	153.09	Smoky Cape Lighthouse	NSW	1957-2010	✓	✓	✓
061055	-32.92	151.80	Newcastle Nobbys Signal Station AWS	NSW	1957-2010		✓	✓
061078	-32.79	151.84	Williamstown RAAF	NSW	1951-2010	✓		
066037	-33.95	151.17	Sydney Airport AMO	NSW	1951-2010	✓	✓	✓
069018	-35.91	150.15	Moruya Heads Pilot Station	NSW	1957-2010	✓	✓	✓
084016	-37.57	149.92	Gabo Island Lighthouse	VIC	1957-2010	✓	✓	✓
092038	-42.12	148.07	Swansea Post Office	TAS	1957-2010	✓	✓	✓
092045	-40.99	148.35	Eddystone Point	TAS	1961-2010	✓	✓	✓
094029	-42.89	147.33	Hobart (Ellerslie Road)	TAS	1893-2010	✓	✓	✓

2.1.3 Observation data processing

For each selected observation site, surface pressure, rainfall and wind data has been extracted. While data may be recorded at intervals ranging from 1 to 24 hours, data was averaged to a daily interval to provide temporal resolution comparable with GCM outputs. All data has been converted to the equivalent SI units shown in Table 2-3.

Where wind direction is provided, wind speed is vectorised into its zonal (u) and meridional (v) directions. Wind orientated in an onshore direction has the greatest potential to induce coastal flooding due to its contribution to extreme waves and storm surge. On the east coasts of the United States and Australia, these are easterly or westward (-u) winds. Vectorised wind from this direction (-u) has therefore been selected for further analysis. As wind data provided by US stations did not include wind direction, absolute wind speed was analysed.

Meridional pressure gradient was calculated as the quotient of the difference in pressure between adjacent observation stations and the meridional distance between the stations.

Table 2-3 Extracted variables

Variable	Unit
Precipitation	mmday ⁻¹
Absolute Mean Wind Speed (United States)	ms ⁻¹
Westward (easterly) Mean Wind Speed (-u) (Australia)	ms ⁻¹
Mean Sea Level Pressure	hPa
Pressure Gradient	hPa/km

2.2 Global Circulation Models

Global Circulation Models are numerical representations of the climate system, which are used to increase the understanding of past and current climates, and to provide projections of future climates (Perkins, 2010 after McGuffie and Henderson-Sellers, 2001). GCMs aim to solve the fundamental equations of physics at each grid cell subject to the relative parameters, at each incremental time step, in order to capture the climatic interactions resulting from complex atmospheric and oceanic physical processes including energy, momentum and mass conservation as well as associated equations of state.

In this study, two types of GCMS have been employed:

a. Reanalysis models

Within reanalysis models, observed data are assimilated into the models during the simulation. Consequently, reanalysis models are a hindcast of observed climate history and their results may be compared directly to observations. They have no forecast capability for changed emission scenarios. During this investigation, the NCEP-NCAR 20th Century Reanalysis V2 and the ECMWF Reanalysis 40 results have been investigated.

b. Predictive-type models

Predictive-type models are initiated with 'spin-up' conditions and propagate according to their internal physics. Consequently, when configured with the greenhouse gas emissions representative of recent history, predictive-type models should yield statistical distributions of atmospheric behaviour that are consistent with measured data. These models have a predictive capability for future climates when configured with a corresponding emission scenario. For this study, model results for the IPCC AR-4 investigation have been used.

For each model, land and ocean cells zonally adjacent to each observation station were selected for comparison. This was undertaken to assess whether there is significant difference in the modelled variables between adjacent land and ocean cells.

Data is converted from GCM standard output form to a form comparable with observed data. The GCM convention for winds (10 m elevation) is U winds positive from West to East (westerly or eastward wind) and V winds positive from South to North (southerly or northward wind). Within the GCM datasets, precipitation is provided as a flux in units of kg/m²/s. This is converted to total mm of precipitation per 24 hour period.

The key characteristics of the GCMs employed during this investigation are briefly summarised in the following subsections.

2.2.1 NCEP-NCAR 20th Century Reanalysis V2

The NCEP-NCAR 20th Century Reanalysis V2 (20CRv2) dataset (Compo et al., 2011) is a hindcast model for the years 1871 to 2008. The model assimilates observed surface pressure and sea level pressure from the International Surface Pressure Databank and the International Best Track Archive for Climatic Stewardship every six hours. Using these assimilated data, the model determines a short-term forecast from an ensemble of integrations of an NCEP numerical weather prediction model using the Ensemble Kalman Filter technique to produce an estimate of the complete state of the atmosphere, and the uncertainty in that estimate (NCEP, 2011). The model domain resolution is approximately 1.875° x ~1.904° in the horizontal and 28 levels in the vertical.

20th Century Reanalysis V2 data including daily precipitation, mean surface level pressure and wind speed (u, v) were extracted at locations corresponding to observation stations on the United States and Australian East Coasts (Appendix B). Data was provided by the NOAA/OAR/ESRL PSD, Boulder, Colorado, USA.

2.2.2 ECMWF ERA-40

The European Centre for Medium-Range Weather Forecasts (ECMWF) Reanalysis 40 (ERA40) dataset (Uppala et al., 2005) is a global atmospheric reanalysis of the 45-year period 1 September 1957 - 31 August 2002. The reanalysis used the ECMWF Integrated Forecast Model (IFS Cy28r3) run at a horizontal resolution of 1.5° x 1.5° with 28 vertical levels. Observations including satellite and field observation data were assimilated at 6-hourly intervals (Kallberg et al., 2007).

Reanalysis data including daily precipitation, mean surface level pressure and wind speed (u, v) were obtained at 2.5° x 2.5° horizontal resolution for comparable observation station locations (Appendix B). ECMWF ERA-40 data used in this study/project have been provided by ECMWF from the ECMWF Data Server.

2.2.3 AR-4 Models

Seven coupled Atmospheric and Oceanic General Circulation Models (AOGCMs) used in the IPCC AR4 study and that include the variables of interest and relevant scenarios have been selected for comparison. These are shown within Table 2.4 and include two models developed by Australian research institutes, four models developed by American research institutes and one model developed by joint German and Korean research institutes.

GCM scenarios have been selected for assessment including:

- 20c3m (Present Scenario: 1960 – 2000), and
- OsresA2 (Future Scenarios: 2044 – 2065; 2080 – 2099)

All relevant model data covering the scenarios and regions of interest has been obtained from the World Climate Research Programme's (WCRP's) Coupled Model Intercomparison Project phase 3 (CMIP3) multi-model dataset (Meehl et al., 2007).

Table 2-4 List of GCMs to be Used in Present Assessment

Model ID	Sponsor, Country	Resolution	
		Horizontal (°)	Vertical (levels)
CSIRO-Mk3.0	Commonwealth Scientific Industrial and Research Organisation, Australia	~ 1.9° x 1.9°	L18
CSIRO-Mk3.5	Commonwealth Scientific Industrial and Research Organisation, Australia	~ 1.9° x 1.9°	L18
GFDL-CM2.0	Geophysical Fluid Dynamics Laboratory, United States of America	2.5° x 2.0°	L24
GFDL-CM2.1	Geophysical Fluid Dynamics Laboratory, United States of America	2.5° x 2.0°	L24
GISS-ER	NASA/ Goddard Institute for Space Studies, United States of America	5.0° x 4.0°	L20
NCAR-CCSM3	National Centre for Atmospheric Research, United States of America	~ 1.4° x 1.4°	L26
MIUBEG ECHO-G	Meteorological Institute of the University of Bonn, Meteorological Research Institute of KMA, and Model & Data Group, Germany/ Korea	~ 3.9° x 3.9°	L19

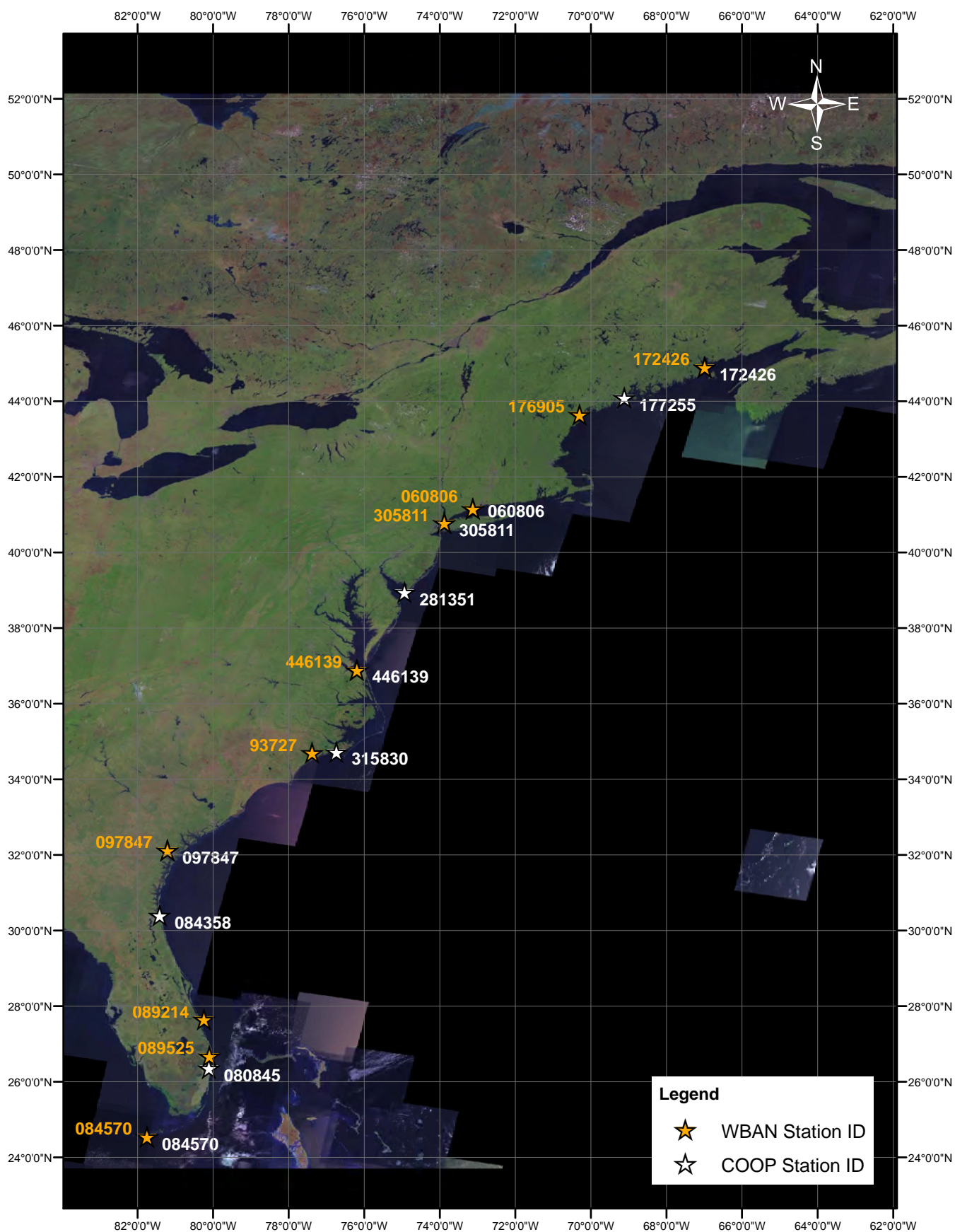
Model results from two scenarios are extracted. These include the ***Climate of the 20th Century experiment (20C3M)*** and the 21st Century ***SRES A2 experiment (OsresA2)***. The 20c3m model is a representation of 20th Century development and observed increases carbon dioxide (CO₂) emission rates while the 21st Century models represent various socio-economic *storylines* with consequent changes in CO₂ emission rates. The A2 scenario assumes Economic development is primarily regionally oriented and slower per capita economic growth and technological change (IPCC, 2007). This scenario predicts medium to high increase in CO₂ emissions with climate models generally predicting higher increases in global temperature and sea level (IPCC, 2007). The 20th Century scenario produces results for the 1960 – 2000 period and the 21st century OsresA2 scenario produces results for two output periods: 2044 – 2065 and 2080 – 2099.

Each 20th Century model comprises a number of ***Runs*** corresponding to differing initialisation times from a pre-industrial control experiment (***Picntrl***). These initialisation times differ by between 10 and 20 years dependent on model. For example, the CSIR-Mk3.0 20C3M Run 1 is initiated at from Picntrl at the year 1870, Run 2 in 1880 and Run 3 in 1890 (Program for Climate Model Diagnosis and Intercomparison; <http://www-pcmdi.llnl.gov/>).

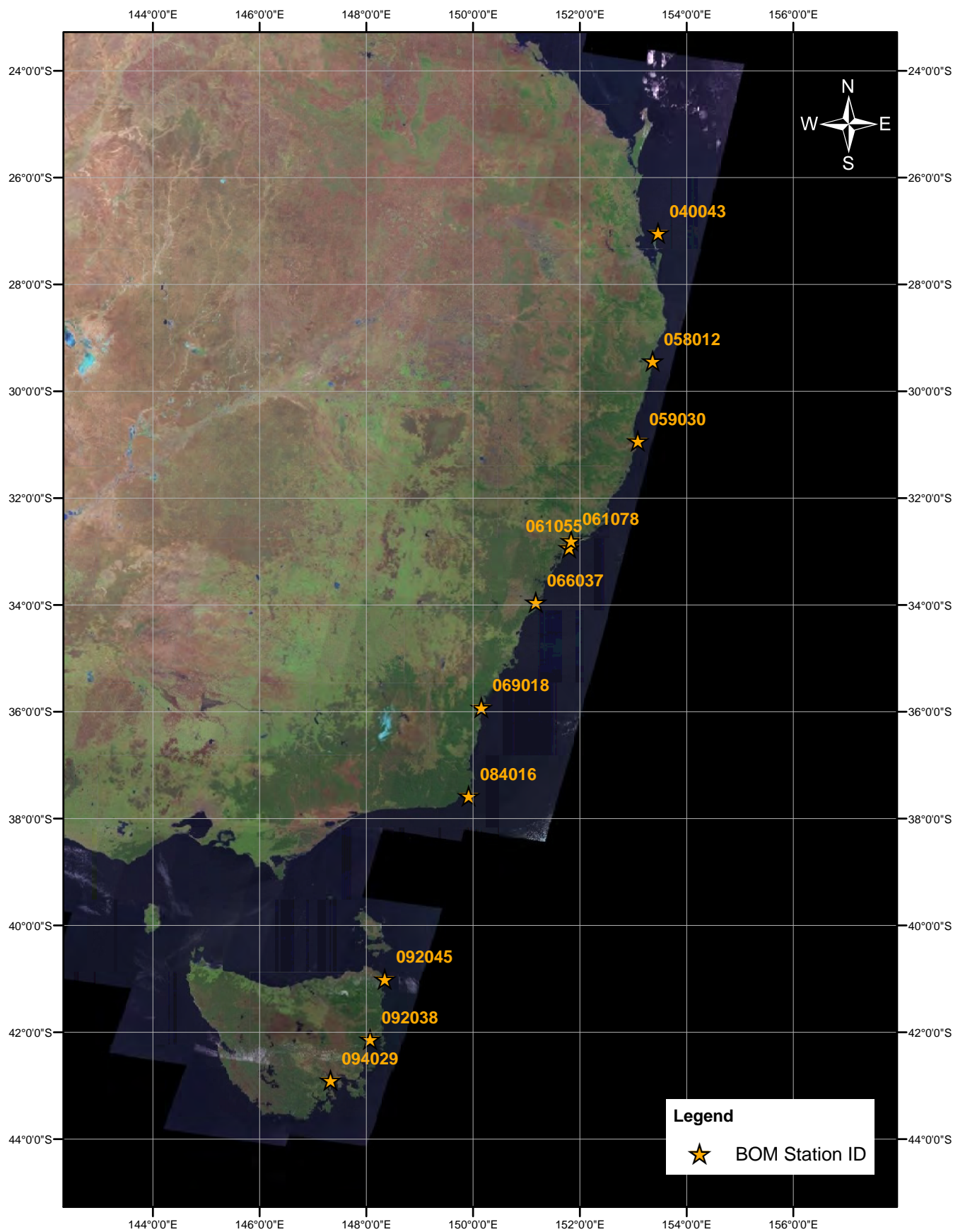
A summary of the extracted datasets for each observation station are provided within Table 2-5.

Table 2-5 Number of GCM datasets compared to each observation station used in present assessment

Model ID	Variables	Land/Sea cells	Scenarios Outputs	Runs	Total
CSIRO-Mk3.0	3	2	3	3	54
CSIRO-Mk3.5	3	2	3	3	54
GFDL-CM2.0	3	2	3	1	18
GFDL-CM2.1	3	2	3	1	18
GISS-ER	3	2	3	1	18
NCAR-CCSM3	3	2	3	3	54
MIUBEG ECHO-G	3	2	3	3	54
<i>Total</i>					<i>252</i>



United States East Coast Observation Stations



Australian East Coast Observation Stations

3. Methodology

The skill of the various Reanalysis and AR-4 models in simulating characteristics of the physical environment along the East Coasts of the United States and Australia is evaluated by comparing statistical characteristics of the modelled datasets with observed. These assessments include comparison of the central tendency of data, the distribution of the data and comparison of extreme values derived from the data. These measures are described below and illustrated in Figure 3-1).

3.1 Mean skill

The mean skill ($Mean_{skill}$) is assessed as the relative difference between the arithmetic mean of the modelled (\overline{M}) and the observed data (\overline{O}) (Eqn. 1) and provides an initial comparison of the model's ability to replicate the central tendency of the observed datasets.

$$Mean_{skill} = \frac{\overline{M}}{\overline{O}} \quad (1)$$

3.2 PDF skill

The empirical probability density function of the observed data is compared to each GCM dataset and an S_{score} metric is assigned based on Perkins et al. (2007) and expressed within Eqn. (2). This measure of agreement between modelled and observed datasets provides values ranging from zero indicating no overlap between PDFs and one, indicating complete overlap.

$$S_{score} = \sum_1^n \min(Z_M, Z_O) \quad (2)$$

Where n is the number of bins used to calculate the PDF and Z_m is Z_o are the frequency of occurrence within a given bin for the model and observed data respectively.

3.3 Extreme value skill

The skill of a model in replicating extreme characteristics of a natural process is of critical importance in determining future design values for adaptation planning and economic analyses. The model skill in replicating such extreme characteristics is evaluated by assessing the relative difference in extreme values estimated from the datasets using an extreme value distribution.

Low probability events are generally defined in terms of an average recurrence interval (ARI). A generalised extreme value (GEV) distribution, with its cumulative distribution function given by Eqn. 3 in Kotz and Nadarajah (2000), has been used to estimate these recurrence intervals. Annual maxima of the data are fitted to the distribution using the method of probability weighted moments (Hosking et al., 1985) to obtain Location, Scale and Shape parameters. Return values are then estimated for average recurrence intervals (ARI) between 2 and 100 years and 90% Confidence Intervals are estimated using a negative log-likelihood function and the delta method (Coles, 2004).

$$F_X(x) = \begin{cases} e^{-(1+\xi((x-\mu)/\sigma))^{-1/\xi}} & -\infty < x \leq \mu - \sigma/\xi & \text{for } \xi < 0 \\ \mu - \sigma/\xi \leq 0 < \infty & & \text{for } \xi > 0 \\ e^{-e^{-(x-\mu)/\sigma}} & -\infty < x < \infty & \text{for } \xi = 0 \end{cases} \quad (3)$$

Where $F_X(x)$ is distribution function of the variable, x , μ is the location parameter, σ is the scale parameter and ξ is the shape parameter.

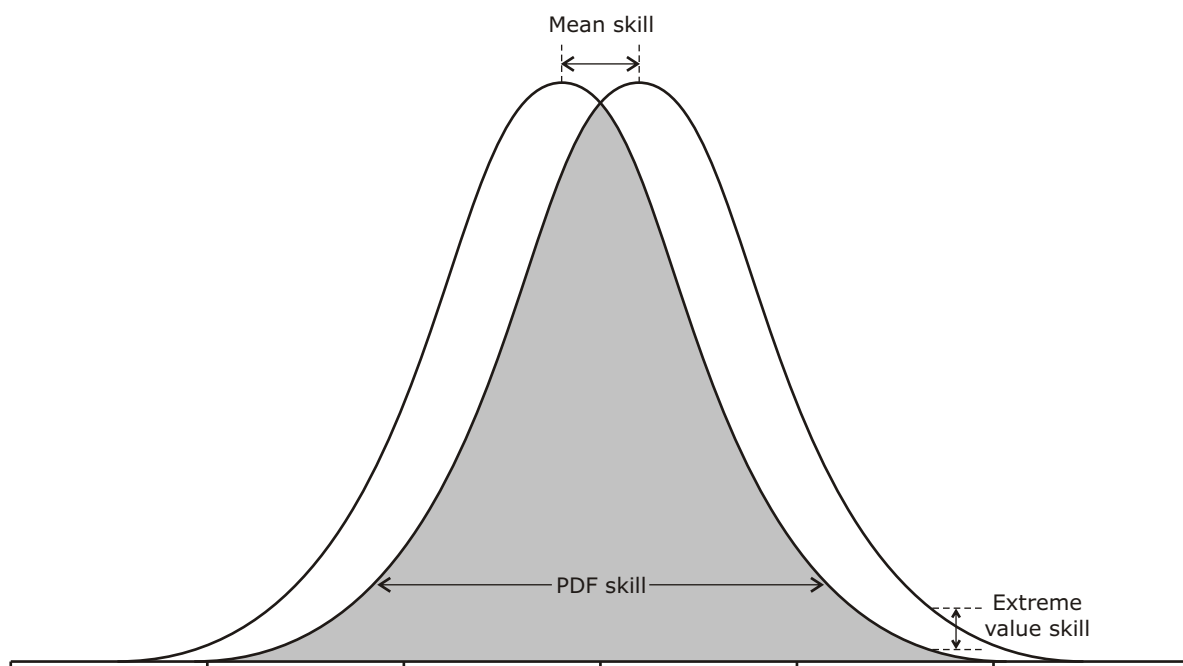
The model skill in representing extreme values ($Extreme_{skill}$) is evaluated by assessing the ratio of the modelled 20yr ARI return value (X_{20-M}) to observed value (X_{20-O}) (Eqn. 4) or an annual exceedance probability of 5%. This value provides an appropriately extreme condition without requiring extrapolation to lower probability values which are subject to much larger confidence intervals (Kharin et al., 2007).

$$Extreme_{skill} = \frac{X_{20-M}}{X_{20-O}} \quad (4)$$

3.4 Processing and comparison

For each observation station, each variable is compared to the corresponding reanalysis and GCM model dataset according to the methods described above. Figure 3-2 provides an example of mean sea level pressure observed at the Norfolk Intl. airport, VA being compared the GFDL-CM2.0 model for the 20c3m scenario. Both the adjacent land and ocean GCM datasets are compared with the mean, $mean_{skill}$, S_{score} , 20yr ARI value and $Extreme_{skill}$ values being extracted for each. All coincident model outputs are compared with the observed data in Figure 3-2 to Figure 3-9 as example comparisons for a particular 20th Century 20c3m scenario run for Norfolk Intl. Airport, VA (Latitude 36.90N) and Sydney Airport, NSW (Latitude -33.95). Statistical characteristics including $Mean_{skill}$, S_{score} and the $Extreme_{skill}$ are extracted, run-averaged and presented for each scenario as a function of latitude. These results are presented and discussed within Section 4.

Initial processing showed the NASA GISS-ER model to contain irregularities during the 20th Century 20c3m scenario. Particularly, these irregularities included a substantial shift in magnitude of precipitation data (Figure 3-10) around 1970. No explanation could be found for this irregularity, and GISS-ER model results show substantial divergence from other GCM results within other studies (i.e. Perkins and Pitman, 2009; Fig 15). The GISS-ER model data has therefore been excluded from the precipitation plots and from the GCM ensemble averaged result summaries. While the GISS-ER data for mean sea level pressure and wind speed did not appear to contain the same magnitude shift within the 20c3m timeseries, the resultant mean and extreme statistical characteristics were generally outliers within the GCM results and were therefore excluded from the GCM ensemble averaged result summaries.

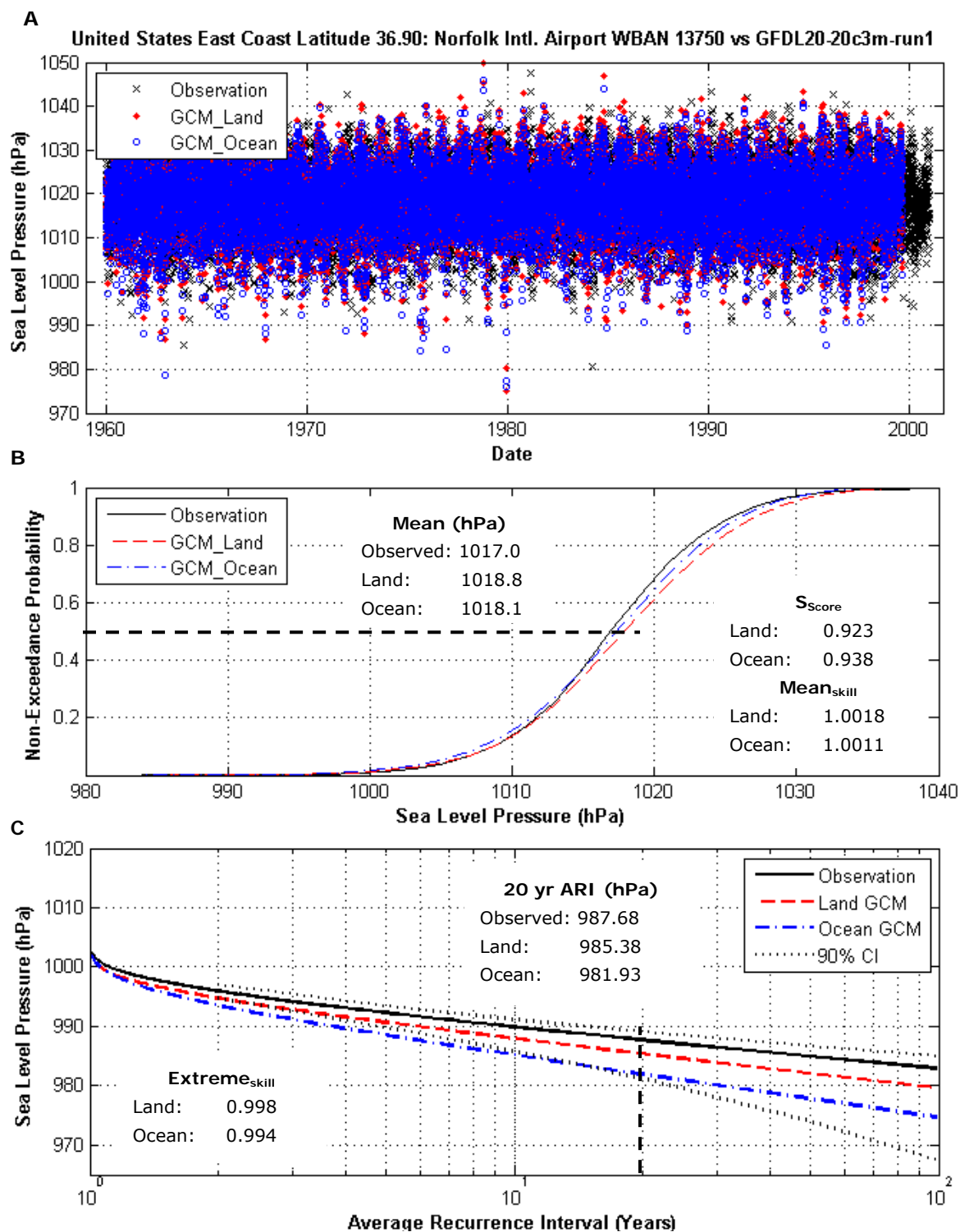


Mean skill is the relative difference between the mean values of two pdfs

PDF skill is the S_{score} corresponding to the overlap between two pdfs

Extreme value skill is the relative difference between the extreme values calculated using two pdfs

**Schematic Diagram of the Methods used to Evaluate
GCM Performance Compared to Observation**
(adapted from Perkins et al., 2007)

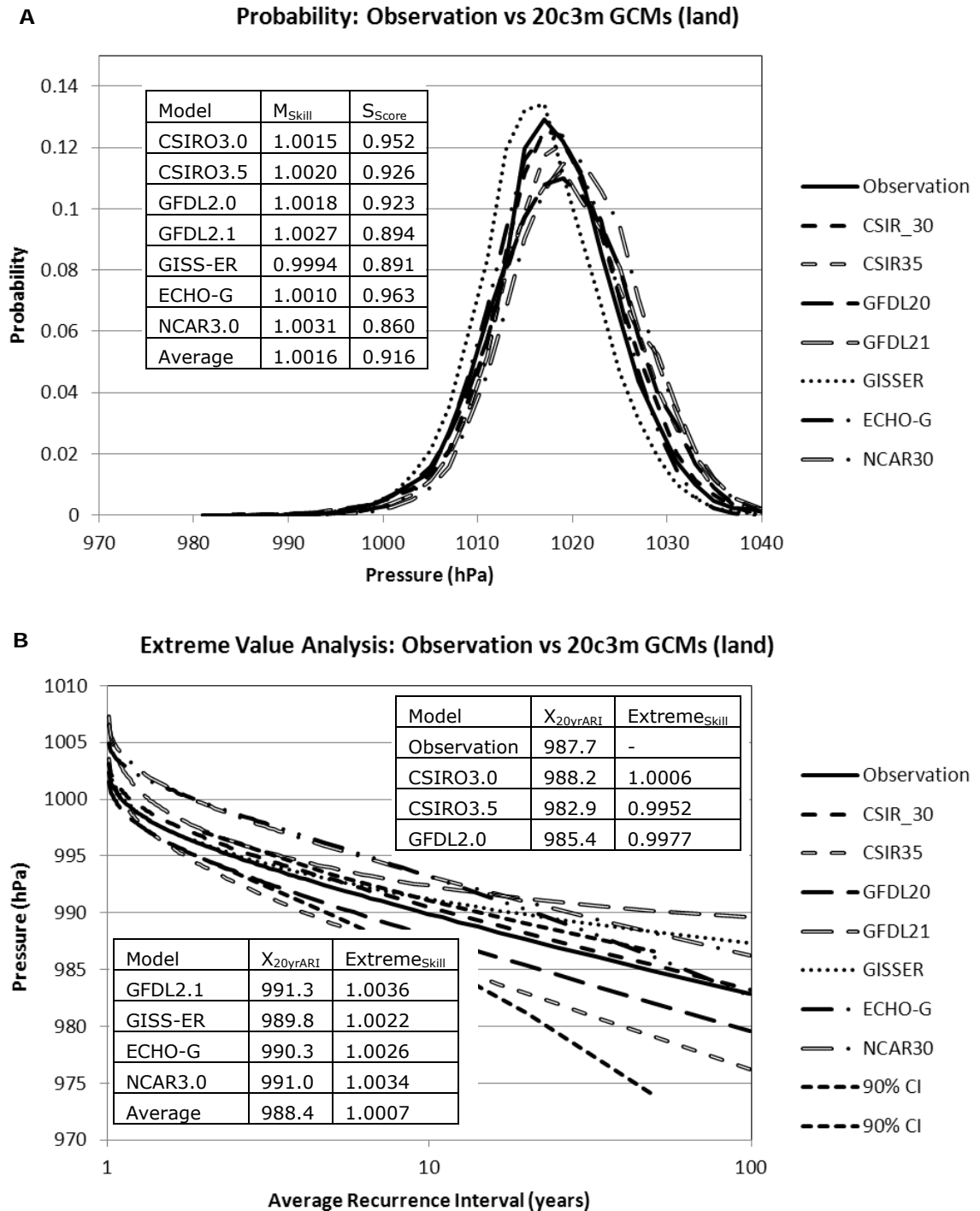


A shows raw observed and modelled timeseries

B show the non-exceedance probability with the calculated $\text{Mean}_{\text{skill}}$ and S_{score} values

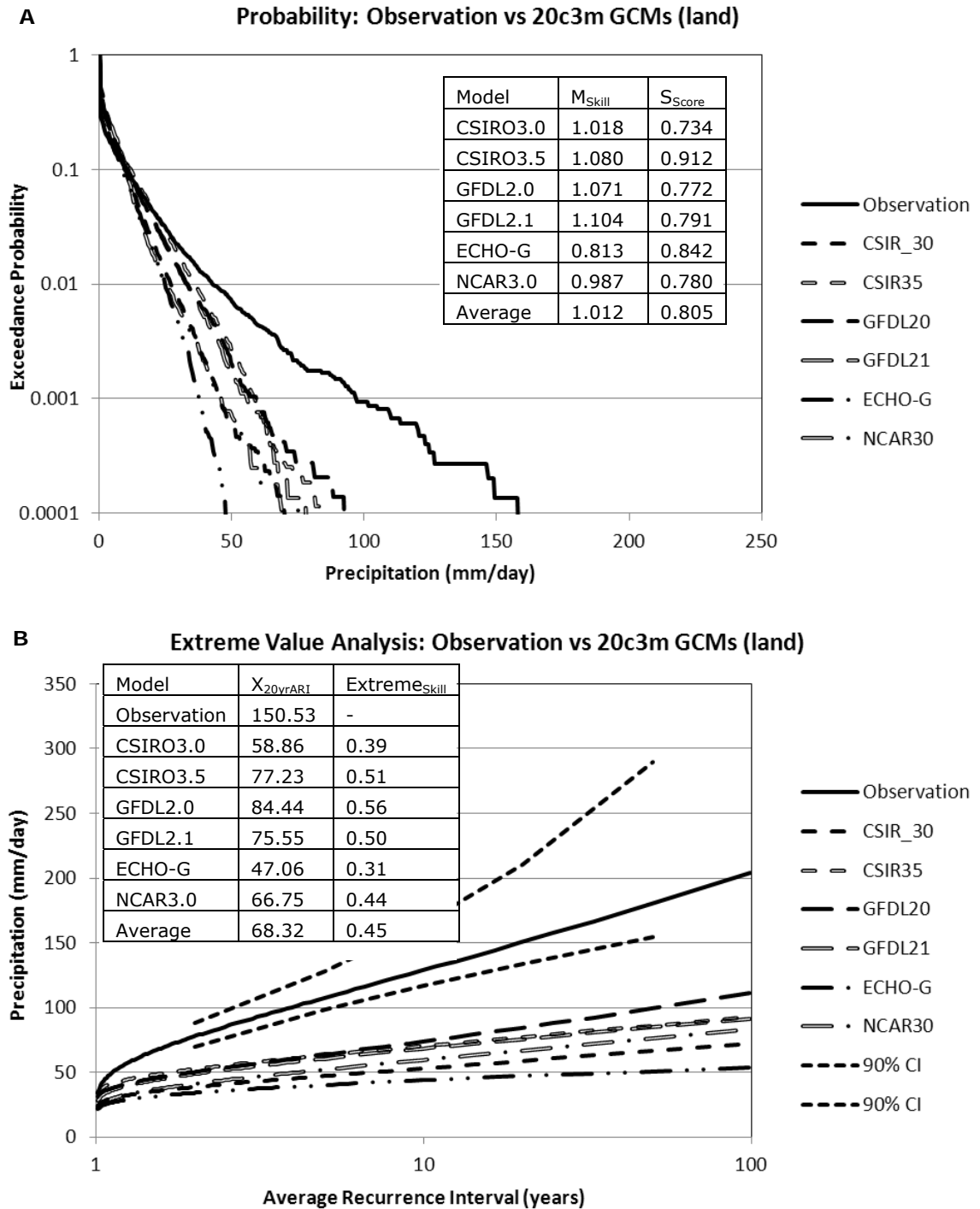
C shows the derived generalised extreme value (GEV) distribution with the 20 year ARI and calculated $\text{Extreme}_{\text{skill}}$ values

Example of an Observed Mean Seal Level Pressure time series at United States East Coast Latitude 36.90 (Norfolk Intl. Airport: WBAN 13750) compared to the GFDL-CM2.0 GCM: Scenario 20c3m, Run1.



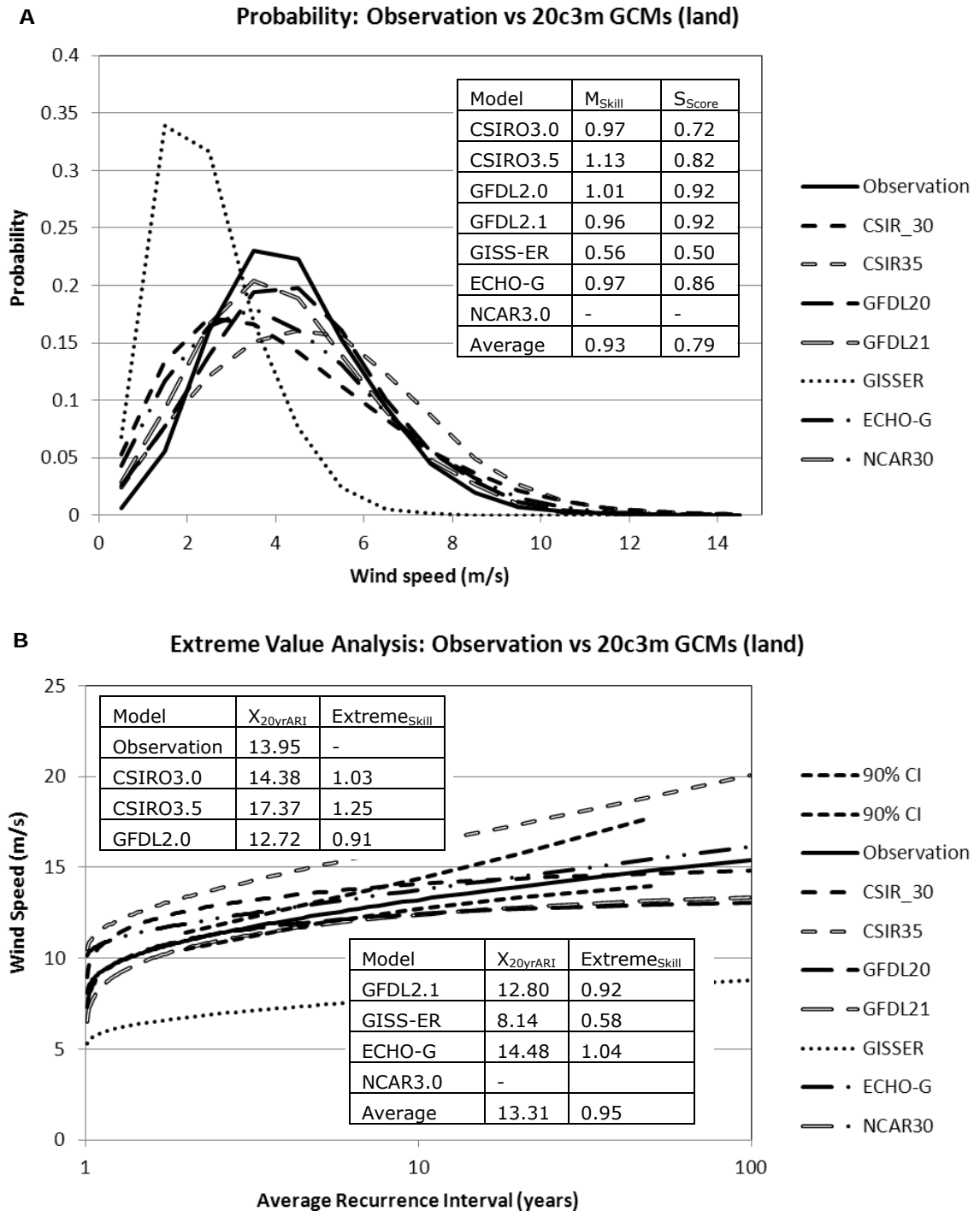
A shows probability distribution function, **B** shows extreme value distribution for observed Mean Sea Level Pressure at United States East Coast Latitude 36.90 (Norfolk Intl. Airport: WBAN 13750) compared to the run-averaged 20th Century (20c3m) GCM land cell results.

Example probability distribution function and extreme value distribution comparison for observed Mean Sea Level Pressure at United States East Coast Latitude 36.90



A shows probability distribution function, **B** shows extreme value distribution for observed Precipitation at United States East Coast Latitude 36.90 (Norfolk Intl. Airport: WBAN 13750) compared to the run-averaged 20th Century (20c3m) GCM land cell results.

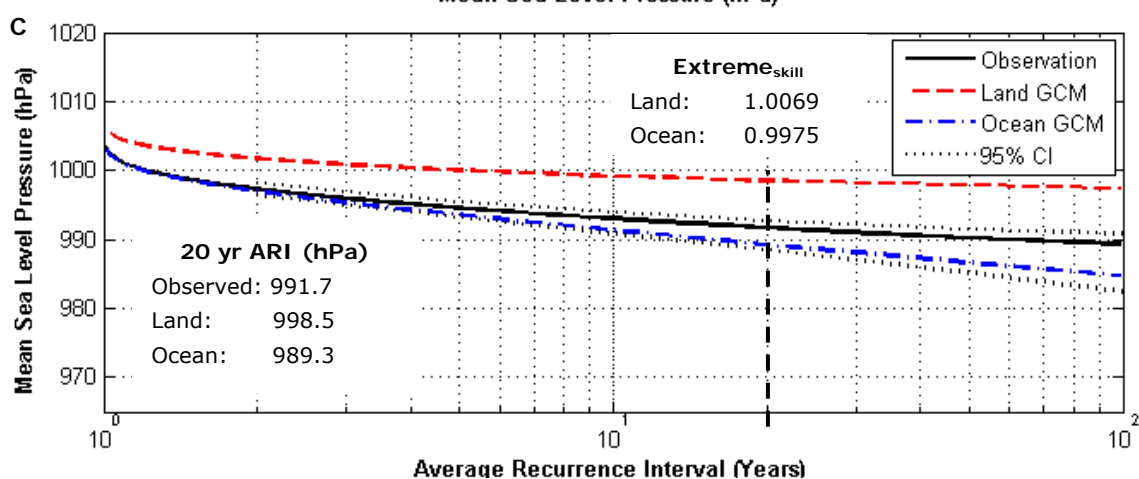
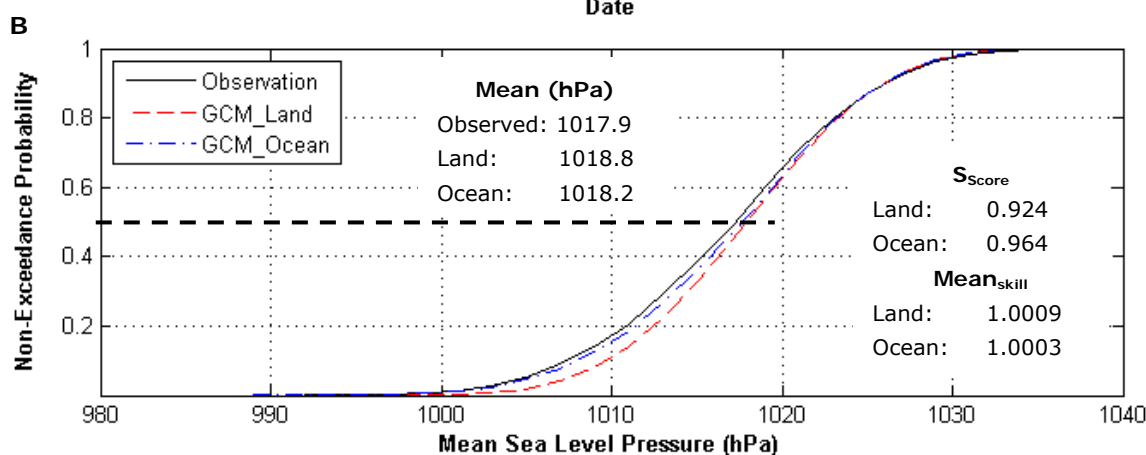
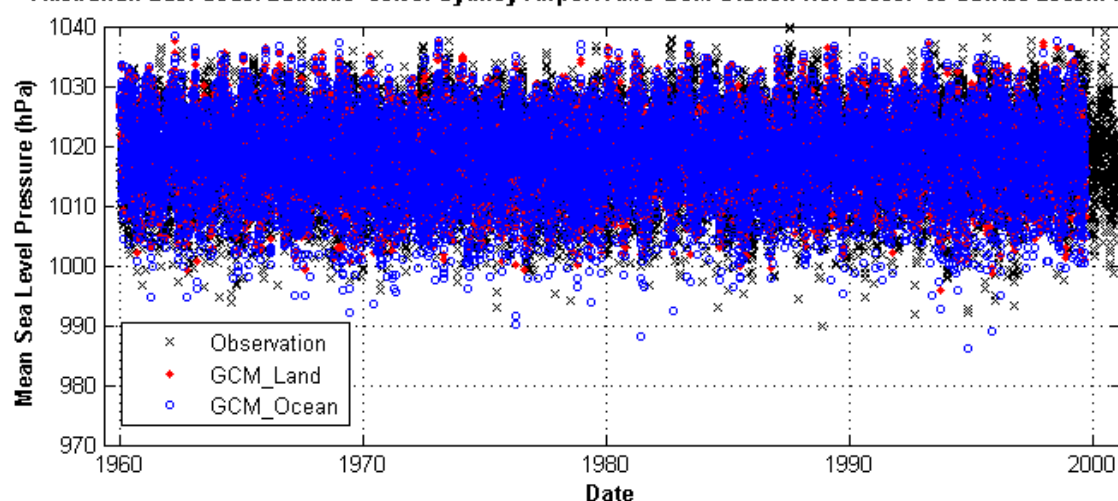
Example probability distribution function and extreme value distribution comparison for observed Precipitation at United States East Coast Latitude 36.90



A shows probability distribution function, **B** shows extreme value distribution for observed Absolute Wind Speed at United States East Coast Latitude 36.90 (Norfolk Intl. Airport: WBAN 13750) compared to the run-averaged 20th Century (20c3m) GCM land cell results.

Example probability distribution function and extreme value distribution comparison for observed Absolute Wind Speed at United States East Coast Latitude 36.90

A Australian East Coast Latitude -33.95: Sydney Airport AMO BoM Station No. 066037 vs CSIR30-20c3m-run2

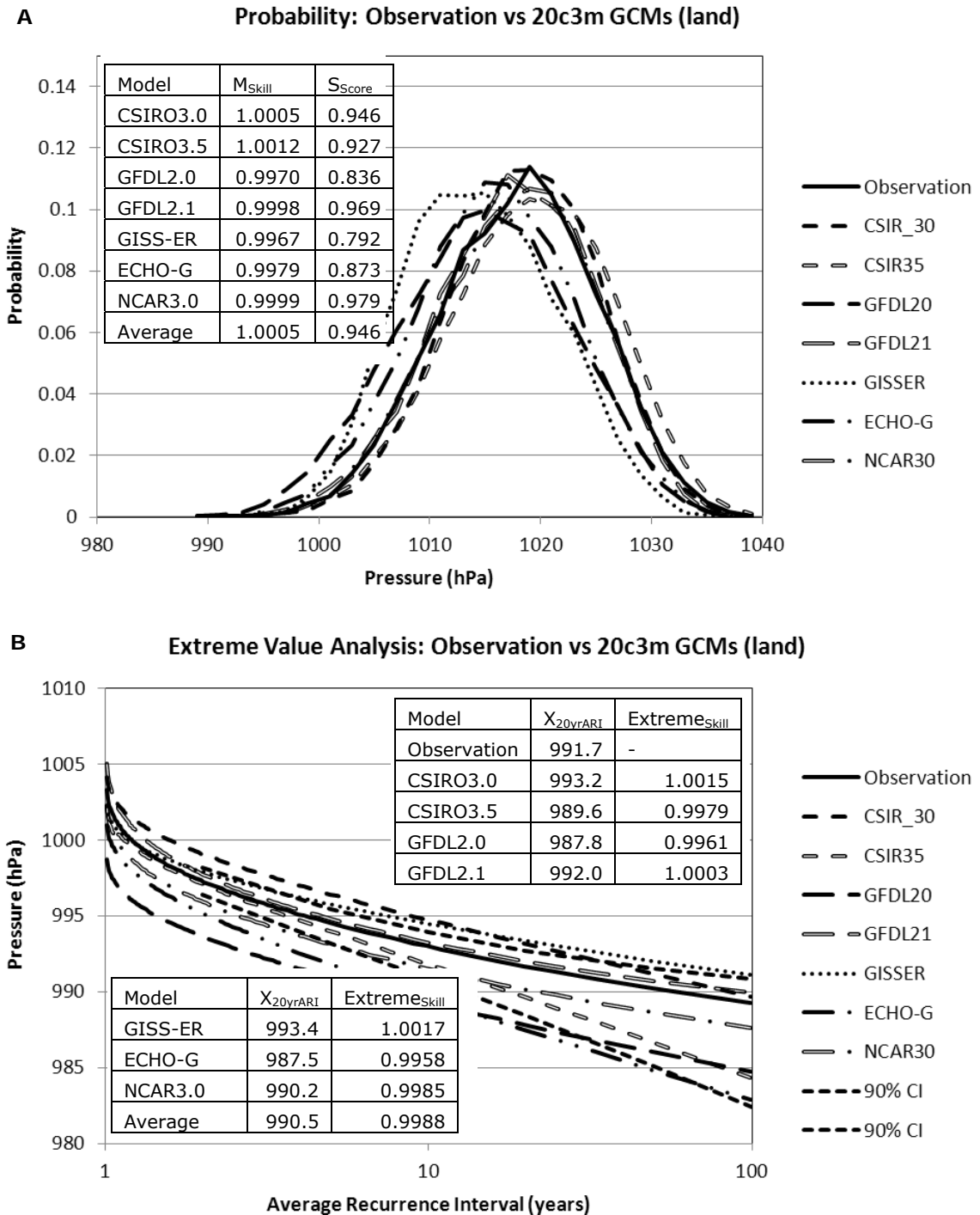


A shows raw observed and modelled timeseries

B show the non-exceedance probability with the calculated Mean_{skill} and S_{score} values

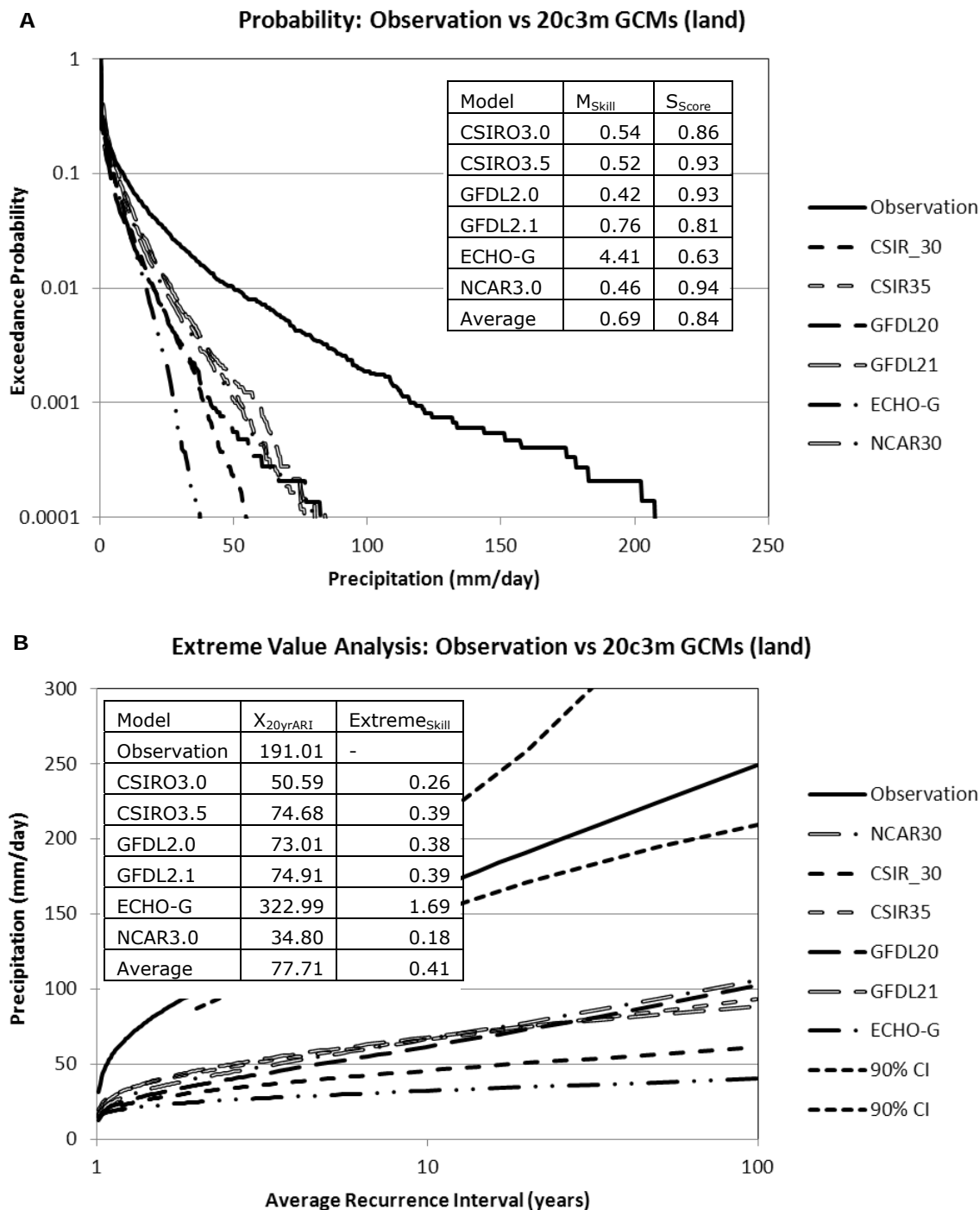
C shows the derived generalised extreme value (GEV) distribution with the 20 year ARI and calculated Extreme_{skill} values

Example of an Observed Mean Seal Level Pressure time series at Australian East Coast Latitude -33.95 (Sydney Airport AMO BoM Station No. 066037) compared to the CSIRO-3.0 GCM: Scenario 20c3m, Run2.



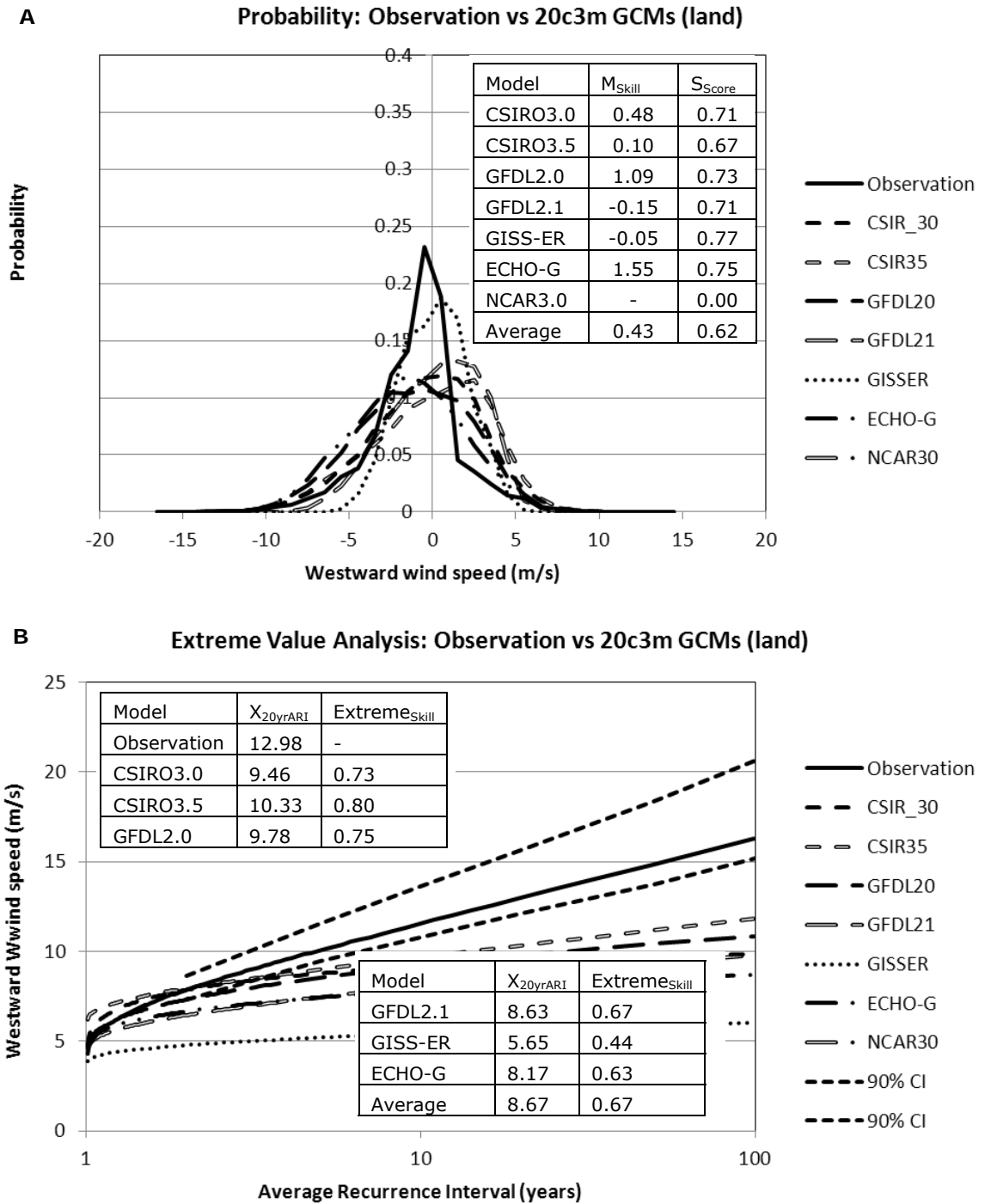
A shows probability distribution function, **B** shows extreme value distribution for observed Mean Sea Level Pressure at Australian East Coast Latitude -33.95 (Sydney Airport AMO BoM Station No. 066037) compared to the run-averaged 20th Century (20c3m) GCM land cell results.

Example probability distribution function and extreme value distribution comparison for observed Mean Sea Level Pressure at Australian East Coast Latitude -33.95



A shows probability distribution function, **B** shows extreme value distribution for observed Precipitation at Australian East Coast Latitude -33.95 (Sydney Airport AMO BoM Station No. 066037) compared to the run-averaged 20th Century (20c3m) GCM land cell results.

Example probability distribution function and extreme value distribution comparison for observed Precipitation at Australian East Coast Latitude -33.95



A shows probability distribution function, **B** shows extreme value distribution for observed Westward (-u) Wind Speed at Australian East Coast Latitude -33.95 (Sydney Airport AMO BoM Station No. 066037) compared to the run-averaged 20th Century (20c3m) GCM land and cell results.

Example probability distribution function and extreme value distribution comparison for observed Westward (-u) Wind Speed at Australian East Coast Latitude -33.95

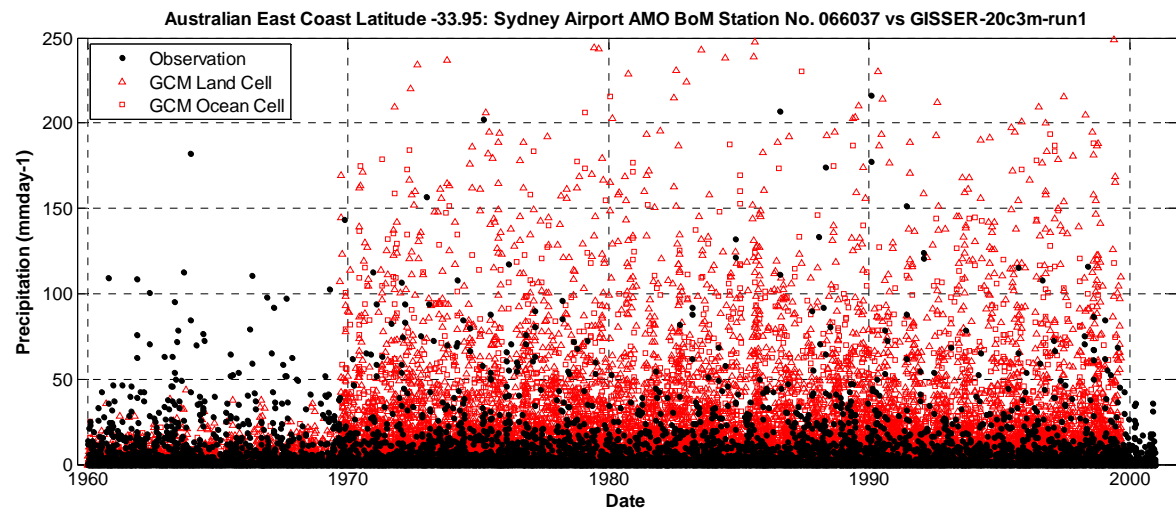


Figure 3-10 Example comparison of observed precipitation at Australian East Coast Latitude - 33.95 with the GISS-ER 20c3m model output.

4. Results and Discussion

Significant quantities of both observational and model data have been processed during the course of this investigation. A primary challenge has been to consolidate that data in such a way that the reader can quickly appreciate the performance of the GCMs and their applicability to coastal engineering assessment.

The assessment has considered two epochs:

- 20th century conditions (Appendix C), and
- the predicted OsresA2 climate scenario (Appendix D).

In both cases, these have been compared directly with the observational data. Changes between the epochs can be obtained by comparing the corresponding values or figures of the epochs.

As discussed in Section 2, reanalysis results can only be obtained for the 20th century conditions but the reanalysis methodology (higher resolution, data assimilation) would be anticipated to yield results that are systematically better than the predictive models.

Each figure in Appendices C and D summarises the quantitative statistics described in Section 3 (see Tables 4-1 and 4-2), with the corresponding model results for adjacent land- and ocean-based cells shown in the left and right columns (respectively) of each figure. Statistical characteristics are model ensemble averaged for each latitude (note the exclusion of the GISS-ER model, refer Section 3.4).

Table 4-1 Figure references in Appendix C for comparison of different GCM characterisations of recent climate with observed data

Model type	Reanalysis		20c3m		Tabular
Variable	US East Coast	Australian East Coast	US East Coast	Australian East Coast	Summary of model averages
Precipitation	Figure C.1a	Figure C.1b	Figure C.1c	Figure C.1d	Table 4-3
Mean Sea Level Pressure	Figure C.2a	Figure C.2b	Figure C.2c	Figure C.2d	Table 4-3
MSLP Gradient	Figure C.3a	Figure C.3b	Figure C.3c	Figure C.3d	Table 4-5
Wind	Figure C.4a	Figure C.4b	Figure C.4c	Figure C.4d	Table 4-7

Table 4-2 Figure references in Appendix D for comparison of different GCM characterisations of future climate with observed data.

Model type	A2 2046-2065		A2 2081-2100		Tabular Summary of average model differences from average 20c3m
Variable	US East Coast	Australian East Coast	US East Coast	Australian East Coast	
Precipitation	Figure D.1a	Figure D.1c	Figure D.1b	Figure D.1d	Table 4-4
Mean Sea Level Pressure	Figure D.2a	Figure D.2c	Figure D.2b	Figure D.2d	Table 4-4
MSLP Gradient	Figure D.3a	Figure D.3c	Figure D.3b	Figure D.3d	Table 4-6
Wind	Figure D.4a	Figure D.4c	Figure D.4b	Figure D.4d	Table 4-8

4.1 Precipitation

The Australian measurements show a systematic decrease in mean precipitation with increasing latitude that is not evident in the US data (Table 4.3). Averages of model mean precipitation are systematically higher over sea than land in both reanalysis and predictive models along the east coast of the USA and east coast Australia.

As an average, both reanalysis and predictive models fail to adequately predict the systematic latitudinal behaviour of east coast Australian precipitation. Models over-predict mean precipitation except in the case of reanalysis of east coast Australian precipitation. While the models do vary locally in their ability to predict mean precipitation, no specific features of individual models warrant comment (Figures C1.a to C1.d).

In terms of precipitation distribution as obtained from an average of the models S_{score} values, no systematically better performance is obtained from the reanalysis models in comparison with the 20c3m predictions. However, on average, the land-based predictions better match the measured coastal data than those over the ocean. Modelled probability precipitation distribution results are systematically better over the Australian east coast than over the east coast US. While the 20c3m results cluster in Figures C1.c and C1.d, the ERA-40 results provide a systematically better stochastic representation of precipitation probability distribution than the NCEP reanalysis.

The averages of the modelled 20 year ARI precipitations are up to a factor of 3 smaller than those measured, thereby indicating systematic attenuation of the rainfall distribution tails. However, the models do replicate the observed increase in extreme intensity that can be observed towards the equator in eastern Australia. The present findings support the Emmanuel et al., (2007) findings of a lack of severe tropical storms on the east coast of the US but we find that this effect is much less significant in eastern Australia. On average, the reanalysis models better predict extreme precipitation than the 20c3m forms. Figures C1.a to C1.d show that ERA-40 provides comparable representation of extreme rainfall to the 20c3m models and both of these model sets yield a significantly better stochastic representation than the NCEP product.

Table 4-4 summarises the predicted changes in coastal rainfall between the A2 scenario and 20c3m conditions. An important first observation is the divergence that can be observed between the different predictive models (compare Figures C1.c and C1.d with Figures D1.a to D1.d) for all statistical characterisations of the model data. The significantly different patterns in predicted rainfall along the meridians by the individual models must also be carefully considered during this assessment. Nonetheless, average model results do show systematic shifts in mean and extreme precipitation as a function of latitude with notable differences between land and ocean. On the east Australian coast, average predicted shifts in mean precipitation are less than 10% to 2100. This will make confirming physical observations difficult to obtain. As would be anticipated, intensification of severe storms is predicted for all monitored locations.

On the US east coast, substantial changes in extreme rainfall are predicted, particularly by the GFDL models. Their predictions warrant careful scrutiny. This clear divergence in the cluster of model results for both mean and extreme precipitation that can be found by comparing, say, Figure C1.c (20c3m) with Figure D1.c (A2 2046-2065). The result divergence can be observed to expand slightly for A2 2081-2100 (Figure D1.d) in comparison with A2 2046-2065. In context of no clear demonstration of superior performance of any single model over another and significant local fluctuations with latitude, localised predictions of future extreme precipitation must be considered.

Table 4-3 Comparison of Observed Precipitation with Ensemble-averaged 20th Century GCM results

Australia East Coast														
Latitude	Mean Precipitation (mmday ⁻¹)					S-score				20 year ARI Precipitation (mmday ⁻¹)				
	Observation	20th C Reanalysis		20c3m		20th C Reanalysis		20c3m		Observation	20th C Reanalysis		20c3m	
		L	O	L	O	L	O	L	O		L	O	L	O
-27.03	4.3	2.2	2.7	2.4	2.6	0.86	0.85	0.81	0.79	218.5	97.3	85.7	79.8	85.2
-29.43	4.2	2.9	3.1	2.7	2.9	0.88	0.85	0.83	0.76	229.7	91.7	95.7	82.1	78.0
-30.92	4.2	2.9	3.2	2.6	3.1	0.85	0.83	0.86	0.75	206.1	93.6	93.4	75.7	75.4
-32.79	3.1	2.3	2.9	2.0	2.5	0.85	0.82	0.88	0.78	158.7	72.3	78.4	67.9	65.4
-32.92	3.1	2.3	2.9	2.0	2.5	0.85	0.83	0.89	0.79	150.1	72.3	78.4	67.9	65.4
-33.95	3.1	2.6	2.9	1.7	2.3	0.84	0.80	0.89	0.79	191.0	79.1	81.9	64.3	62.0
-35.91	2.9	2.5	2.8	1.7	2.2	0.81	0.78	0.87	0.80	180.2	76.0	78.8	58.9	56.6
-37.57	2.6	2.1	2.5	1.5	1.8	0.83	0.84	0.88	0.86	178.5	58.1	67.8	54.6	53.7
-40.99	2.2	-	1.9	1.7	1.8	-	0.81	0.86	0.82	116.9	-	50.1	43.2	43.2
-42.12	1.5	2.0	2.3	1.9	2.1	0.82	0.68	0.75	0.72	98.8	62.6	46.9	42.5	45.4
-42.89	1.6	-	2.2	1.9	2.1	-	0.72	0.78	0.75	82.4	-	45.3	42.5	45.4
United States East Coast														
Latitude	Mean Precipitation (mmday ⁻¹)					S-score				20 year ARI Precipitation (mmday ⁻¹)				
	Observation	20th C Reanalysis		20c3m		20th C Reanalysis		20c3m		Observation	20th C Reanalysis		20c3m	
		L	O	L	O	L	O	L	O		L	O	L	O
44.10	2.8	-	4.4	2.9	2.9	-	0.54	0.63	0.60	169.2	-	81.2	59.1	57.4
41.16	2.8	3.2	4.0	2.9	2.9	0.50	0.56	0.64	0.61	169.2	78.1	88.4	59.1	61.9
40.78	2.9	4.7	4.7	2.7	3.1	0.70	0.69	0.82	0.74	110.9	77.2	88.5	60.8	61.9
36.90	3.1	4.1	5.2	3.1	3.5	0.74	0.70	0.81	0.71	150.5	88.9	109.4	68.3	69.4
34.73	2.9	5.8	5.3	3.3	4.0	0.57	0.57	0.61	0.53	285.5	104.2	103.7	64.0	66.3
32.13	3.5	3.7	4.7	3.1	3.1	0.81	0.76	0.78	0.76	172.4	91.8	97.0	63.2	66.0
26.37	4.0	2.9	3.6	2.8	3.4	0.87	0.83	0.64	0.50	181.7	94.9	92.1	56.4	61.7
24.56	2.8	2.6	3.1	2.7	3.0	0.72	0.67	0.77	0.67	310.2	94.9	92.1	55.3	60.9

Table 4-4 Changes in Ensemble-averaged GCM Precipitation for the 21st Century A2 Scenario from the 20th Century 20Cm3 Scenario

Australia East Coast								
Latitude	Change in Mean Precip (mmday ⁻¹)				Change in X ₂₀ (%)			
	A2 2046-2065		A2 2081-2100		A2 2046-2065		A2 2081-2100	
	L	O	L	O	L	O	L	O
-27.03	-0.12	-0.15	-0.22	-0.20	0.3	13.6	4.2	12.2
-29.43	-0.13	-0.16	-0.18	-0.24	2.7	5.2	7.4	13.0
-30.92	-0.06	-0.12	0.01	-0.13	15.8	10.9	16.2	11.1
-32.79	0.01	0.00	0.10	0.11	-3.7	14.7	8.5	6.1
-32.92	0.01	0.00	0.10	0.11	-3.7	14.7	8.5	6.1
-33.95	0.00	0.06	0.05	0.16	3.7	19.1	9.3	14.9
-35.91	-0.02	0.11	0.00	0.21	1.3	1.3	1.7	7.7
-37.57	-0.07	0.03	-0.08	0.11	-12.2	2.7	0.9	14.2
-40.99	-0.07	0.09	-0.13	0.19	13.2	5.7	11.1	5.7
-42.12	0.02	0.10	-0.02	0.21	0.0	12.2	12.9	24.1
-42.89	0.02	0.10	-0.02	0.21	0.0	12.2	12.9	24.1
United States East Coast								
Latitude	Change in Mean Precip (mmday ⁻¹)				Change in X ₂₀ (%)			
	A2 2046-2065		A2 2081-2100		A2 2046-2065		A2 2081-2100	
	L	O	L	O	L	O	L	O
44.10	0.16	0.19	0.27	0.29	10.3	7.3	25.1	16.2
41.16	0.20	0.19	0.29	0.26	9.2	6.9	16.6	6.0
40.78	0.18	0.23	0.22	0.28	16.0	8.5	22.1	7.1
36.90	0.21	0.17	0.35	0.23	4.4	15.6	11.7	12.4
34.73	0.19	0.25	0.29	0.27	19.4	11.0	25.4	15.6
32.13	0.17	0.11	0.17	0.12	5.6	15.7	22.2	36.1
30.40	0.06	0.08	-0.02	0.02	8.6	6.7	13.8	12.0
26.37	-0.15	-0.18	-0.25	-0.31	-2.6	6.0	0.9	8.1
24.56	-0.12	-0.08	-0.21	-0.19	-1.3	-0.2	1.1	1.4

4.2 Mean Sea Level Pressure

The systematic gradient in average mean sea level pressure on the east coast Australia contrasts strongly with absence of a systematic gradient on the east coast of the US (Table 4-5).

In contrast with precipitation, the average prediction of average mean sea level from the reanalysis models is systematically better than that obtained from the 20c3m ensemble. Indeed, all statistical measures of mean sea level pressure of the reanalysis models are impressive. In general, the NCEP product outperforms the ERA-40 results in this regard (Figures C2.a and C2.b).

In the Australian context, 20 year ARI mean sea level pressure is under predicted by up to 5hPa (~50mm H₂O) at some latitudes implying a slight over estimate in barometric setup by the reanalysis models.

Table 4-5 Comparison of Observed Mean Sea Level Pressure with Ensemble-averaged 20th Century GCM results

Australia East Coast														
Latitude	Mean MSLP (hPa)					S-score				20 year ARI low MSLP (hPa)				
	Observation	20th C Reanalysis		20c3m		20th C Reanalysis		20c3m		Observation	20th C Reanalysis		20c3m	
		L	O	L	O	L	O	L	O		L	O	L	O
-27.03	1017.0	1017.4	1017.0	1017.7	1017.7	0.94	0.95	0.91	0.92	992.5	996.3	993.0	996.2	995.2
-29.43	1017.9	1017.1	1017.0	1017.9	1017.8	0.94	0.94	0.92	0.92	995.0	993.5	991.4	995.6	994.9
-30.92	1017.3	1017.1	1017.0	1017.9	1017.8	0.97	0.96	0.92	0.93	993.6	992.1	989.9	993.1	993.1
-32.79	1018.1	1017.0	1016.9	1017.8	1017.7	0.94	0.94	0.93	0.93	992.9	989.5	988.9	992.6	991.7
-33.95	1017.9	1016.9	1016.8	1016.7	1016.7	0.94	0.94	0.92	0.92	991.7	987.2	986.8	988.1	986.3
-35.91	1017.4	1016.8	1016.6	1015.9	1015.7	0.96	0.95	0.92	0.93	987.6	985.5	984.7	984.7	982.8
-37.57	1016.7	1016.1	1016.0	1013.7	1013.6	0.96	0.96	0.90	0.89	985.2	982.1	980.8	978.0	978.3
-40.99	1015.5	-	1015.0	1012.1	1012.0	-	0.96	0.89	0.89	978.5	-	977.6	973.5	974.0
-42.12	1014.2	1013.1	1013.5	1012.1	1012.0	0.95	0.96	0.88	0.88	974.8	970.7	973.4	973.5	974.0
-42.89	1014.4	-	1013.4	-	-	-	0.95	-	-	974.2	-	972.8	-	-
United States East Coast														
Latitude	Mean MSLP (hPa)					S-score				20 year ARI low MSLP (hPa)				
	Observation	20th C Reanalysis		20c3m		20th C Reanalysis		20c3m		Observation	20th C Reanalysis		20c3m	
		L	O	L	O	L	O	L	O		L	O	L	O
43.65	1016.1	1016.3	1016.1	1015.6	1015.8	0.93	0.93	0.94	0.93	979.0	977.1	973.2	975.7	975.3
41.16	1016.9	1017.3	1017.0	1017.0	1016.8	0.93	0.93	0.92	0.93	983.7	983.8	982.4	978.9	977.2
40.78	1017.0	1017.3	1017.0	1017.6	1017.4	0.94	0.94	0.94	0.93	984.2	983.8	982.4	980.5	978.1
36.90	1017.5	1017.7	1017.6	1019.0	1018.6	0.95	0.95	0.92	0.92	987.7	987.7	986.7	988.4	983.7
34.70	1017.9	1017.8	1017.9	1019.4	1019.0	0.94	0.93	0.89	0.89	991.1	989.9	989.7	991.8	988.1
32.13	1018.3	1017.5	1017.6	1019.5	1019.5	0.90	0.91	0.88	0.87	993.1	993.7	994.1	996.0	993.9
26.68	1017.5	1016.5	1017.1	1018.8	1018.9	0.88	0.93	0.82	0.80	996.8	998.8	998.1	1000.9	1000.4
24.56	1016.3	-	1015.4	1019.2	1018.8	-	0.77	0.81	0.78	997.3	-	1001.2	1000.9	1000.4

The predictions of the 20c3m models are also impressive (Table 4-5, Figures C2.c and C2.d). Differences between modelled and measured mean sea level pressure remain less than 5hPa and the predicted 20 year ARI pressures differ by less than 10hPa. On east coast Australia, the meridional distribution of extreme storm intensity predicted by the models closely replicates the observations. However, on the east coast of the US, the models struggle to capture the lower pressure systems towards the equator (Table 4-5, Figure C2.c).

Global warming predicts a more unstable atmosphere and therefore more intense extreme storms. The present results are interesting because the predictive GCMs generally indicate an increase in storm-related mean sea level pressure and therefore a *decline* in extreme storm intensity from 20c3m to AR2 2046-2065 with conditions for AR2 2081-2100 returning to 20c3m conditions along the east coast US. The effect is not as pronounced along the Australian east coast but there is a systematic decline in extreme storm intensity at higher latitudes.

The model mean values shown in Table 4-6 reflect these trends (compare Figures C2.c and C2.d with their respective counterparts, Figures D2.a to D2.d).

Table 4-6 Changes in Ensemble-averaged GCM Mean Sea Level Pressure for the 21st Century A2 Scenario from the 20th Century 20Cm3 Scenario

Australia East Coast								
Latitude	Change in Mean MSLP (hPa)				Change in X ₂₀ (%)			
	A2 2046-2065		A2 2081-2100		A2 2046-2065		A2 2081-2100	
	L	O	L	O	L	O	L	O
-27.03	0.47	0.54	0.77	0.90	0.2	0.0	0.0	-0.7
-29.43	0.49	0.57	0.87	1.01	0.1	0.8	0.6	-0.4
-30.92	0.63	0.66	1.06	1.20	0.5	1.1	1.7	0.6
-32.79	0.57	0.62	1.01	1.11	1.5	2.1	2.0	1.8
-33.95	0.70	0.72	1.28	1.37	3.1	2.6	3.9	2.7
-35.91	0.86	0.88	1.54	1.59	2.7	2.9	3.2	2.2
-37.57	1.00	0.83	1.83	1.63	2.5	2.8	2.4	3.1
-40.99	1.11	0.95	1.99	1.79	3.7	2.7	3.4	1.9
-42.12	1.11	0.95	1.99	1.79	3.7	2.7	3.4	1.9
United States East Coast								
Latitude	Change in Mean MSLP (hPa)				Change in X ₂₀ (hPa)			
	A2 2046-2065		A2 2081-2100		A2 2046-2065		A2 2081-2100	
	L	O	L	O	L	O	L	O
43.65	0.18	0.36	0.36	0.61	0.5	0.8	-0.1	-0.4
41.16	0.14	0.35	0.29	0.57	1.8	2.5	1.4	0.4
40.78	0.14	0.33	0.23	0.51	0.0	2.5	0.2	1.3
36.90	0.03	0.18	0.10	0.31	-0.1	1.2	-0.3	-1.4
34.70	0.08	0.21	0.11	0.32	-0.6	0.6	-0.3	-1.0
32.13	0.06	0.11	0.03	0.10	-1.9	-2.1	-0.7	-1.7
26.68	-0.07	0.04	-0.02	0.08	-0.5	-0.2	-0.1	-0.8
24.56	-0.10	-0.05	-0.12	-0.05	-0.5	-0.3	-0.3	-1.1

4.3 Sea Level Pressure Gradient

Although sea level pressure gradients derived from synoptic charts have traditionally been used to determine surface winds, their numerical counterparts tend to suffer from numerical noise arising from differentiation.

For completeness during this study, we have endeavoured to compute the corresponding quantities for both data and models but as shown in Tables 4-7 and 4-8 as well as Figures C.3a to C.3d and D.3a to D.3d, the results are noisy and therefore not of particular use.

Table 4-7 Comparison of Observed MSLP Gradient with Ensemble-averaged 20th Century GCM results

Australia East Coast								
Latitude	Mean MSLP Grad (hPakm ⁻¹)			S-score		20 year ARI MSLP Grad (hPakm ⁻¹)		
	Observation	20c3m		20c3m		Observation	20c3m	
		L	O	L	O		L	O
-29.43	-0.003	-0.001	0.000	0.83	0.81	0.064	0.029	0.044
-30.92	0.004	-0.005	0.000	0.63	0.72	0.087	0.034	0.037
-32.79	-0.004	0.001	0.002	0.77	0.70	0.066	0.041	0.035
-35.91	0.002	0.004	0.005	0.85	0.84	0.059	0.041	0.049
-37.57	0.004	0.003	0.004	0.65	0.72	0.072	0.052	0.050
United States East Coast								
Latitude	Mean MSLP Grad (hPakm ⁻¹)			S-score		20 year ARI MSLP Grad (hPakm ⁻¹)		
	Observation	20c3m		20c3m		Observation	20c3m	
		L	O	L	O		L	O
41.16	-0.005	-0.005	-0.006	0.58	0.59	-	0.075	0.078
36.90	-0.006	0.002	-0.002	0.43	0.44	-	0.059	0.048
34.70	-0.005	-0.002	-0.002	0.25	0.28	-	0.042	0.056
32.13	-0.001	0.005	-0.001	0.58	0.58	-	0.059	0.044
27.65	0.009	0.006	0.001	0.22	0.21	-	0.032	0.025

Table 4-8 Changes in Ensemble-averaged GCM MSLP Gradient for the 21st Century A2 Scenario from the 20th Century 20Cm3 Scenario

Australia East Coast								
Latitude	Change Mean MSLP Grad (hPakm⁻¹)				Change in X₂₀ (%)			
	A2 2046-2065		A2 2081-2100		A2 2046-2065		A2 2081-2100	
	L	O	L	O	L	O	L	O
-29.43	0.000	-0.001	-0.001	-0.001	-8.5	-6.1	-5.9	-7.4
-30.92	0.000	0.000	0.004	-0.001	-8.2	-5.9	-11.1	-10.5
-32.79	0.000	0.000	0.000	-0.001	-7.1	-7.9	-8.3	-5.3
-35.91	-0.001	0.000	-0.001	-0.001	-3.0	-7.6	-1.6	-12.7
-37.57	0.000	0.000	-0.002	-0.001	-12.9	-3.3	-15.1	0.8
United States East Coast								
Latitude	Change Mean MSLP Grad (hPakm⁻¹)				Change in X₂₀ (hPakm⁻¹)			
	A2 2046-2065		A2 2081-2100		A2 2046-2065		A2 2081-2100	
	L	O	L	O	L	O	L	O
41.16	0.000	0.000	0.000	0.000	-0.8	-10.3	-8.0	-6.7
36.90	-0.004	0.000	-0.004	0.000	-6.8	-4.7	-7.7	-0.3
34.70	0.000	0.000	0.000	-0.001	0.2	-9.2	0.5	-6.2
32.13	-0.003	0.000	-0.003	0.000	-3.4	-2.5	-5.7	10.0
27.65	0.000	0.000	-0.001	0.000	-1.4	0.2	-2.3	-0.4

4.4 Wind

Comparing mean modelled and measured winds is often not a robust process as conventional anemometers are notoriously bad at capturing low velocity winds. Consequently, the average wind data in Table 4-9 and the upper panels of Figure C4.a to C4.d and D4.a and D4.d should be treated with caution.

Significant differences in the frequency of the vectorially resolved wind speeds are observed in the modelled and observed wind speeds in panel A of Figure 3.7, for example.

Surface wind intensity is a function of local pressure gradient and the surface roughness. Unfortunately, as discussed in the previous section, it did not prove possible to obtain a robust comparison of surface pressure gradients.

Winds over land are systematically lower than those over water, reflecting the relative smoothness of the sea (Figures C4.a and C4.b). Consequently, coastal anemometers are vulnerable to systematic differences depending on the direction of the wind. This is reflected in the model data more extreme wind events for which winds over water are systematically higher than those over adjacent land cells.

For the extreme events, model behaviour in east coast Australia and US is strongly contrasting.

For the east coast US, both the reanalysis and 20c3m model predictions are systematically higher than the observed data. Along the east Australian coast the converse is true.

This pattern of behaviour is such that the performance of the reanalysis and 20c3m models in relation to the data is very similar. Along the east coast US, winds over land most closely resemble the data and along the east coast of Australia, winds over water bear the greatest similarity to the data.

Nonetheless, these results are encouraging and indicate that the wind intensities generated by the models are of similar magnitude to those observed. Consequently, the limited ability to quantify reliable pressure gradients is of secondary importance as there is significant reliability in extreme winds generated by the models.

When compared to the climate change scenarios, a warmer climate should mean greater atmospheric instability and therefore greater storm (and wind) intensity. On the Australian east coast there is a systematic decline in extreme wind intensity for future climates, particularly towards the equator (lower two panels of Figures C.4d, D.4c and D.4d). Along the east coast of the US also, while individual models predict local changes, there is an overall slight decline in extreme wind intensity (lower two panels of Figures C.4c, D.4a and D.4b).

When the models are assessed as an ensemble, these observations are clearly demonstrated in Table 4-10 although no significant differences can be observed between the results for A2 2081-2100 in comparison with A2 2046-2065.

Table 4-9 Comparison of Observed Wind with Ensemble-averaged 20th Century GCM results

Australia East Coast														
Latitude	Mean Westward Wind (ms ⁻¹)					S-score				20 year ARI Westward Wind (ms ⁻¹)				
	Observation	20th C Reanalysis		20c3m		20th C Reanalysis		20c3m		Observation	20th C Reanalysis		20c3m	
		L	O	L	O	L	O	L	O		L	O	L	O
-27.03	1.1	0.4	1.2	1.1	1.6	0.56	0.73	0.50	0.60	22.8	9.5	17.4	8.5	15.4
-29.43	-0.5	0.5	0.5	0.7	0.9	0.55	0.55	0.53	0.48	23.9	14.7	17.3	8.8	15.6
-30.92	-2.0	0.6	0.2	0.0	0.0	0.54	0.59	0.57	0.53	20.2	16.0	17.5	9.1	15.8
-32.79	-1.6	0.4	-0.1	-0.2	-0.4	0.61	0.67	0.61	0.61	11.5	15.3	17.3	7.0	15.0
-32.92	-2.3	0.4	-0.1	-0.2	-0.4	0.64	0.72	0.55	0.62	19.7	15.3	17.3	7.0	15.0
-33.95	-1.1	-0.3	-0.6	-0.5	-1.0	0.57	0.58	0.60	0.51	13.0	16.2	18.0	7.7	15.2
-35.91	-0.9	-1.0	-1.5	-1.0	-1.5	0.67	0.68	0.68	0.59	15.4	17.5	19.2	7.9	14.5
-37.57	-2.4	-2.1	-2.2	-1.6	-2.4	0.81	0.82	0.56	0.65	18.2	17.3	18.2	7.0	15.2
-40.99	-1.9	-	-3.1	-2.8	-3.4	-	0.79	0.61	0.61	15.7	-	16.3	9.6	14.8
-42.12	-0.9	-4.2	-4.1	-3.5	-4.2	0.46	0.45	0.39	0.36	13.1	14.9	15.3	9.8	15.2
-42.89	-1.5	-	-4.2	-3.5	-4.2	-	0.49	0.43	0.38	7.8	-	15.8	9.8	15.2
United States East Coast														
Latitude	Mean Absolute Wind (ms ⁻¹)					S-score				20 year ARI Absolute Wind (ms ⁻¹)				
	Observation	20th C Reanalysis		20c3m		20th C Reanalysis		20c3m		Observation	20th C Reanalysis		20c3m	
		L	O	L	O	L	O	L	O		L	O	L	O
43.65	3.8	7.3	7.6	4.3	6.5	0.51	0.49	0.70	0.54	11.9	25.6	25.1	14.2	20.3
41.16	5.0	6.7	7.5	4.1	6.9	0.66	0.59	0.71	0.63	15.1	23.3	25.3	13.7	22.2
40.78	5.3	6.7	7.5	4.2	6.8	0.64	0.59	0.64	0.63	15.5	23.3	25.3	13.7	21.4
36.90	4.4	6.1	7.2	4.4	7.2	0.68	0.58	0.85	0.56	14.0	19.7	22.5	14.3	22.1
34.70	2.8	6.7	6.9	4.6	6.9	0.42	0.41	0.63	0.39	11.4	20.9	21.2	14.4	20.3
32.13	3.3	5.1	6.0	3.6	5.5	0.63	0.52	0.79	0.56	10.1	16.2	19.0	11.4	17.0
26.68	4.4	5.8	5.9	4.0	5.8	0.68	0.66	0.82	0.70	13.7	17.6	17.1	12.0	16.7
24.56	4.1	-	5.1	4.0	5.5	-	0.72	0.85	0.72	15.5	-	14.5	11.8	15.1

Table 4-10 Changes in Ensemble-averaged GCM Wind Speed for the 21st Century A2 Scenario from the 20th Century 20Cm3 Scenario

Australia East Coast								
Latitude	Change Mean Westward Wind (ms⁻¹)				Change in X₂₀ (%)			
	A2 2046-2065		A2 2081-2100		A2 2046-2065		A2 2081-2100	
	L	O	L	O	L	O	L	O
-27.03	0.24	0.38	0.50	0.76	-9.7	-10.5	-14.4	-9.5
-29.43	0.22	0.45	0.48	0.83	-11.1	-11.0	-13.0	-12.5
-30.92	0.27	0.48	0.55	0.88	-2.4	-7.5	-9.2	-9.2
-32.79	0.24	0.35	0.50	0.74	-7.0	-11.7	-7.1	-10.0
-32.92	0.24	0.35	0.50	0.74	-7.0	-11.7	-7.1	-10.0
-33.95	0.27	0.26	0.54	0.63	-9.6	-1.8	-9.2	-6.4
-35.91	0.27	0.12	0.51	0.41	-9.3	-3.3	-10.6	-9.7
-37.57	0.26	0.15	0.49	0.45	-9.5	-9.3	-8.5	-8.6
-40.99	0.02	-0.19	0.17	-0.05	-12.0	-12.2	-9.6	-9.9
-42.12	-0.03	-0.12	0.01	-0.11	-11.5	-4.9	-9.3	-5.0
-42.89	-0.03	-0.12	0.01	-0.11	-11.5	-4.9	-9.3	-5.0
United States East Coast								
Latitude	Change in Mean Absolute Wind (ms⁻¹)				Change in X₂₀ (%)			
	A2 2046-2065		A2 2081-2100		A2 2046-2065		A2 2081-2100	
	L	O	L	O	L	O	L	O
43.65	-0.11	-0.22	-0.14	-0.28	-3.6	-5.7	-4.3	-5.5
41.16	-0.18	-0.23	-0.22	-0.31	-6.1	-3.7	-9.1	-2.1
40.78	-0.09	-0.22	-0.14	-0.28	-1.9	-2.0	-0.4	-0.2
36.90	-0.63	-0.18	-0.65	-0.24	-14.6	-1.4	-15.7	-4.8
34.70	-0.48	-0.18	-0.50	-0.23	-12.5	-1.9	-11.4	-3.5
32.13	-0.59	-0.12	-0.58	-0.11	-19.5	-5.9	-16.2	-2.5
26.68	-0.24	-0.04	-0.26	-0.04	-5.7	-0.7	-6.4	-3.5
24.56	-0.26	0.02	-0.26	0.04	-3.7	0.3	-4.6	-4.1

5. Conclusions and Recommendations

During this investigation, we have undertaken a detailed review of the performance of both reanalysis and predictive global circulation models in predicting the atmospheric behaviour most important for extreme inundation in coastal regions.

Differences between individual model predictions are significant and so an assembly of characterisations of mean, probability distribution and extreme behaviour have been assembled to quantify model behaviour.

Mean Sea Level Pressure

Atmosphere mean sea level pressure is the best predicted variable by the GCMs and the different meridional average gradients along the US and Australian east coasts are well predicted.

As anticipated, the reanalysis models perform better at predicting representative probability distributions of mean sea level pressure than the predictive models for present climate.

The 20 year ARI mean sea level pressure is underpredicted by 5hPa by the reanalysis models thereby implying systematic slight overestimate of barometric set up.

The meridional distribution of modelled 20 year ARI minimum mean sea level pressures closely replicates the observed distribution along the east Australian coast and most of the US east coast. Consistent with Emmanuel et al. (2008), the intensity of more tropical storms is systematically underpredicted in the US.

Comparison of extreme mean sea level pressures for the A2 scenarios indicates only small (<3%) average changes in storm intensity from present conditions.

Although gradients in mean sea level pressure have traditionally been used to predict winds, during this study it was found that these differential quantities were very noisy and were of negligible value in comparison with the model predicted winds themselves.

Winds

Conventional anemometers struggle to capture low velocity winds and therefore comparison of mean wind speeds is usually subject to significant errors.

As anticipated, the models predicted higher 10m wind speeds over water than over land.

In spite of the generally good performance of the GCMs in predicting extreme mean sea level pressures along both coastlines, analysis of extreme winds showed contrasting behaviours. Along the US east coast, the models predicted 20 year ARI winds that were higher than those observed. In Australia, the predictions were systematically lower than the observations.

Nonetheless, the wind intensities generated by the models are of similar magnitude to those measured. Appropriate downscaling that recognises these features should be capable of generating wind fields that are consistent with extreme large-scale low pressure systems.

Although the predicted future changes with climate show local variability, on average the models predict modest declines in extreme wind speeds on both coasts.

Precipitation

There are significant differences in the meridional distribution of mean precipitation between the US and Australian east coasts: along the Australian east coast there is a significant gradient in mean rainfall.

Both reanalysis and predictive models fail to capture this gradient in mean precipitation along the east coast of Australia.

Averaged 20 year ARI precipitations are generally a factor of 3 smaller in both reanalysis and predictive models than those observed along both coasts, indicating significant attenuation of the distribution tails.

However, systematic extreme distributions of precipitation can be obtained from the GCMs. While the individual values may contain significant error, appropriate downscaling techniques should be able to be developed to yield representative extreme rainfalls.

There is clear divergence in the predictions of future rainfall distributions obtained from the suite of GCMs investigated in this study. In the absence of clear superior regional performance of one model over others, future predictions of extreme rainfall must acknowledge this broader model context and caution used when interpreting highly localised and model-specific results.

Engineering Assessment of Coastal Storms

As discussed in the introduction to this report, coastal flooding has both potential marine and inland contributions and, to date, defining the joint probabilities of the individual contributions has been a longstanding coastal engineering problem.

During this investigation, the representation of the atmospheric forcing associated with storm systems with durations greater than 1 day in GCMs has been quantified.

Although the models exhibit different levels of skill in their ability to represent mean sea level pressure, wind and precipitation, clear extreme distributions of the relevant state variable for larger-scale coastal flooding can be defined. These extreme distributions are associated with the passage of large-scale storm events.

When combined with appropriate downscaling, the ability to relate a suite of state variables to individual storm events yields a new method of estimating the joint probability of the individual contributions to coastal flooding.

Unfortunately, these models do not yield estimates of shorter duration events. However, extreme short duration events are produced within a broader climatic context. Joint correlations of the atmospheric forcing variables amongst themselves and their climatic context should be able to be used to develop appropriate stochastic characterisations of short duration events.

6. Acknowledgements

Funding for this project was provided by the US Army Engineer Research and Development Centre International Research Office (ERDC-IRO) under Federal Grant 1413-EN-01 and by the Australian National Climate Change Adaptation Research Facility: Settlements and Infrastructure (ACCARNSI) within the National Climate Change Adaptation Research Facility (NCCARF).

Australian observation data is provided by the Australian Bureau of Meteorology. Observation data from the United States is provided by the NCDC Climate Services Branch (CSB).

NCEP 20th Century Reanalysis V2 data provided by the NOAA/OAR/ESRL PSD, Boulder, Colorado, USA. ERA-40 Reanalysis Data is provided by the European Centre for Medium-Range Weather Forecasting (ECMWF).

We acknowledge the modelling groups, the Program for Climate Model Diagnosis and Intercomparison (PCMDI) and the WCRP's Working Group on Coupled Modelling (WGCM) for their roles in making available the WCRP CMIP3 multi-model dataset. Support of this dataset is provided by the Office of Science, U.S. Department of Energy.

The authors were assisted by Brett Miller and Xavier Barthelemy at the Water Research Laboratory in the extraction of GCM data from model databases. Their assistance is gratefully acknowledged.

References

- AIR Corporation, 2008. The coastline at risk: 2008 update to the estimated insured value of U.S. coastal properties. June
- Bengtsson, L. M., K. I. Hodges, M. Esch, N. Keenlyside, L. Kornbleuh, J.-J. Luo, and T. Yamagata (2007): How may tropical cyclones change in a warmer climate? *Tellus*, 59A, 539-561
- Beven, K. J. (2001). *Rainfall-Runoff Modelling*. John Wiley & Sons Ltd. 372 p.
- Caron, L.-P., and C.G. Jones, (2008). Analysing present, past and future tropical cyclone activity as inferred from an ensemble of Coupled Global Climate Models, *Tellus, Series A: Dynamic Meteorology and Oceanography*, 60 A(1), 80-96.
- Coles, S. (2004). An introduction to statistical modelling of extreme values. *Springer series in statistics*.
- Compo, G.P., J.S. Whitaker, P.D. Sardeshmukh, N. Matsui, R.J. Allan, X. Yin, B.E. Gleason, R.S. Vose, G. Rutledge, P. Bessemoulin, S. Brönnimann, M. Brunet, R.I. Crouthamel, A.N. Grant, P.Y. Groisman, P.D. Jones, M. Kruk, A.C. Kruger, G.J. Marshall, M. Maugeri, H.Y. Mok, Ø. Nordli, T.F. Ross, R.M. Trigo, X.L. Wang, S.D. Woodruff, and S.J. Worley (2011): The Twentieth Century Reanalysis Project. *Quarterly J. Roy. Meteorol. Soc.*, 137, 1-28. DOI: 10.1002/qj.776 Free and Open Access.
- Emanuel, K., R. Sundararajan, and J. Williams (2008): Hurricanes and global warming - results from downscaling IPCC AR4 simulations. *Bull. Amer. Met. Soc.*, 89, 347-367
- Hosking, J.R.M, Wallis, J.R. and Wood E.F. (1985). Estimation of the generalized extreme-value distribution by the method of probability-weighted moments. *Technometrics* (27), pp. 251-261
- IPCC, (2007). *Climate Change 2007 - The Physical Science Basis. Contribution of Working Group I to the Fourth Assessment Report of the Intergovernmental Panel on Climate Change*, (ISBN 978 0521 88009-1 Hardback; 978 0521 70596-7 Paperback), [Solomon, S., D. Qin, M. Manning, Z. Chen, M. Marquis, K.B. Averyt, M. Tignor and H.L. Miller (eds.)]. Cambridge University Press, Cambridge, United Kingdom and New York, NY, USA, 996 pp.
- Kallberg, P. Simmons, A. Uppala, S. and Fuentes, M. (2007). The ERA-40 Archive. *ERA-40 Project Report Series*. ECMWF.
- Kharin, V.V., Zwiers, F.W., Zhang, X and Hegerl, G.C. (2007). Changes in Temperature and Precipitation Extremes in the IPCC Ensemble of Global Coupled Model Simulations. *J. Climate*, 20, 1419 – 1444.
- Kotz, S. and Madarajah, S. 2000. *Extreme value distributions: theory and applications*. Imperial College Press, London. 185p.
- Lambert, S.J., and J.C. Fyfe, (2006). Changes in winter cyclone frequencies and strengths simulated in enhanced greenhouse warming experiments: Results from the models participating in the IPCC diagnostic exercise, *Climate Dynamics*, 26(7-8), 713-728.

Mearns, L.O., I. Brogardi, et al. (1999). Comparison of climate change scenarios generated from regional climate model experiments and statistical downscaling, *Journal of Geographical Research*, 104(D6), 6603-6621.

Meehl, G. A., C. Covey, T. Delworth, M. Latif, B. McAvaney, J. F. B. Mitchell, R. J. Stouffer, and K. E. Taylor, (2007): The WCRP CMIP3 multi-model dataset: A new era in climate change research, *Bulletin of the American Meteorological Society*, **88**, 1383-1394.

NCCOE, (1993), *At what price data?* Institution of Engineers Australia National Committee on Coastal and Ocean Engineering. ISBN 0858255960

NSW PWD, (1985). *Elevated Ocean Levels. Storms affecting the NSW Coast 1880-1990*. Public Works Department Coastal Branch Report No. 85041 prepared by Blain Bremner and Williams Pty. Ltd. and Weatherex Meteorological Services Pty. Ltd.

Perkins, S. E., and A. J. Pitman, (2009). Do weak AR4 models bias projections of future climate changes over Australia?, *Climatic Change*, 93(3-4), 527-558.

Perkins, S.E., Pitman, A.J., Holbrook, N.J. and McAneney, J. (2007). Evaluation of the AR4 Climate Models' Simulated Daily Maximum Temperature, Minimum Temperature and Precipitation over Australia using Probability Density Functions. *J. Climate*, 20, 4356 – 4756.

Sinclair, M. R., and I. G. Watterson, (1999). Objective assessment of extratropical weather systems in simulated climates. *J. Climate*, 12, 3467-3485

Sun, Y.S., Solomon, S., Dai, A and Portmann, R.W. (2007). How often will it rain? *J. Climate*, 20, 4801-4818.

Uppala, S.M., Kållberg, P.W., Simmons, A.J., et al. (2005). The ERA-40 re-analysis. *Quart. J. R. Meteorol. Soc.*, 131, 2961-3012. doi:10.1256/qj.04.176

Wernli, H. and Schwierz, C. (2006). Surface Cyclones in the ERA-40 Dataset (1958–2001). Part I: Novel Identification, Method and Global Climatology. *J. Atmos. Sci.*, 63, 2486-2507

Wilby, R.L., and T.M.L. Wigley, (1997). Downscaling general circulation model output: a review of methods and limitations, *Progress in Physical Geography*, 21(4), 530-548.

Model Information of Potential Use to the IPCC Lead Authors and the AR4.

CSIRO-Mk3.0

31 January 2005

I. Model identity:

A. Institution, sponsoring agency, country

CSIRO, Australia

B. Model name (and names of component atmospheric, ocean, sea ice, etc. models)

CSIRO Mark 3.0 (abbrev. CSIRO-Mk3.0)

C. Vintage (i.e., year that model version was first used in a published application)

2001

D. General published references and web pages

Gordon, H. B., Rotstayn, L. D., McGregor, J. L., Dix, M. R., Kowalczyk, E. A., O'Farrell, S. P., Waterman, L. J., Hirst, A. C., Wilson, S. G., Collier, M. A., Watterson, I. G., and Elliott, T. I. (2002): The CSIRO Mk3 Climate System Model [Electronic publication]. Aspendale: CSIRO Atmospheric Research. (CSIRO Atmospheric Research technical paper; no. 60). 130 pp.
(http://www.dar.csiro.au/publications/gordon_2002a.pdf)

Cai, W., Collier, M.A., Durack P.D., Gordon H.B., Hirst A.C., O'Farrell S.P. and Whetton P.H., 2003: The response of climate variability and mean state to climate change: preliminary results from the CSIRO Mark 3 coupled model. *CLIVAR Exchanges*, **28**, 8-11.

Cai, W., M. A. Collier, H. B. Gordon, and L. J. Waterman, 2003: Strong ENSO variability and a super-ENSO pair in the CSIRO coupled climate model. *Monthly Weather Review*, **131**, 1189-1210.

Cai, W., M. J. McPhaden, M. A. Collier, 2004: Multidecadal fluctuations in the relationship between equatorial Pacific heat content anomalies and ENSO amplitude. *Geophys. Res. Let.*, **31**, L01201, doi:10.1029/2003GL018714

Cai, W., H. Hendon, and G. Meyers, 2005: An Indian Ocean Dipole-like variability in the CSIRO Mark 3 climate model. *J. Climate*, in press.

Cai, W., G. Meyers, and G. Shi, 2005: Transmission of ENSO signals to the Indian Ocean, *Geophys. Res. Let.*, in press.

Cai, W., G. Shi, Y. Li, 2005: Multidecadal fluctuations of winter rainfall over southwest Western Australia simulated in the CSIRO Mark 3 coupled model, *Geophys. Res. Let.*, submitted.

Watterson, I.G., and M. R. Dix, 2005: Effective sensitivity and heat capacity in the response of climate models to greenhouse gas and aerosol forcings. *Q. J. Roy. Met. Soc.*, **131**, 259-280.

Watterson, i.G., 2005: The intensity of precipitation during extra-tropical cyclones in global warming simulations: a link to cyclone intensities? *Tellus A*. Accepted subject to minor revision.

- E. References that document changes over the last ~5 years (i.e., since the IPCC TAR) in the coupled model or its components. We are specifically looking for references that document changes in some aspect(s) of model performance.
[See technical report – Gordon et al, 2002.](#)
- F. IPCC model version's global climate sensitivity (KW^{-1}m^2) to increase in CO_2 and how it was determined (slab ocean expt., transient expt--Gregory method, $\pm 2\text{K}$ Cess expt., etc.)
[Slab ocean doubled \$\text{CO}_2\$ experiment has warming 3.07 K \(average over last 30 years\). In the CSIRO Mk3 model the doubled \$\text{CO}_2\$ radiative forcing was \$3.5 \text{ W m}^{-2}\$, so sensitivity = \$0.88 \text{ KW}^{-1}\text{m}^2\$.](#)
- G. Contacts (name and email addresses), as appropriate, for:
1. coupled model – Hal.Gordon@csiro.au
 2. atmosphere – Hal.Gordon@csiro.au
 3. ocean – Tony.Hirst@csiro.au
 4. sea ice – Siobhan.O'Farrell@csiro.au
 5. land surface – Eva.Kowalczyk@csiro.au
 6. vegetation – Eva.Kowalczyk@csiro.au

II. Besides atmosphere, ocean, sea ice, and prescription of land/vegetated surface, what can be included (interactively) and was it active in the model version that produced output stored in the PCMDI database?

- A. atmospheric chemistry? - [No](#)
B. interactive biogeochemistry? - [No](#)
C. what aerosols and are indirect effects modeled?
[Direct effect of aerosols only using monthly mean sulfate \(Penner et al, 1994\).](#)
D. dynamic vegetation? - [No](#)
E. ice-sheets? - [No](#)

III. List the community based projects (e.g., AMIP, C4MIP, PMIP, PILPS, etc.) that your modeling group has participated in and indicate if your model results from each project should carry over to the current (IPCC) version of your model in the PCMDI database.

[Participation carrying over to the IPCC version \(CSIRO-Mk3.0\):
PILPS 1, 2a,2b,2d, C1](#)

Model Information of Potential Use to the IPCC Lead Authors and the AR4.

CSIRO-Mk3.5

13 July 2007

I. Model identity:

A. Institution, sponsoring agency, country

CSIRO, Australia

B. Model name (and names of component atmospheric, ocean, sea ice, etc. models)

CSIRO Mark 3.5 (abbrev. CSIRO-Mk3.5)

C. Vintage (i.e., year that model version was first used in a published application)

2006

D. General published references and web pages

Gordon, H. B., Rotstayn, L. D., McGregor, J. L., Dix, M. R., Kowalczyk, E. A., O'Farrell, S. P., Waterman, L. J., Hirst, A. C., Wilson, S. G., Collier, M. A., Watterson, I. G., and Elliott, T. I. (2002): The CSIRO Mk3 Climate System Model [Electronic publication]. Aspendale: CSIRO Atmospheric Research. (CSIRO Atmospheric Research technical paper; no. 60). 130 pp.
(http://www.dar.csiro.au/publications/gordon_2002a.pdf)

Cai, W., Collier, M.A., Durack P.D., Gordon H.B., Hirst A.C., O'Farrell S.P. and Whetton P.H., 2003: The response of climate variability and mean state to climate change: preliminary results from the CSIRO Mark 3 coupled model. *CLIVAR Exchanges*, **28**, 8-11.

Cai, W., M. A. Collier, H. B. Gordon, and L. J. Waterman, 2003: Strong ENSO variability and a super-ENSO pair in the CSIRO coupled climate model. *Monthly Weather Review*, **131**, 1189-1210.

Cai, W., M. J. McPhaden, M. A. Collier, 2004: Multidecadal fluctuations in the relationship between equatorial Pacific heat content anomalies and ENSO amplitude. *Geophys. Res. Let.*, **31**, L01201, doi:10.1029/2003GL018714

Cai, W., H. Hendon, and G. Meyers, 2005: An Indian Ocean Dipole-like variability in the CSIRO Mark 3 climate model. *J. Climate*, in press.

Cai, W., G. Meyers, and G. Shi, 2005: Transmission of ENSO signals to the Indian Ocean, *Geophys. Res. Let.*, in press.

Cai, W., G. Shi, Y. Li, 2005: Multidecadal fluctuations of winter rainfall over southwest Western Australia simulated in the CSIRO Mark 3 coupled model, *Geophys. Res. Lett.*, submitted.

Watterson, I.G., and M. R. Dix, 2005: Effective sensitivity and heat capacity in the response of climate models to greenhouse gas and aerosol forcings. *Q. J. Roy. Met. Soc.*, **131**, 259-280.

Watterson, I.G., 2005: The intensity of precipitation during extra-tropical cyclones in global warming simulations: a link to cyclone intensities? *Tellus A*. Accepted subject to minor revision.

- E. References that document changes over the last ~5 years (i.e., since the IPCC TAR) in the coupled model or its components. We are specifically looking for references that document changes in some aspect(s) of model performance.
[See technical report – Gordon et al, 2002.](#)
- F. IPCC model version's global climate sensitivity (KW^{-1}m^2) to increase in CO_2 and how it was determined (slab ocean expt., transient expt--Gregory method, $\pm 2\text{K}$ Cess expt., etc.)
[Not available yet.](#)
- G. Contacts (name and email addresses), as appropriate, for:
1. coupled model – Hal.Gordon@csiro.au
 2. atmosphere – Hal.Gordon@csiro.au
 3. ocean – Tony.Hirst@csiro.au
 4. sea ice – Siobhan.O'Farrell@csiro.au
 5. land surface – Eva.Kowalczyk@csiro.au
 6. vegetation – Eva.Kowalczyk@csiro.au

II. Besides atmosphere, ocean, sea ice, and prescription of land/vegetated surface, what can be included (interactively) and was it active in the model version that produced output stored in the PCMDI database?

- A. atmospheric chemistry? - [No](#)
- B. interactive biogeochemistry? - [No](#)
- C. what aerosols and are indirect effects modeled?
[Direct effect of aerosols only using monthly mean sulfate \(Penner et al, 1994\).](#)
- D. dynamic vegetation? - [No](#)
- E. ice-sheets? - [No](#)

III. List the community based projects (e.g., AMIP, C4MIP, PMIP, PILPS, etc.) that your modeling group has participated in and indicate if your model results from each project should carry over to the current (IPCC) version of your model in the PCMDI database.

[Participation carrying over to the IPCC version \(CSIRO-Mk3.0\):](#)
[PILPS 1, 2a,2b,2d, C1](#)

Model Information of Potential Use to the IPCC Lead Authors and the AR4.

GFDL-CM2.0 and GFDL-CM2.1

2 May 2005

I. Model identity:

A. Institution, sponsoring agency, country

Geophysical Fluid Dynamics Laboratory

NOAA

USA

B. Model name (and names of component atmospheric, ocean, sea ice, etc. models)

CM2.0 - AOGCM

AM2P13 – atmosphere

OM3P4 - ocean

LM2 - land

SIS – sea ice

C. Vintage (i.e., year that model version was first used in a published application)

2005

D. General published references and web pages

Delworth, T.L. and co-authors, 2004: GFDL's CM2 global coupled climate models -- Part 1: Formulation and simulation characteristics, submitted to J. Climate.

Gnanadesikan, A. and co-authors, 2004: GFDL's CM2 global coupled climate models -- Part 2: The baseline ocean simulation, submitted to J. Climate.

<http://data1.gfdl.noaa.gov/nomads/forms/deccen/>

E. References that document changes over the last ~5 years (i.e., since the IPCC TAR) in the coupled model or its components. We are specifically looking for references that document changes in some aspect(s) of model performance.

CM2.0 was not developed using GFDL's TAR model (MCM) as a starting point. It is a completely new formulation.

References:

Delworth, T.L. and co-authors, 2004: GFDL's CM2 global coupled climate models -- Part 1: Formulation and simulation characteristics, submitted to J. Climate.

Gnanadesikan, A. and co-authors, 2004: GFDL's CM2 global coupled climate models -- Part 2: The baseline ocean simulation, submitted to J. Climate.

Wittenberg, A.T., A. Rosati, N-C Lau, and J. Ploshay, 2004: GFDL's CM2 global coupled climate models, Part 3: Tropical Pacific Climate and ENSO, submitted

to J. Climate.

GFDL GAMDT, 2004: The new GFDL global atmosphere and land model AM2-LM2: Evaluation with prescribed SST simulations, J. Climate, 17, 4641-4673.

Milly, P.C.D, and A.B. Shmakin, 2002: Global modeling of land water and energy balances, Part I: The land dynamics (LaD) model, Journal of Hydrometeorology, 3, 283-299.

Griffies, S.M., A. Gnanadesikan, K.W. Dixon, J.P. Dunne, R. Gerdes, M.J. Harrison, I.M. Held, A. Rosati, J. Russell, B.L. Samuels, M.J.

Spelman, M. Winton, and R. Zhang, 2005: Formulation of an ocean model for global climate simulations, in preparation for Ocean Modelling.

F. IPCC model version's global climate sensitivity (KW-1m2) to increase in CO2 and how it was determined (slab ocean expt., transient expt--Gregory method, $\pm 2K$ Cess expt., etc.)

2.9K for a CO2 doubling in a slab model

Reference:

Knutson, T.R., A.J. Broccoli, B.J. Soden, R. Gudgel, R. Hemler, S.A. Weber, and M. Winton, 2005: Equilibrium sensitivity of the GFDL AM2 slab-ocean climate model to a doubling of atmospheric CO2, in preparation.

Transient 1%/yr sensitivity at 2xCO2: 1.6 K

Reference:

Stouffer, R.J, A.J Broccoli, T.L. Delworth, K.W. Dixon, R. Gudgel, I. Held, T. Knutson, H-C Lee, M.D. Schwarzkopf, B. Soden, M.J. Spelman, M. Winton, and F. Zeng, 2004: GFDL's CM2 Global Coupled Climate Models -- Part 4:

Idealized climate response, submitted to J. Climate.

G. Contacts (name and email addresses), as appropriate, for:

1. coupled model
2. atmosphere
3. ocean
4. sea ice
5. land surface
6. vegetation
7. other?

All queries: gfdl.climate.model.info@noaa.gov

II. Besides atmosphere, ocean, sea ice, and prescription of land/vegetated surface, what can be included (interactively) and was it active in the model version that produced output stored in the PCMDI database?

A. atmospheric chemistry?

Not yet

B. interactive biogeochemistry?

Model Information of Potential Use to the IPCC Lead Authors and the AR4.

GISS-EH and GISS-ER

7 April 2006

I. Model identity:

A. Institution, sponsoring agency, country

Goddard Institute for Space Studies (GISS), NASA, USA

B. Model name (and names of component atmospheric, ocean, sea ice, etc.. models)

Two versions were submitted to the IPCC archive: GISS ModelE-H and GISS ModelE-R (which differ only in ocean component)

Atmospheric and sea ice model:

GISS ModelE (Schmidt et al, 2005, J. Clim, accepted)

<http://www.giss.nasa.gov/tools/modelE>

Ocean models:

GISS-ModelE-R - Russell et al (1995; 2000)

GISS-ModelE-H - HYCOM (Bleck 2000; 2002)

C. Vintage (i.e., year that model version was first used in a published application)

2004

D. General published references and web pages

Main web page: <http://www.giss.nasa.gov/tools/modelE>

AGCM description and evaluation:

Schmidt, G. A. , Reto Ruedy, James E. Hansen, Igor Aleinov, Nadine Bell, Mike Bauer, Susanne Bauer, Brian Cairns, Vittorio Canuto, Ye Cheng, Anthony DelGenio, Greg Faluvegi, Andrew D. Friend, Tim M. Hall, Yongyun~Hu, Max Kelley, Nancy Y. Kiang, Dorothy Koch, Andy A. Lacis, Jean~Lerner, Ken~K.~Lo, Ron L. Miller, Larissa Nazarenko, Valdar Oinas, Jan~Perlwitz, Judith Perlwitz, David Rind, Anastasia Romanou, Gary L. Russell, Makiko~Sato, Drew T. Shindell, Peter H. Stone, Shan Sun, Nick Tausnev, Duane Thresher, Mao-Sung Yao 2005. Present day atmospheric simulations using GISS ModelE: Comparison to in-situ, satellite and reanalysis data. J. Climate, 19, 153-192.

<http://www.giss.nasa.gov/tools/modelE/>

Hansen et al., 2006. The Efficacy of Climate Forcings. J. Geophys. Res. 100, D18104.

<http://www.giss.nasa.gov/data/simodel/efficacy/>

Sun, S., R. Bleck 2006. Multi-Century Simulations with the Coupled GISS-HYCOM Climate Model: Control Experiments. Climate Dynamics 26, 407-428.

The Impact of the ocean component on coupled model simulations in GISS ModelE. Romanou, A., G. A. Schmidt, L. Nazarenko, R. Miller, Y. Hu, S. Sun and N. Tausnev. J. Climate. in preparation.

E. References that document changes over the last ~5 years (i.e., since the IPCC TAR) in the coupled model or its components. We are specifically looking for references that document changes in some aspect(s) of model performance.

As above, but also:

Del Genio, A.D., W. Kovari, M.-S. Yao and J. Jonas, 2005: Cumulus microphysics and climate sensitivity. J. Clim., in press.

Friend, A. D. and N. Y. Kiang (2005). "Land Surface Model Development for the GISS GCM: Effects of Improved Canopy Physiology on Simulated Climate." J. Clim. (in press)

Schmidt, G. A., C. M. Bitz, U. Mikolajewicz and L.-B. Tremblay. 2004. Ice-ocean boundary conditions for coupled models. Ocean Modelling, 7, 59--74

F. IPCC model version's global climate sensitivity (KW-1m2) to increase in CO2 and how it was determined (slab ocean expt., transient expt.--Gregory method, $\pm 2K$ Cess expt., etc.)

Slab ocean sensitivity to 2xCO2: 2.7 deg C

G. Contacts (name and email addresses), as appropriate, for:

1. coupled model
2. atmosphere
3. ocean
4. sea ice
5. land surface
6. vegetation
7. other?

For 1,2,4,7: Gavin Schmidt (gschmidt@giss.nasa.gov)

For 3 (ModelE-R): Gavin Schmidt (gschmidt@giss.nasa.gov) and Gary Russell (cmglr@giss.nasa.gov)

For 4 (ModelE-H): Shan Sun (ssun@giss.nasa.gov)

For 5,6: Igor Aleinov (ialeinov@giss.nasa.gov)

For data, forcing info, etc.: Reto Ruedy (rruedy@giss.nasa.gov)

II. Besides atmosphere, ocean, sea ice, and prescription of land/vegetated surface, what can be included (interactively) and was it active in the model version that produced output stored in the PCMDI database?

Model Information of Potential Use to the IPCC Lead Authors and the AR4.

CCSM3

31 January 2005

I. Model identity:

A. Institution, sponsoring agency, country

National Center for Atmospheric Research (NCAR),
NSF (a primary sponsor), DOE (a primary sponsor), NASA, and NOAA
USA

B. Model name (and names of component atmospheric, ocean, sea ice, etc. models)

Coupled model - Community Climate System Model, version 3.0 (CCSM3)
Atmosphere - Community Atmosphere Model, version 3.0 (CAM3)
Ocean - Parallel Ocean Program, version 1.4.3 (POP 1.4.3)
Sea ice - Community Sea Ice Model, version 5.0 (CSIM5)
Land - Community Land Model, version 3.0 (CLM3)

C. Vintage (i.e., year that model version was first used in a published application)

First control runs and IPCC runs were run and submitted for publication in 2004. First publication containing CCSM3 results will appear in 2005.

D. General published references and web pages

Main website - <http://www.ccsm.ucar.edu>

Publications submitted to a special issue of the Journal of Climate describing CCSM3 are available from http://www.ccsm.ucar.edu/publications/jclim04/Papers_JCL04.html

E. References that document changes over the last ~5 years (i.e., since the IPCC TAR) in the coupled model or its components. We are specifically looking for references that document changes in some aspect(s) of model performance.

There are a series of NCAR technical reports available from <http://www.ucar.edu/communications/technotes/technotes401-.shtml>

TN-455+STR The Sea Ice Simulation of the Community System Model, Version Two, B.P. Briegleb, E.C. Hunke, C.M. Bitz, W.H. Lipscomb, M.M. Holland, J.L. Schramm, and R.E. Moritz, CGD. 38 pp. January 2004. NTIS #PB2004-105849.

TN-461+STR Technical Description of the Community Land Model (CLM), Keith

W. Oleson, Yongjiu Dai, Gordon Bonan, Mike Bosilovich, Robert Dickinson, Paul Dirmeyer, Forrest Hoffman, Paul Houser, Samuel Levis, Guo-Yue Niu, Peter Thornton, Mariana Vertenstein, Zong-Liang Yang, Xubin Zeng, CGD. 183 pp. May 2004, NTIS #PB2004-105836.

TN-463+STR Scientific Description of the Sea Ice Component in the Community Climate System Model, Version Three, B.P. Briegleb, C.M. Bitz, E.C. Hunke, W.H. Lipscomb, M.M. Holland, J.L. Schramm, and R.E. Moritz, CGD, 75 pp. June 2004, NTIS #PB2004-106574.

TN-464+STR Description of the NCAR Community Atmosphere Model (CAM 3.0), W.D. Collins, P.J. Rasch, B.A. Boville, J.R. McCaa, D.L. Williamson, J.T. Kiehl, B. Briegleb, C. Bitz, S.-J. Lin, M. Zhang, and Y. Dai, CGD, 214 pp. June 2004.

LANL technical reports:

Smith, R. D. and P. R. Gent, 2002: Reference manual for the Parallel Ocean Program (POP), ocean component of the Community Climate System Model (CCSM2.0 and 3.0). Technical Report LA-UR-02-2484, Los Alamos National Laboratory, available online at <http://www.ccsm.ucar.edu/models/ccsm3.0/pop>.

Refereed papers (partial list):

Bonan, G. B., K. W. Oleson, M. Vertenstein, S. Levis, X. Zeng, Y. Dai, R. E. Dickinson and Z.-L. Yang, 2002: The land surface climatology of the Community Land Model coupled to the NCAR Community Climate Model. *J. Clim.*, 15, 3123-3149.

Bonan, G. B., S. Levis, L. Kergoat, and K. W. Oleson, 2001: Landscapes as patches of plant functional types: An integrating approach for climate and ecosystem models. *Glob. Biogeochem. Cycles*, 16, 5.1-5.23.

Boville, B. A. and C. S. Bretherton, 2003: Heating and dissipation in the NCAR Community Atmosphere Model. *J. Clim.*, 16, 3877-3887.

Collins, W. D., 2001: Parameterization of generalized cloud overlap for radiative calculations in general circulation models. *J. Atmos. Sci.*, 58, 3224-3242.

Collins, W. D., J. K. Hackney, and D. P. Edwards, 2002: A new parameterization for infrared emission and absorption by water vapor in the National Center for Atmospheric Research Community Atmosphere Model. *J. Geophys. Res.*, 107, 8028, doi:10.1029/2000JD000032.

Connolley, W. M., J. M. Gregory, E. C. Hunke, and A. J. McLaren, 2004: On the consistent scaling of terms in the sea ice dynamics equation. *J. Phys. Oceanogr.*, 1776-1780.

Model Information of Potential Use to the IPCC Lead Authors and the AR4.

ECHO-G

27 August 2005

I. Model identity:

- A. Institution, country: Meteorological Institute of the University of Bonn (Germany), Institute of KMA (Korea), and Model and Data Group.
- B. Model name (and names of component atmospheric, ocean, sea ice, etc. models):
ECHO-G = ECHAM4 + HOPE-G
- C. Vintage: 2001
- D. General published references and web pages:
http://mad.zmaw.de/Models/Modelliste1_neu.html
- E. The atmosphere is identical to the first release of ECHAM4 (ECHAM4.0) used for AMIP1 besides a flux aggregation method for cells containing sea ice (Grötzner et al. 1996).
- F. IPCC model version's global climate sensitivity (KW^{-1}m^2) to increase in CO_2 :
slab ocean: $0.8 \text{ K W}^{-1}\text{m}^2$ with $2\times\text{CO}_2$ (3.18 K temperature increase with 4W/m^2 radiative forcing)
transient coupled: 20 yr (69-79) mean temperature difference centered at CO_2 doubling is 1.73 K
- G. Contacts (name and email addresses), as appropriate, for:
 - 1. IPCC experiments: Seung-Ki Min (skmin@uni-bonn.de)
 - 2. coupling: Stephanie Legutke (legutke@dkrz.de)
 - 3. atmosphere: Ulrich Schlese (schlese@dkrz.de)
 - 4. ocean: Stephanie Legutke (legutke@dkrz.de)
 - 5. sea ice: Stephanie Legutke (legutke@dkrz.de)
 - 6. land surface: Ulrich Schlese (schlese@dkrz.de)
 - 7. vegetation: Ulrich Schlese (schlese@dkrz.de)
 - 8. aerosols scheme: Ulrich Schlese (schlese@dkrz.de)

II. Besides atmosphere, ocean, sea ice, and prescription of land/vegetated surface, what can be included (interactively) and was it active in the model version that produced output stored in the PCMDI database?

- A. atmospheric chemistry? No
- B. interactive biogeochemistry? No
- C. what aerosols and are indirect effects modeled? Sulfate aerosol is treated as described in in Feichter et al. (1997) and includes direct and indirect effects.
- D. dynamic vegetation? No
- E. ice-sheets? No. Precipitation on ice sheets is converted to discharge into the ocean.

III. List the community based projects (e.g., AMIP, C4MIP, PMIP, PILPS, etc.) that your modeling group has participated in and indicate if your model results from each project should carry over to the current (IPCC) version of your model in the PCMDI database.

AMIP1 (no)

CMIP2++ (yes)

IV. Component model characteristics (of current IPCC model version):

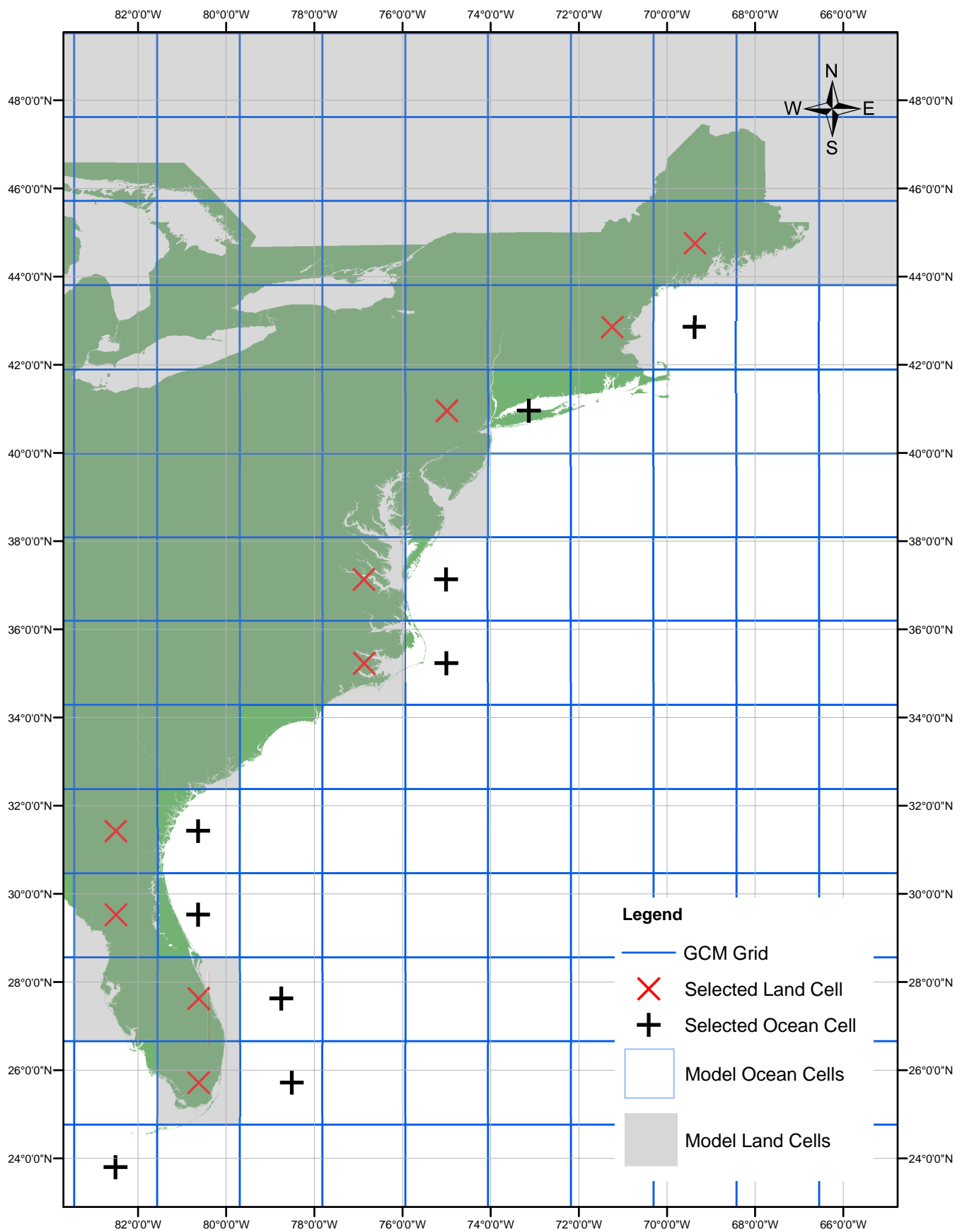
A. Atmosphere (Roeckner et al., 1996)

1. resolution: T30 L19
2. numerical scheme/grid: spectral; hybrid sigma-pressure coordinate (Simmons and Strüfing, 1981); top level at 10 hPa (ca. 30 km); 7 layers above 200 hPa, 5 layers below 850 hPa; semi-implicit leap-frog time stepping; transport of water vapor, cloud water, and (optionally) tracers by a semi-lagrangian scheme (Williamson and Rasch, 1994);
3. list of prognostic variables: vorticity, divergence, temperature, log surface pressure, water vapor, mixing ratio of total cloud water;
4. major parameterizations:
 - a. clouds: Sundquist(1978) type prognostic scheme for stratiform fractional clouds; optical cloud properties and cloud water determined by Mie theory (Rockel et al., 1991; Roeckner, 1995);
 - b. convection: shallow, mid-level, and deep cumulus convection with Tiedke (1989) mass flux scheme and adjustment closure for deep convection as described by Nordeng (1996);
 - c. boundary layer: surface fluxes of momentum, heat, water vapor, and cloud water calculated with Monin-Obukhov theory (Luis, 1979), with eddy diffusivity coefficients depending on roughness length and Richardson No.; above the surface layer, the coefficients depend on wind shear, thermal stability, and mixing length;
 - d. SW radiation: Fouquart and Bonnel(1980), LW radiation: Morcrette et al. (1986) includes methane, nitrous oxide, and 16 CFC species, ozone (14.6 μm), and various types of aerosols (optional) effects; revised water vapor continuum (Giorgetta and Wild, 1995);

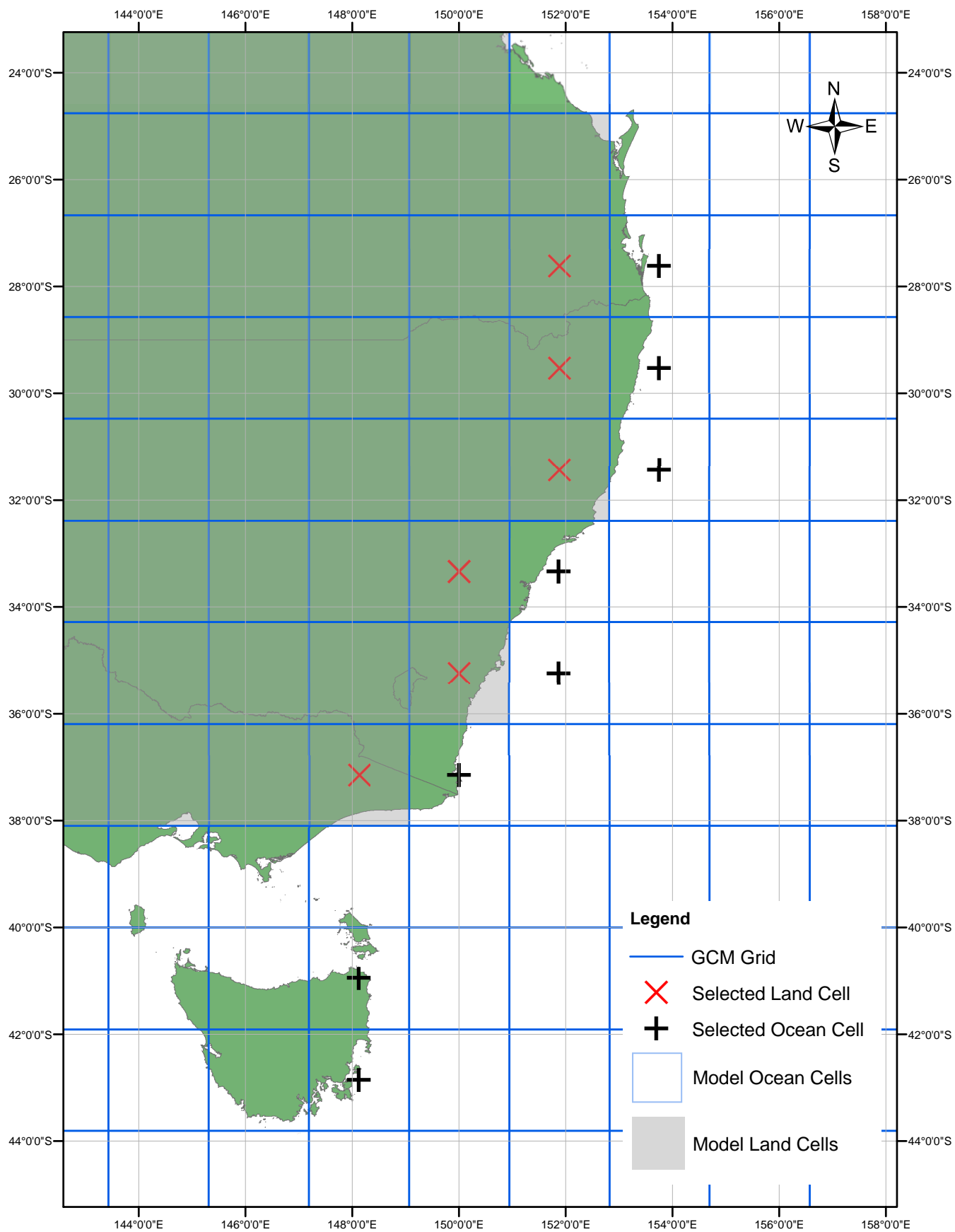
B. Ocean (Legutke and Maier-Reimer, 1999)

1. resolution: even grid rows (E/W) correspond to a T42 Gaussian grid in high and mid latitudes; towards the equator the meridional distances decrease (min = 0.5 deg); 20 levels;
2. numerical scheme/grid: Arakawa E grid; z-level coordinates with partial bottom cells (Adcroft et al., 1997); implicit solver for barotropic mode; free surface; freshwater fluxes;
3. list of prognostic variables and tracers: potential temperature, salinity, zonal and meridional velocity, surface elevation;
4. parameterizations:
 - a. harmonic and shear-dependent eddy diffusion of tracers;
 - b. tracer advection with a predictor-corrector central differencing scheme;

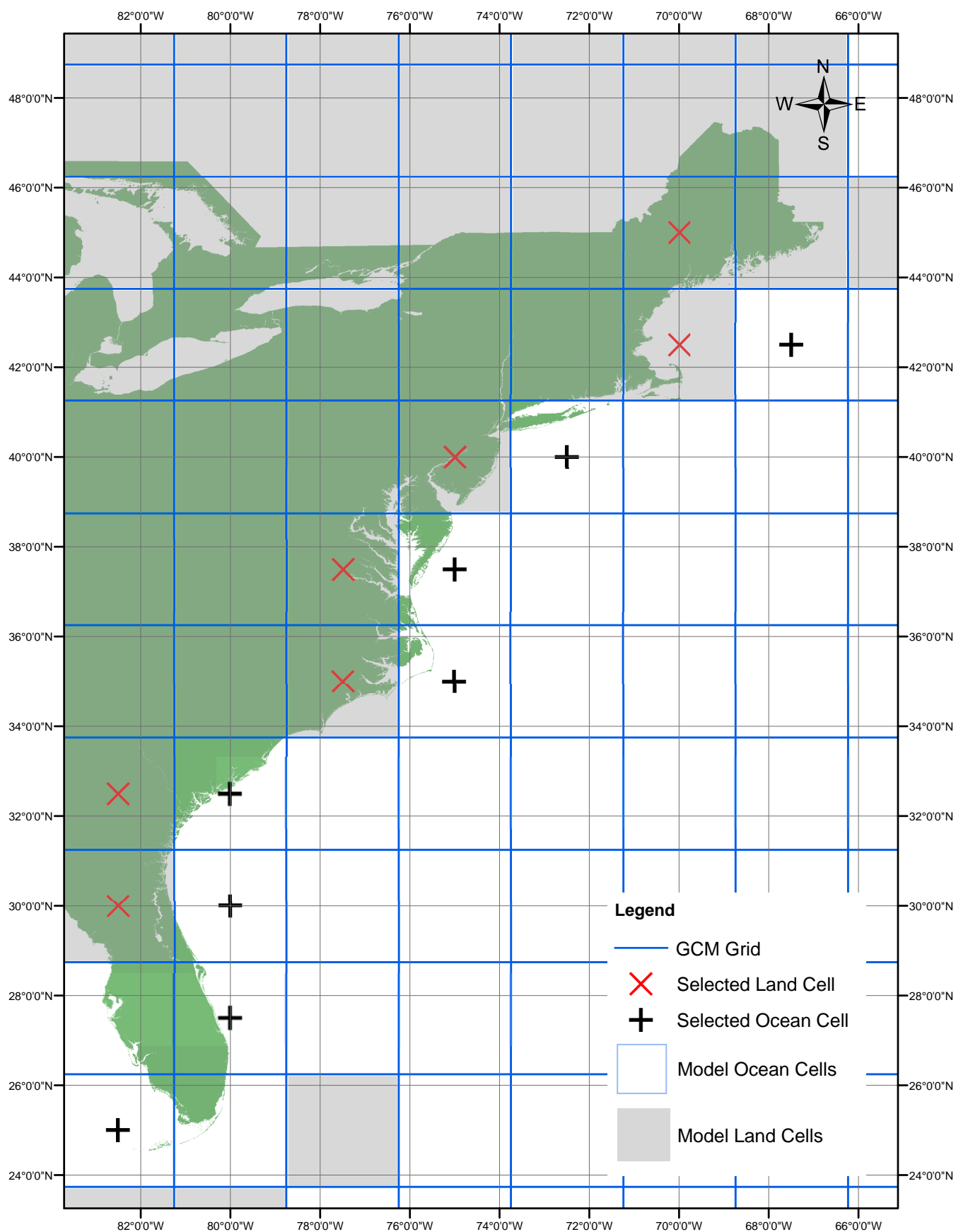
Appendix B GCM Data Extraction Locations



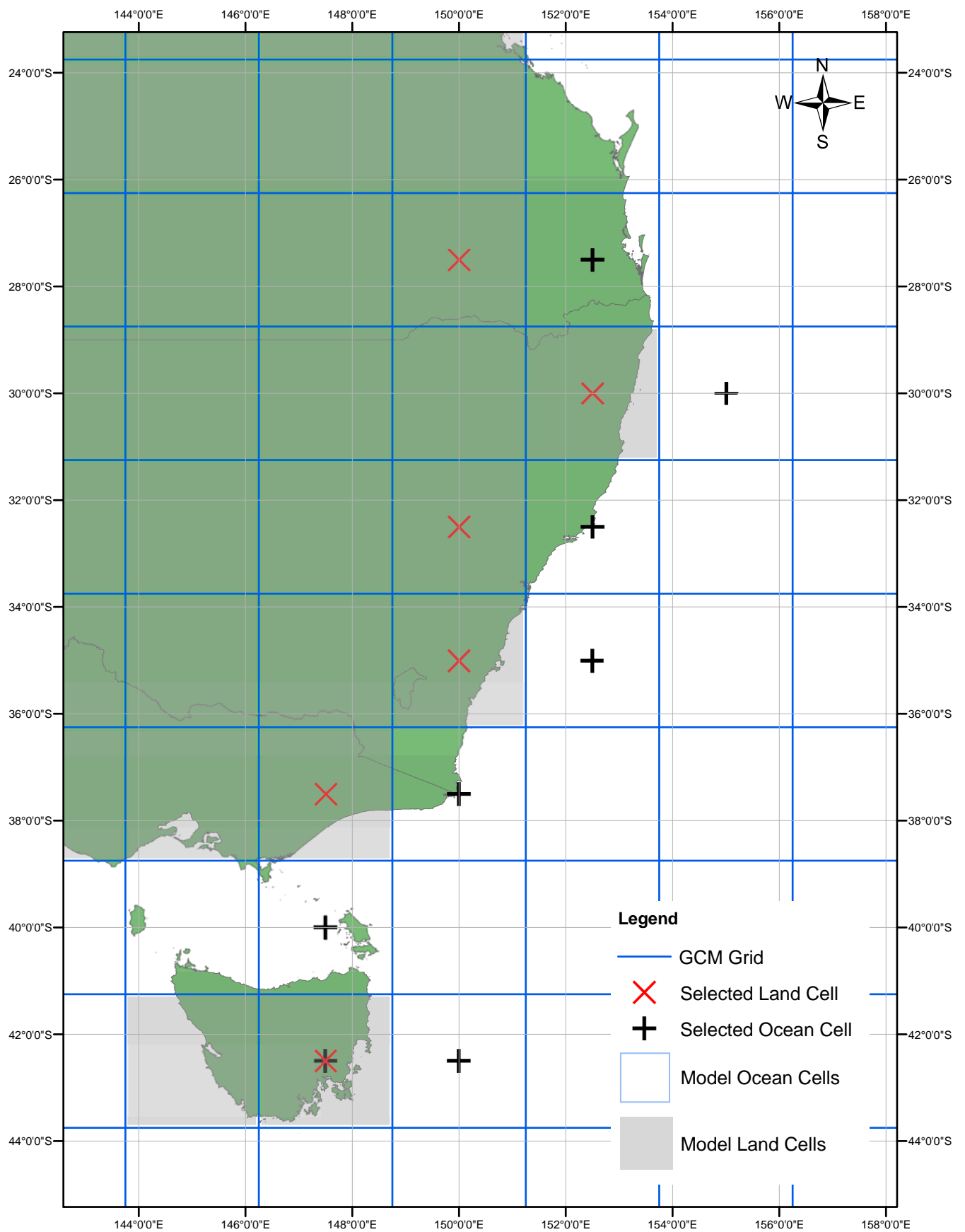
Data extraction locations for NCEP 20CRv2 model



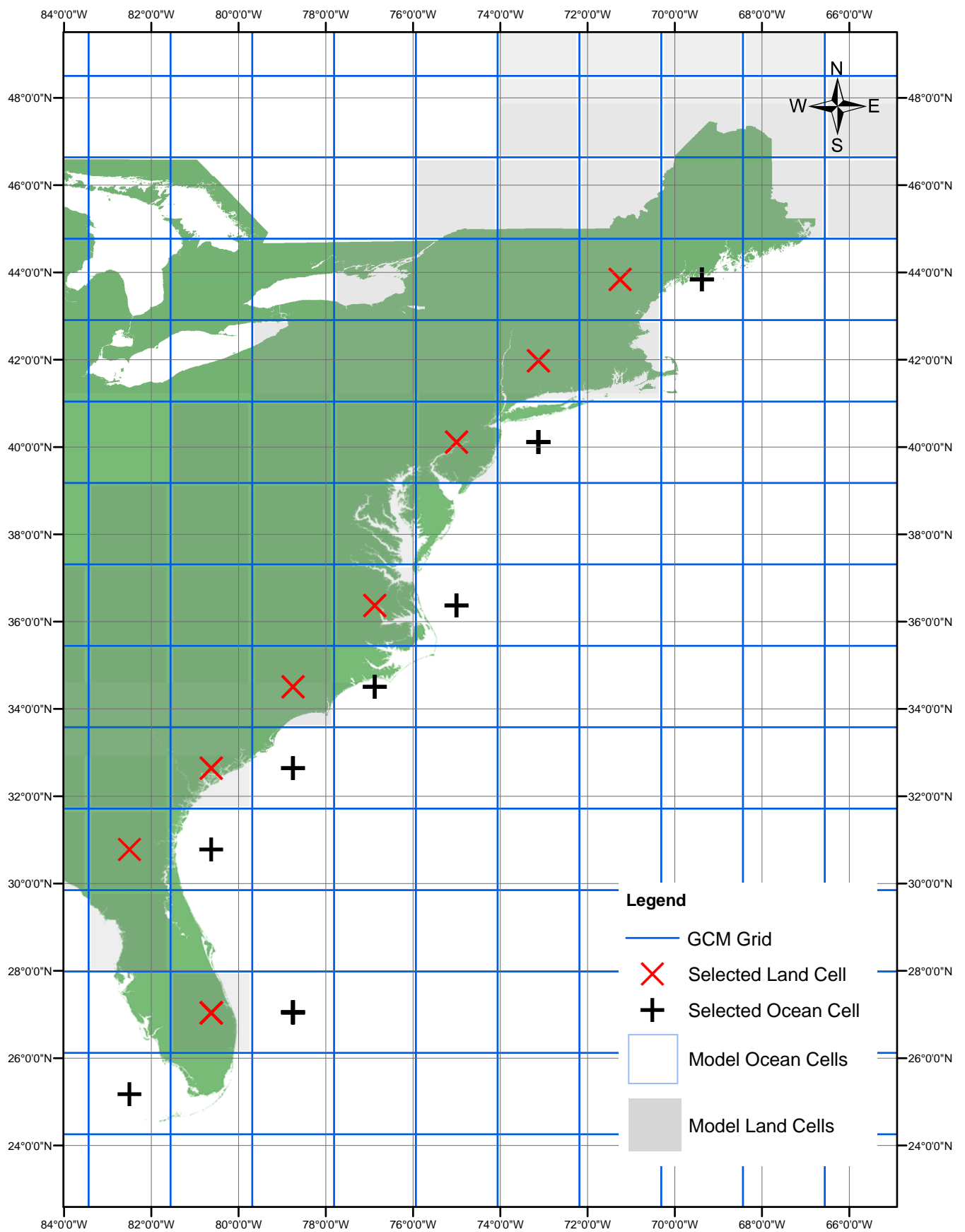
Data extraction locations for NCEP 20CRv2 model



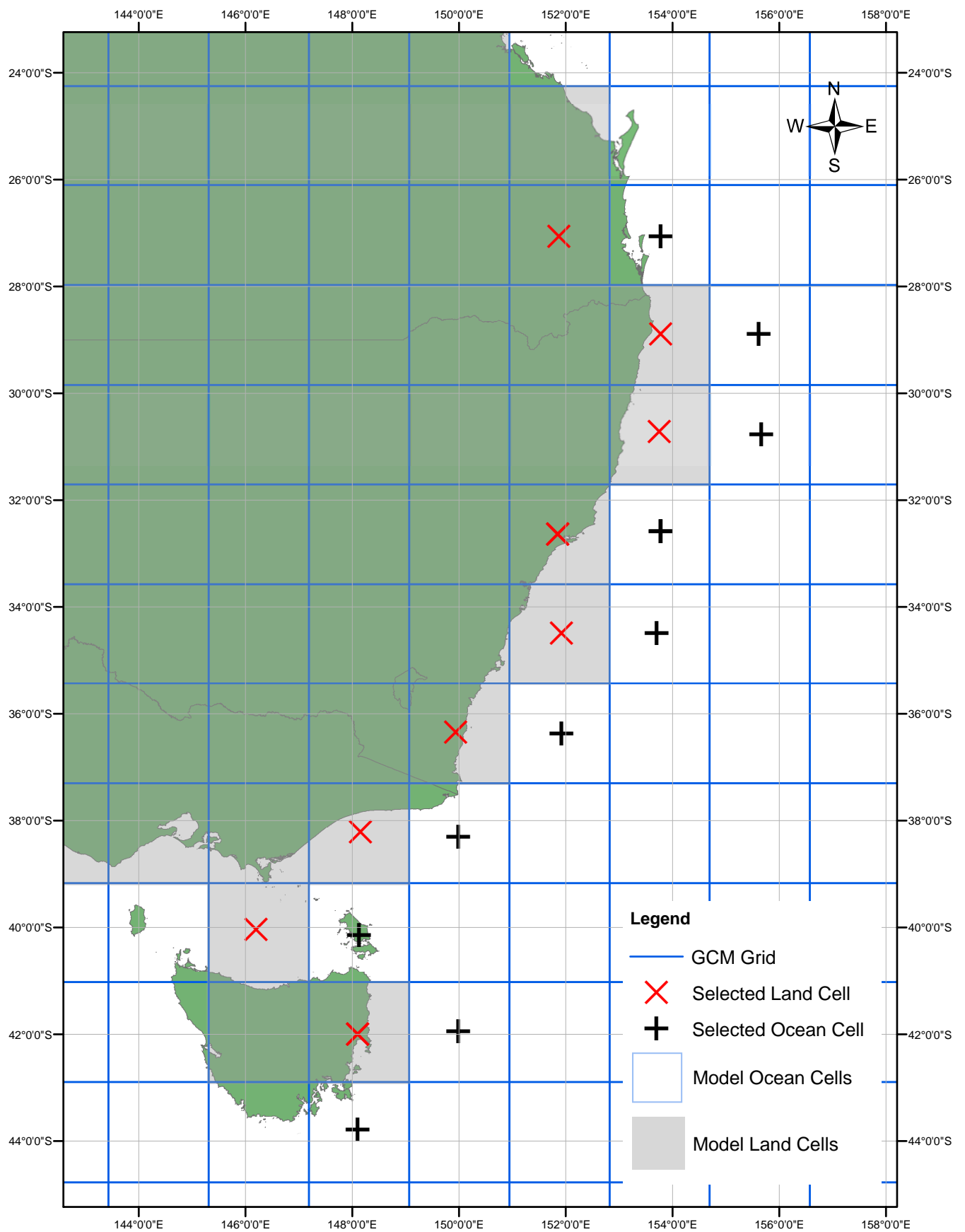
Data extraction locations for ERA40 model



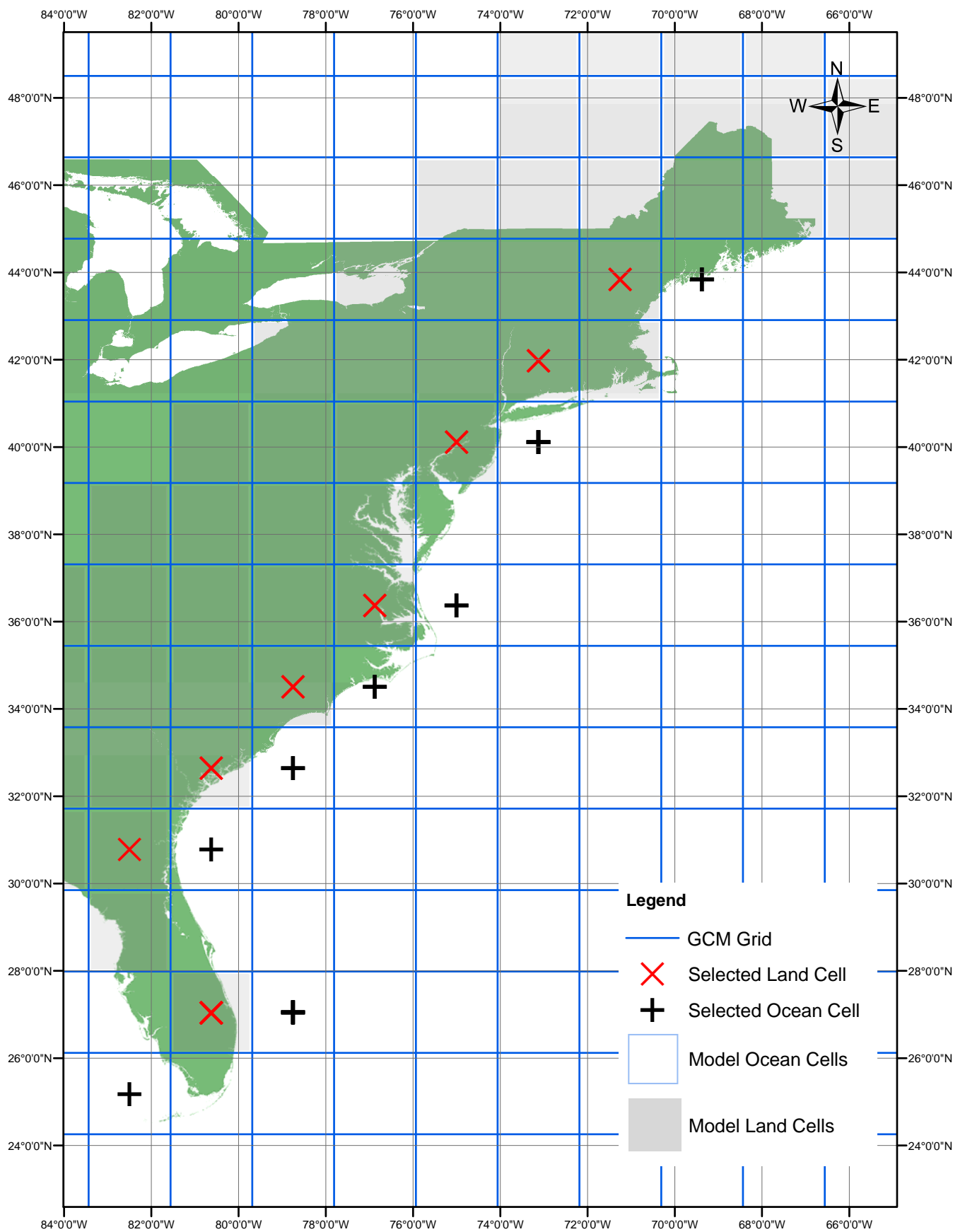
Data extraction locations for ERA40 model



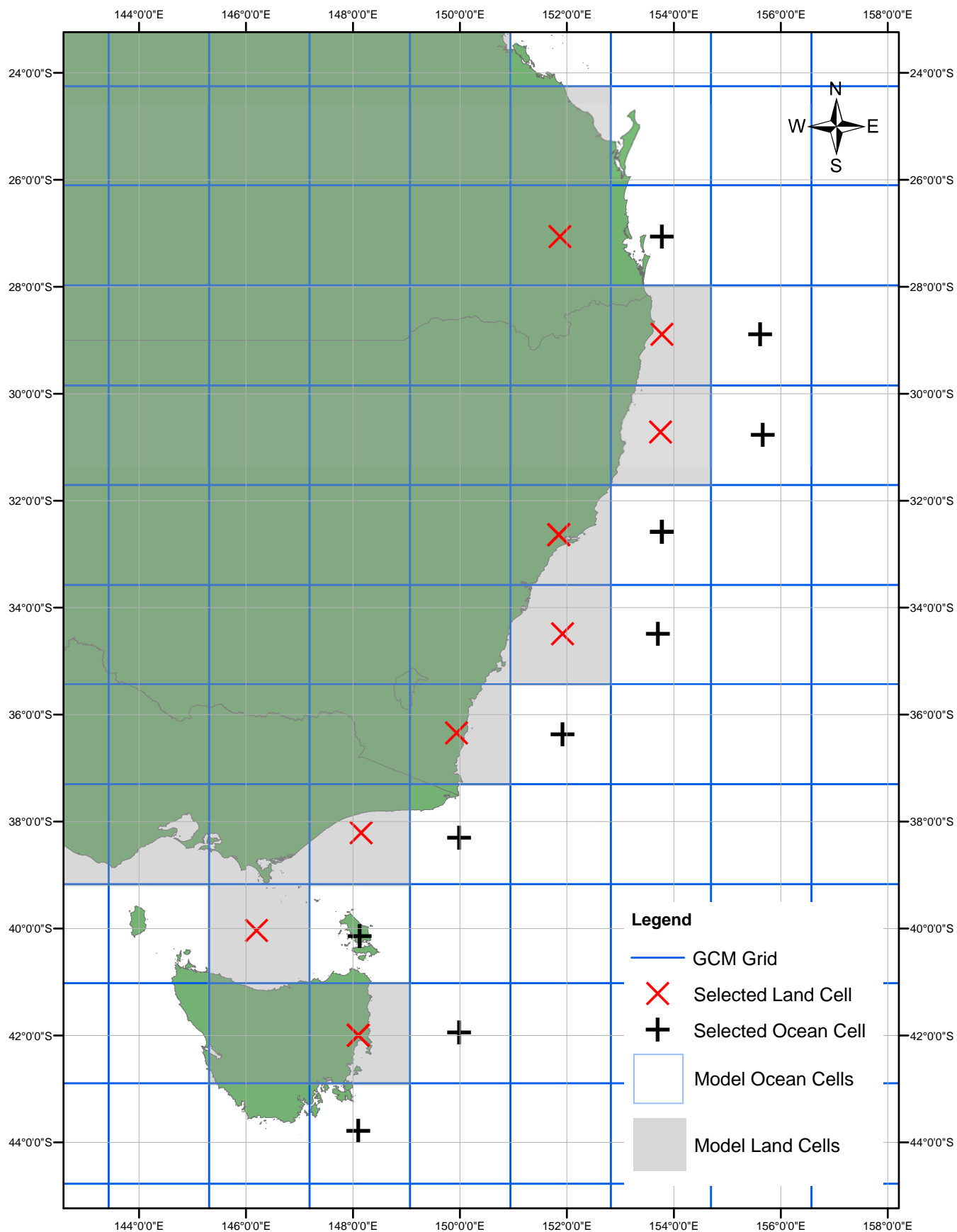
Data extraction locations for CSIRO-Mk3.0 model



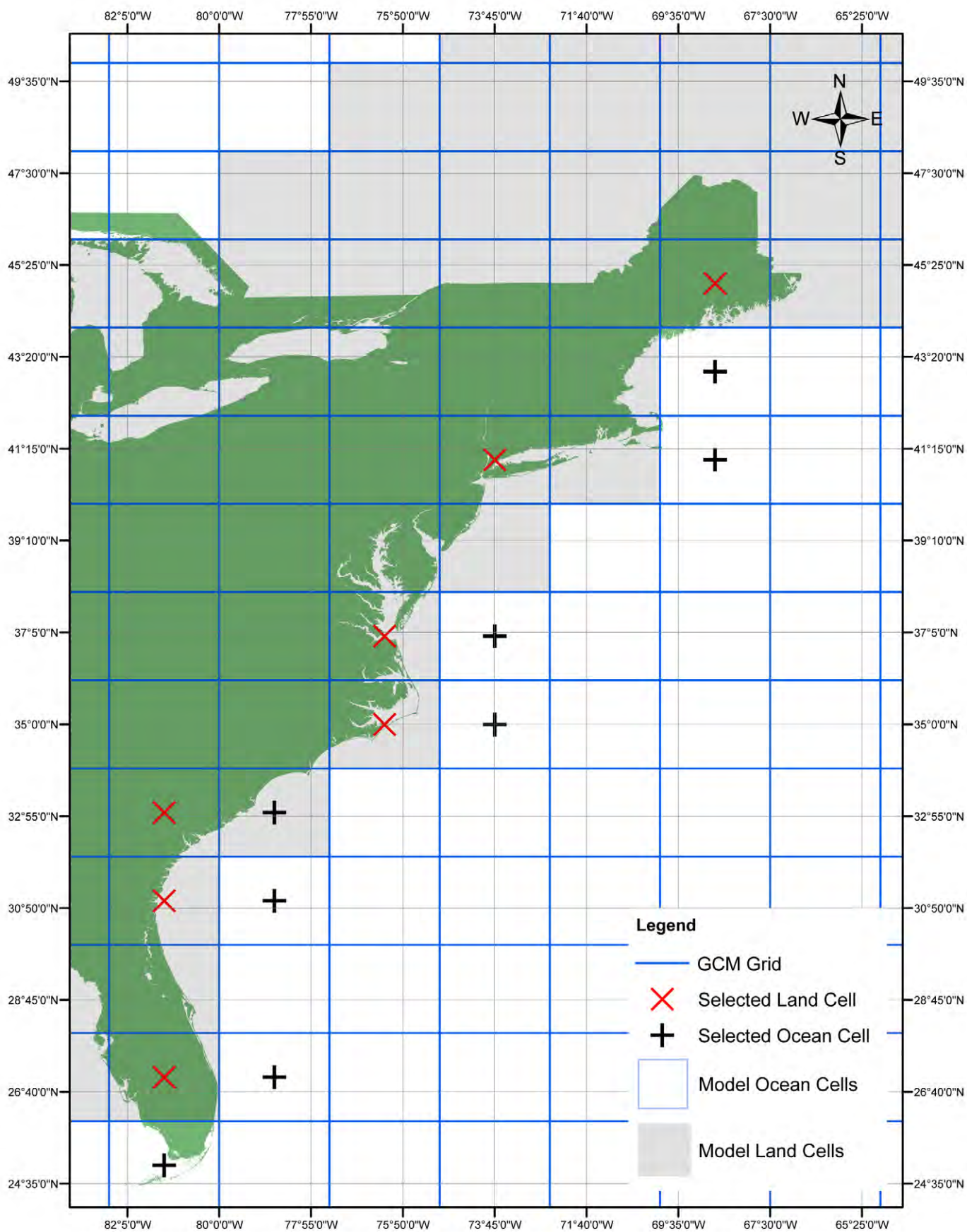
Data extraction locations for CSIRO-Mk3.0 model



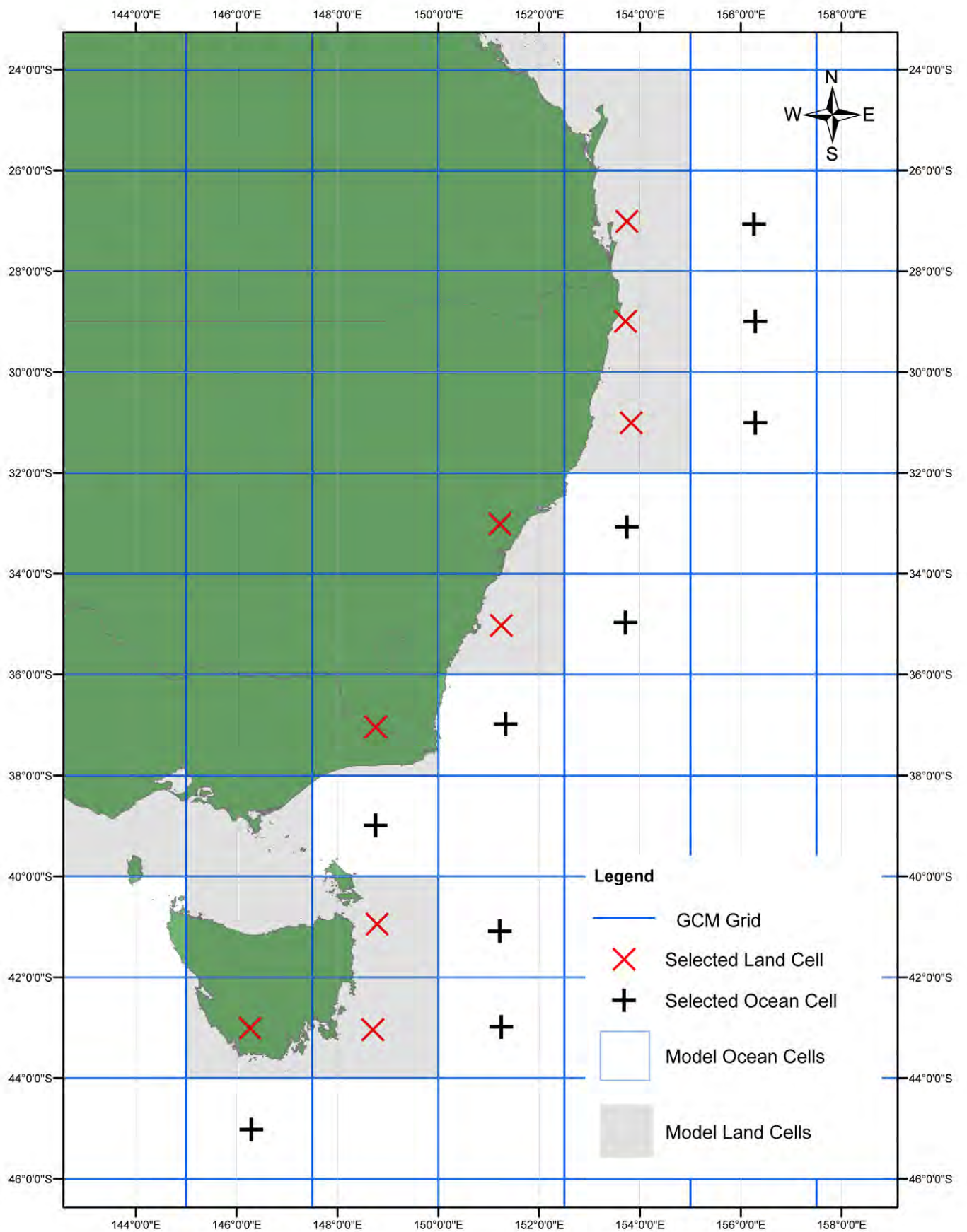
Data extraction locations for CSIRO-Mk3.5 model



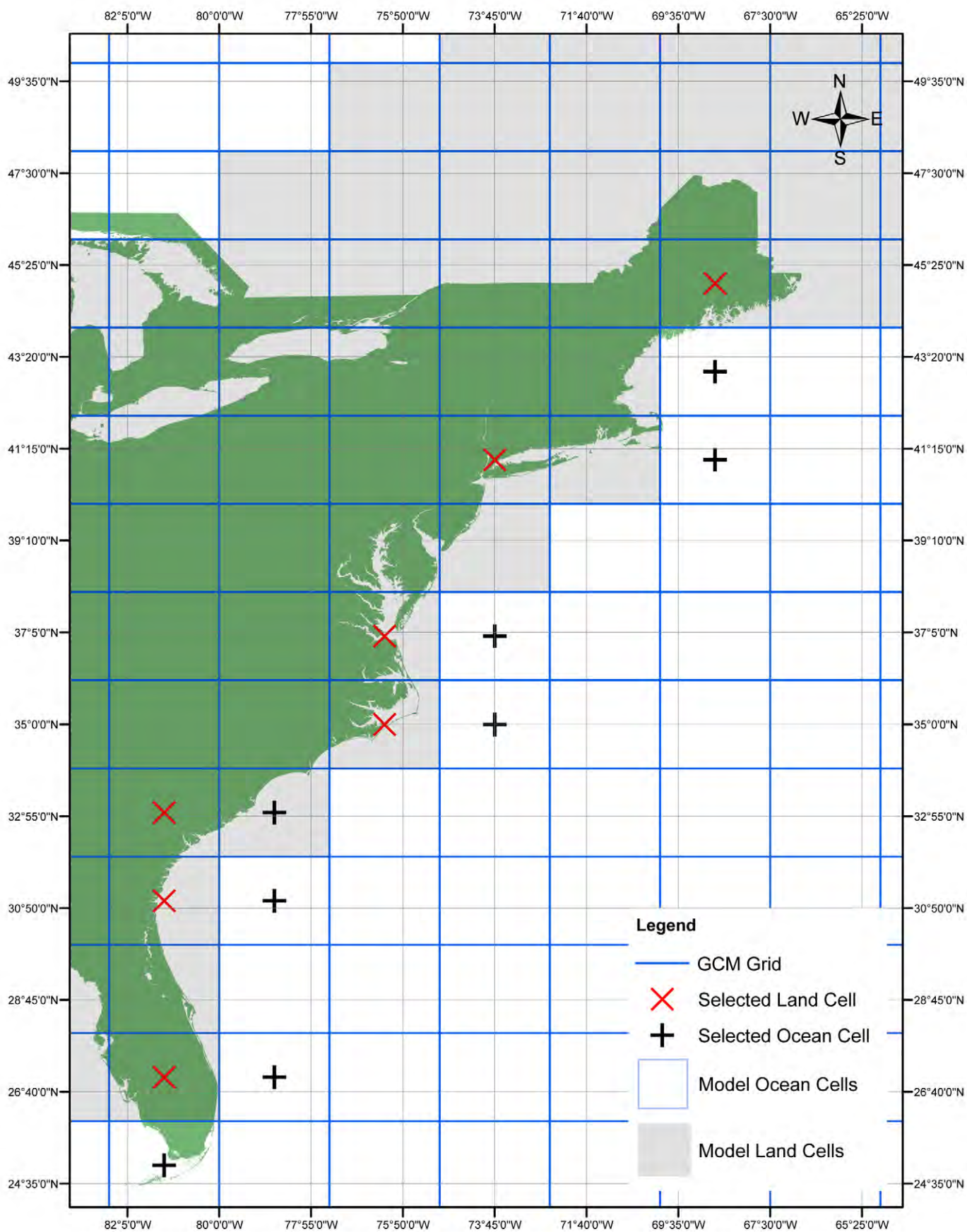
Data extraction locations for CSIRO-Mk3.5 model



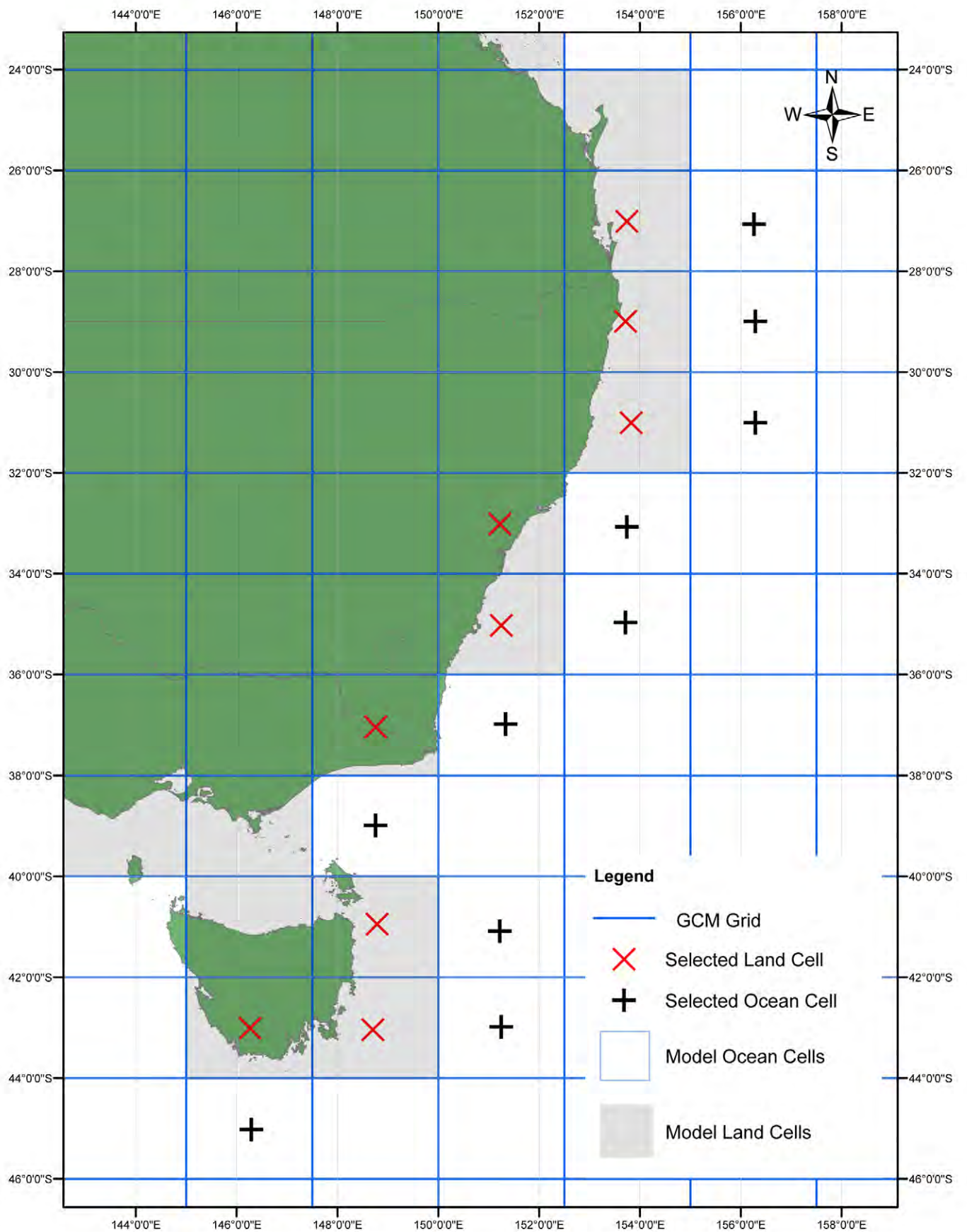
Data extraction locations for GFDL-CM2.0 model



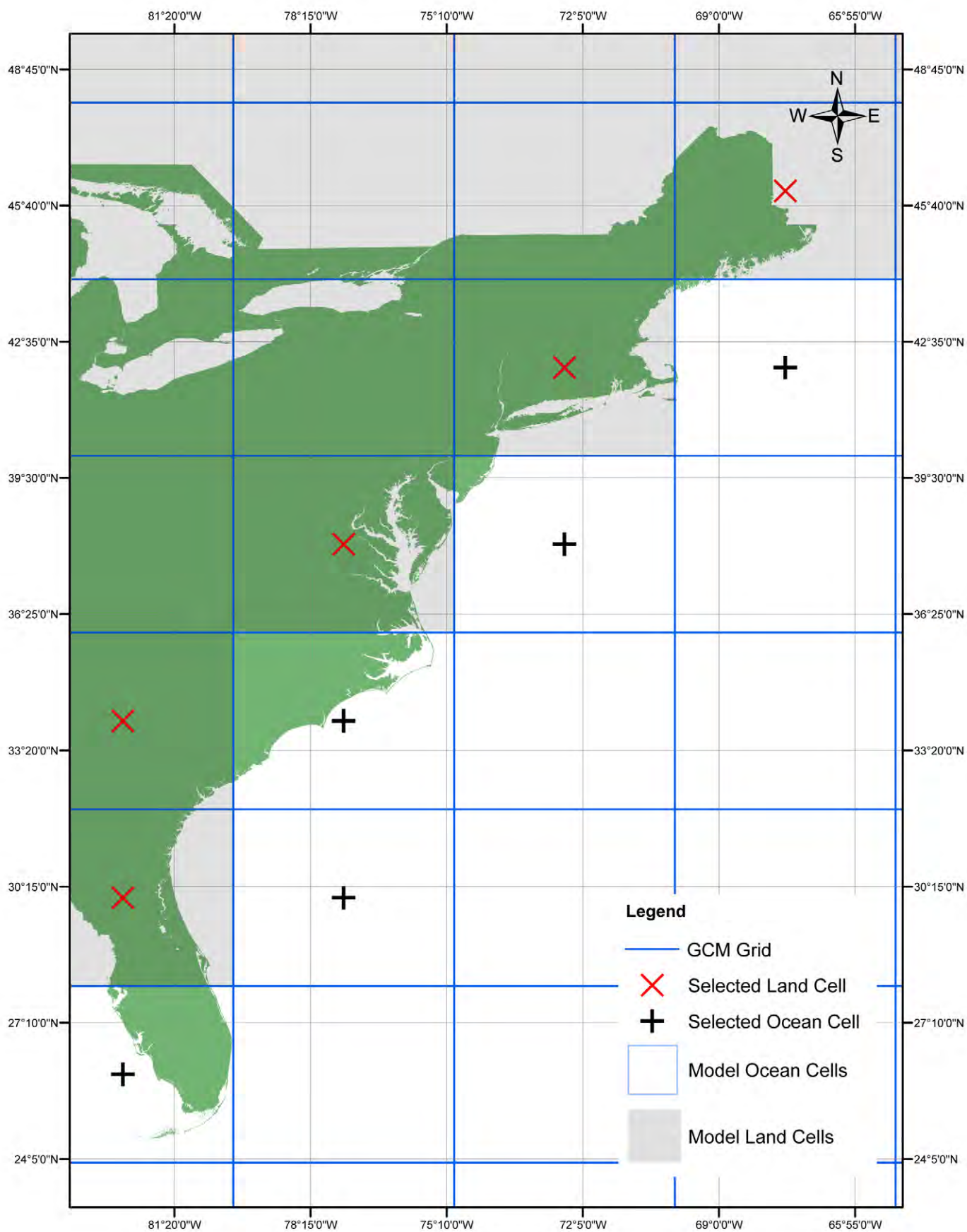
Data extraction locations for GFDL-CM2.0 model



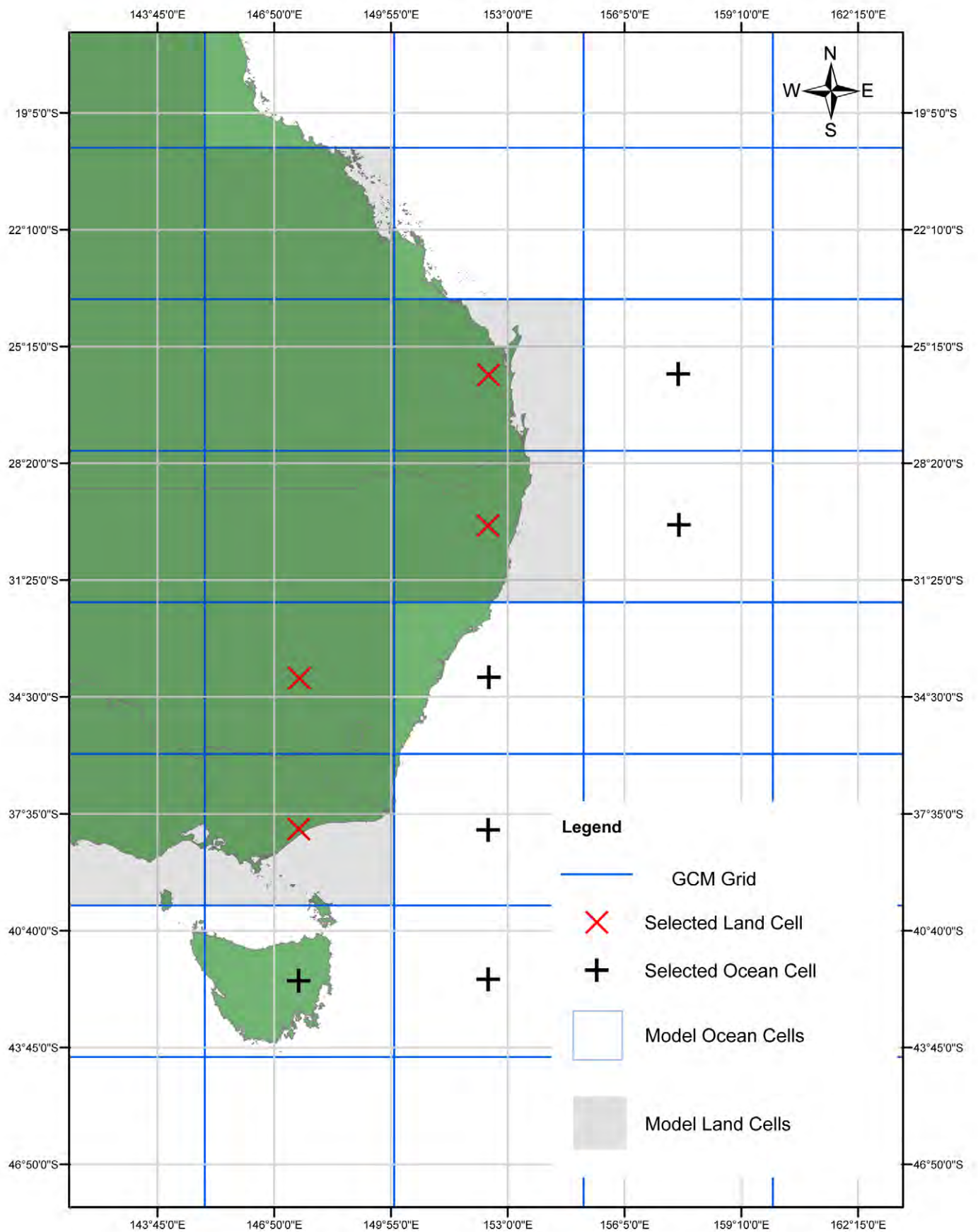
Data extraction locations for GFDL-CM2.1 model



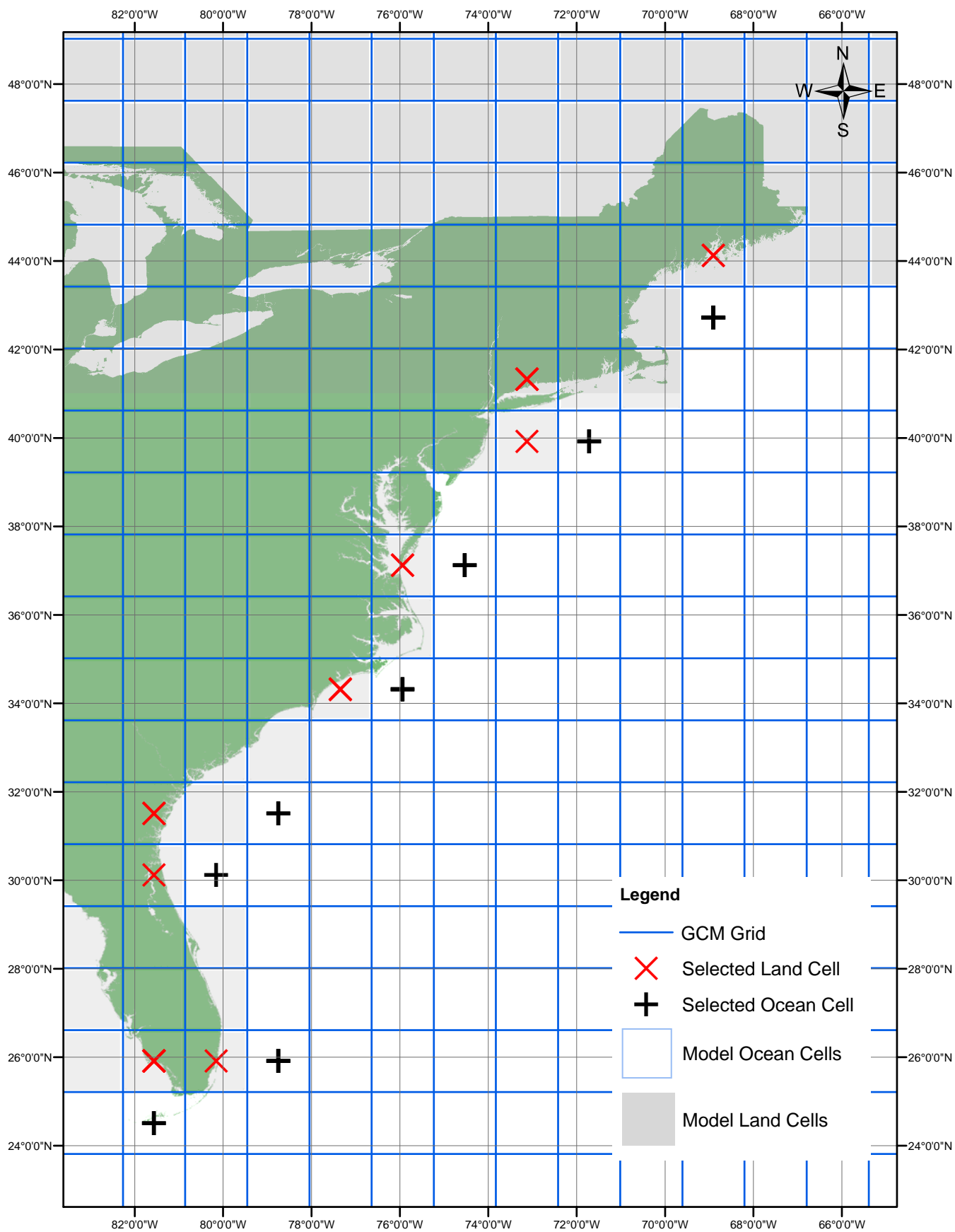
Data extraction locations for GFDL-CM2.1 model



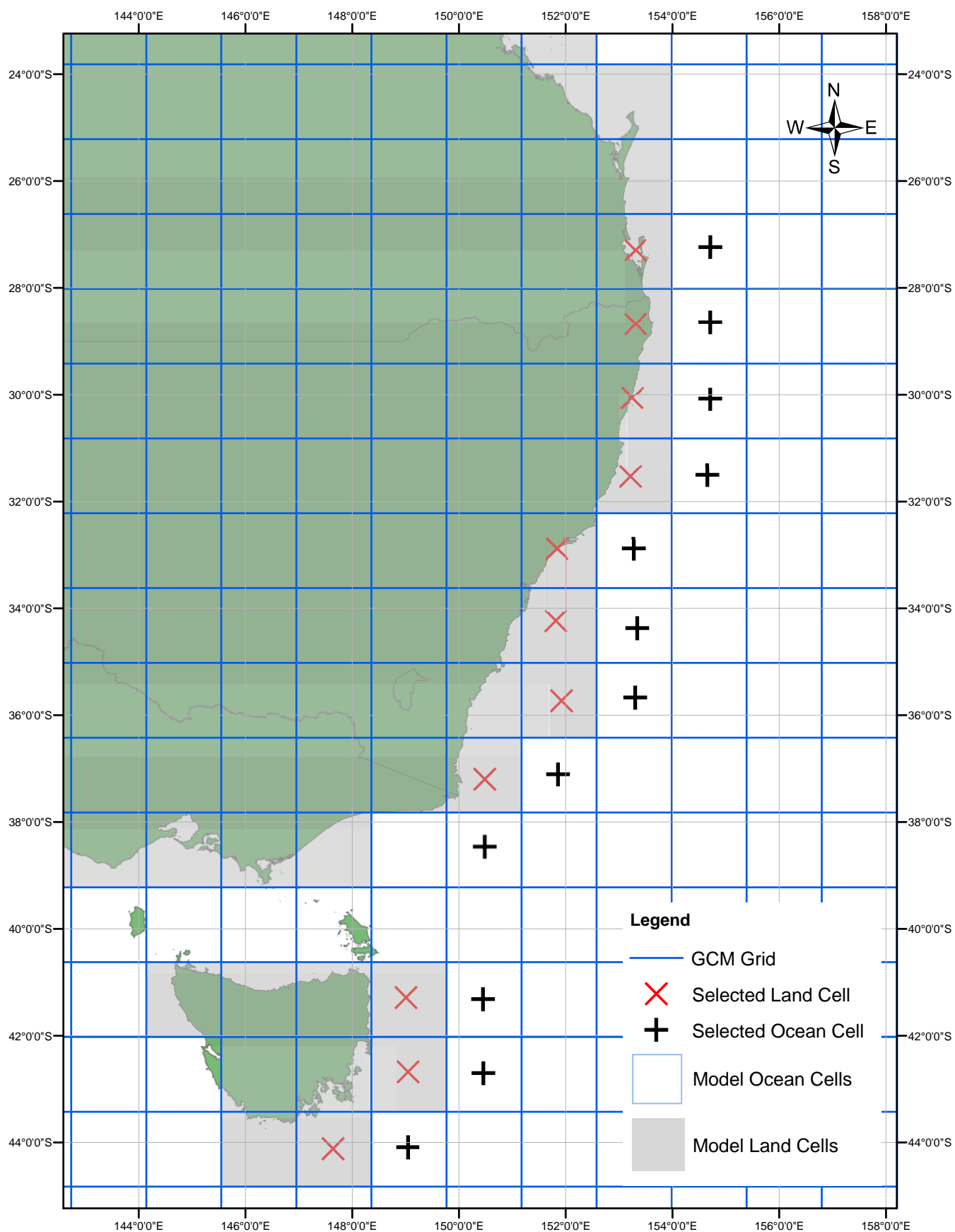
Data extraction locations for GISS-ER model



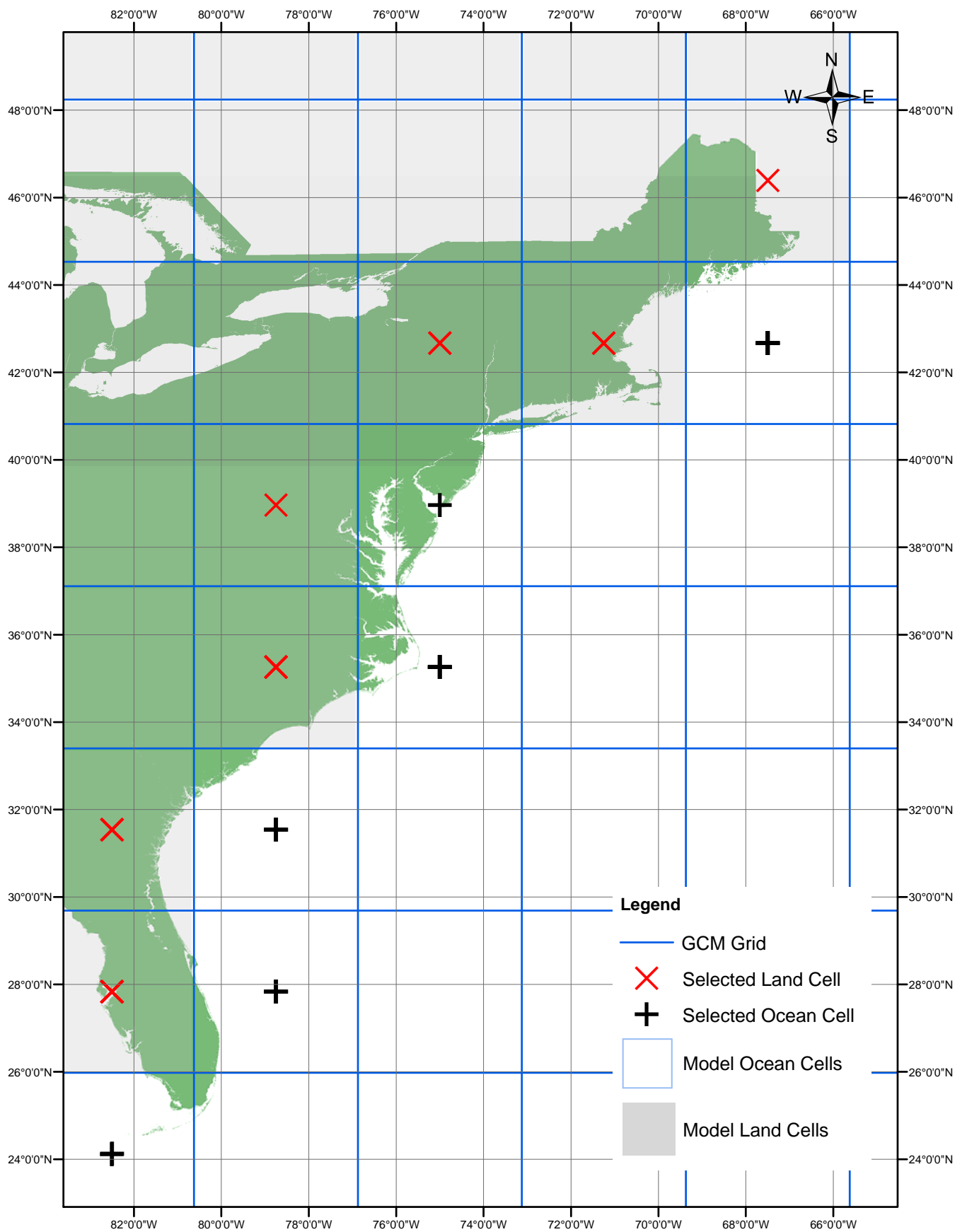
Data extraction locations for GISS-ER model



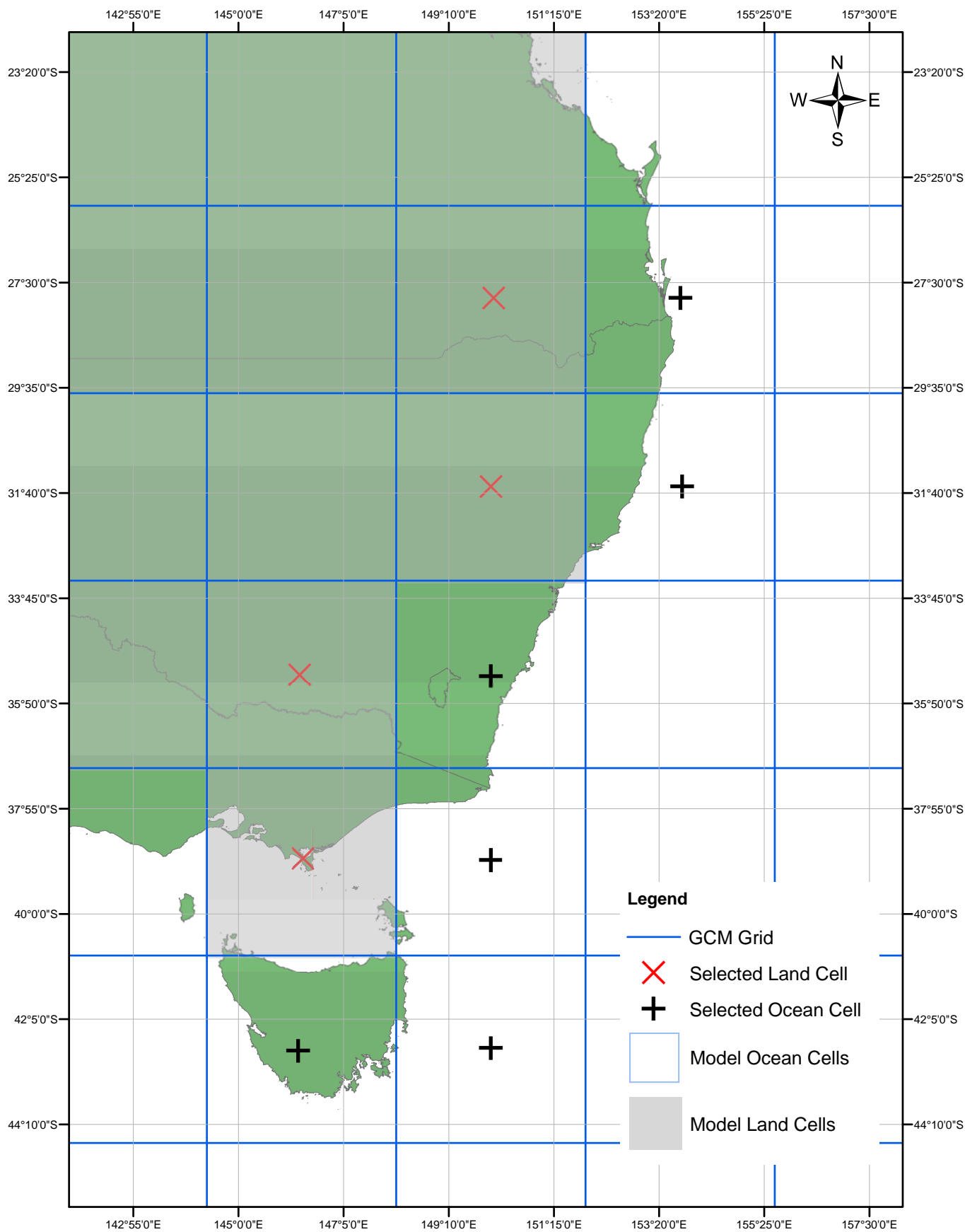
Data extraction locations for NCAR-CCSM3 model



Data extraction locations for NCAR-CCSM3 model



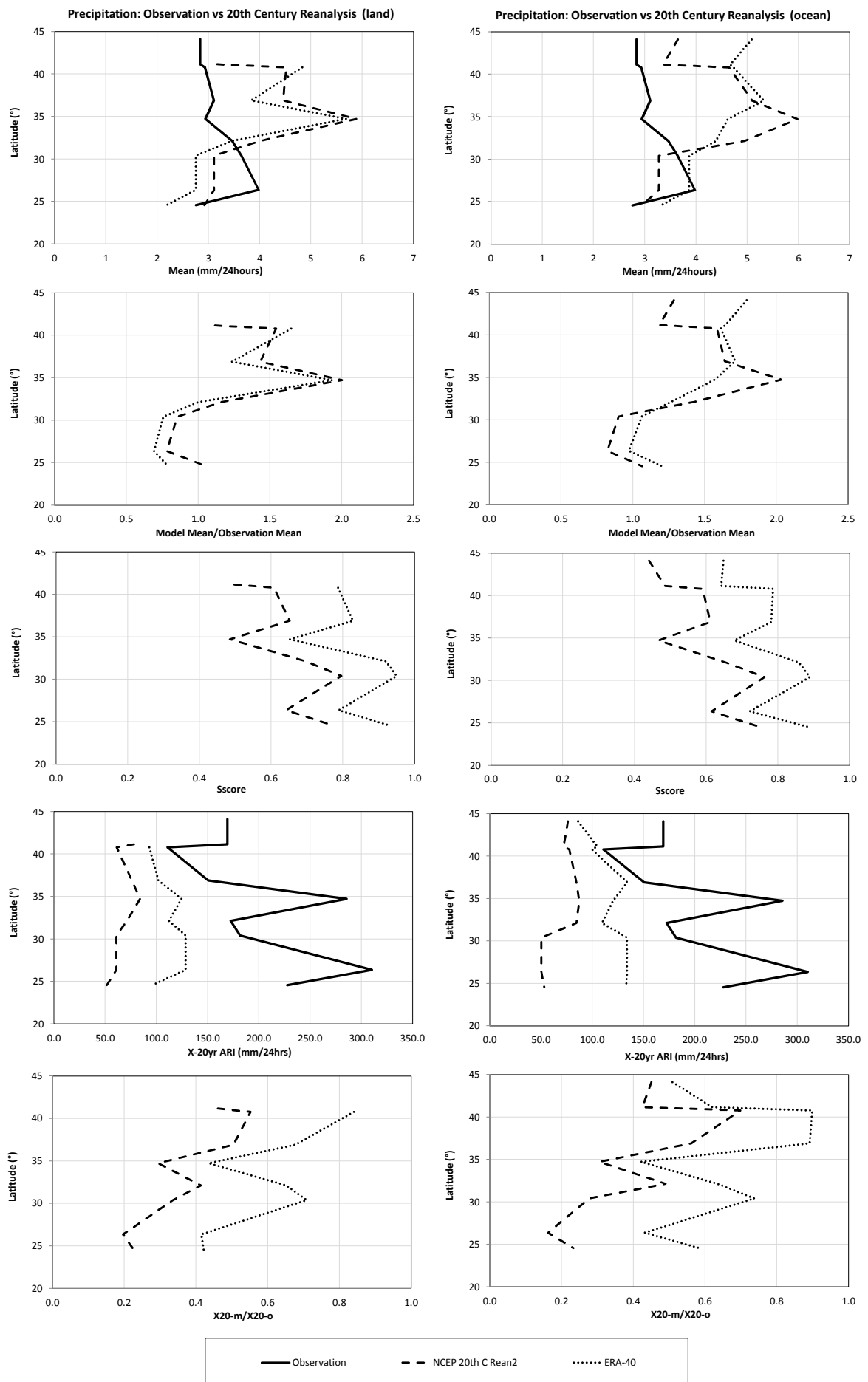
Data extraction locations for MIUBEG ECHO-G model



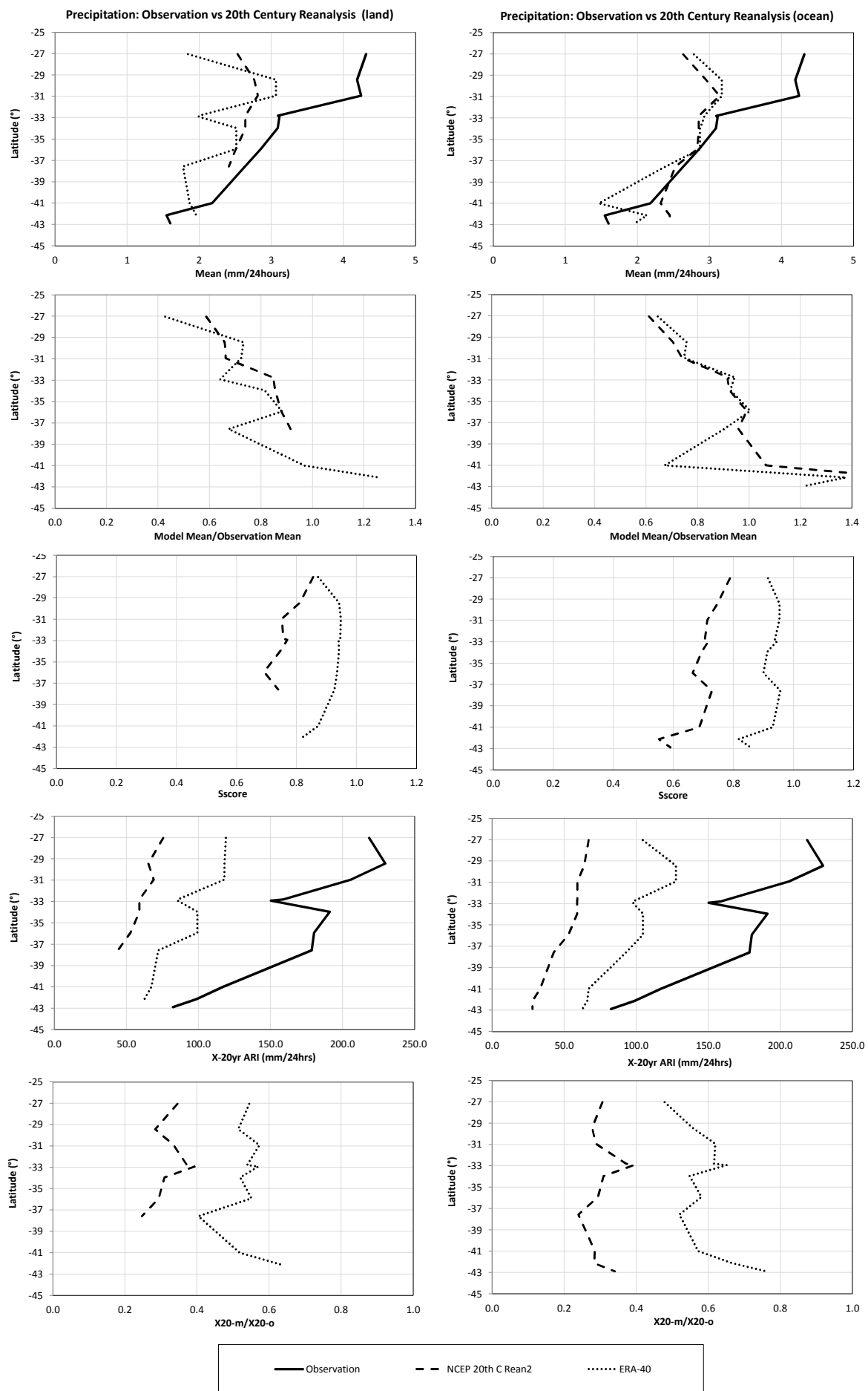
Data extraction locations for MIUBEG ECHO-G model

Appendix C 20th Century Results

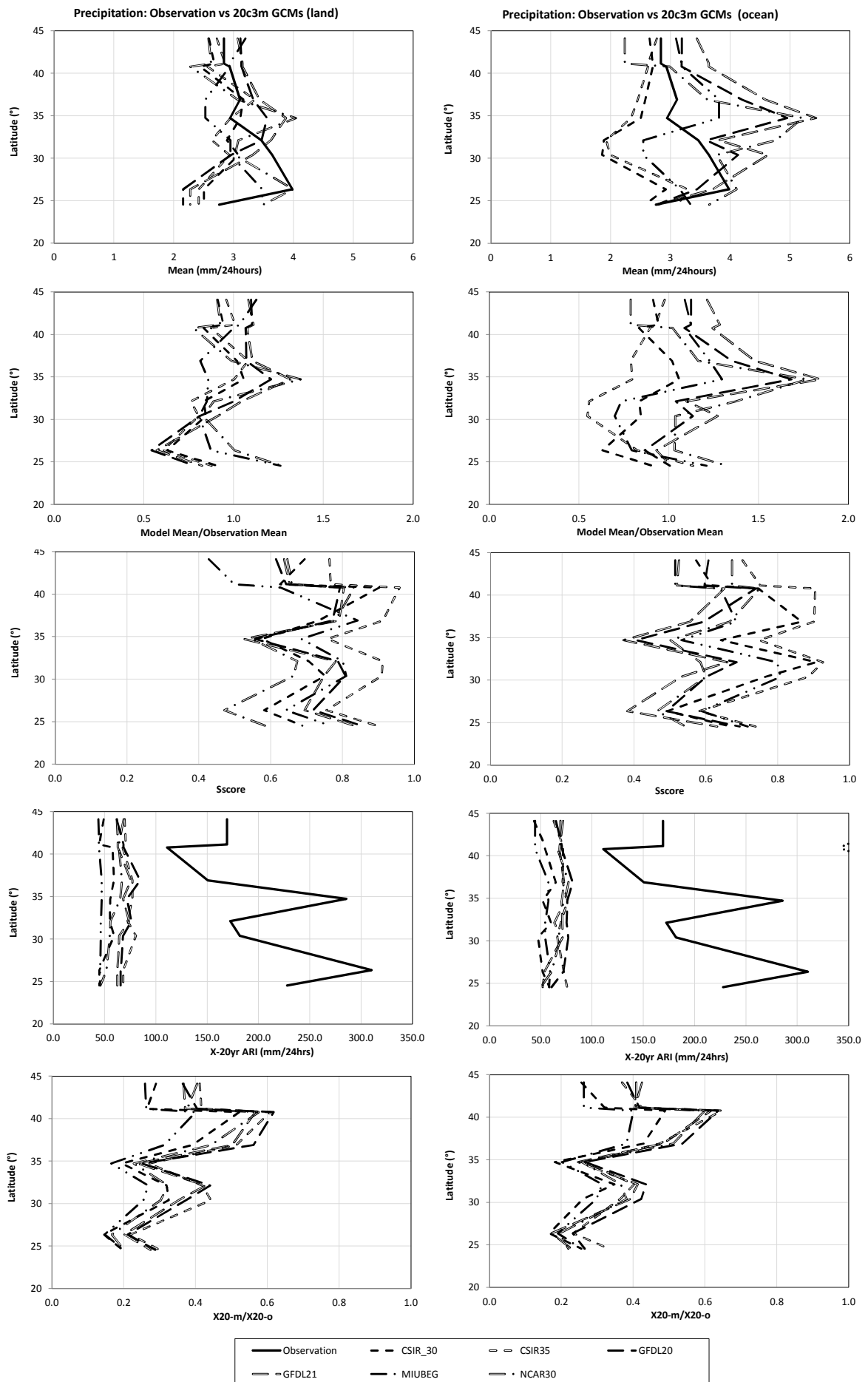
Figure Number	Figure Name
C-1a	US East Coast Precipitation: Observation vs 20th Century Reanalysis GCMs
C-1b	Aus East Coast Precipitation: Observation vs 20th Century Reanalysis GCMs
C-1c	US East Coast Precipitation: Observation vs 20c3m GCMs
C-1d	Aus East Coast Precipitation: Observation vs 20c3m GCMs
C-2a	US East Coast MSLP: Observation vs 20th Century Reanalysis GCMs
C-2b	Aus East Coast MSLP: Observation vs 20th Century Reanalysis GCMs
C-2c	US East Coast MSLP: Observation vs 20c3m GCMs
C-2d	Aus East Coast MSLP: Observation vs 20c3m GCMs
C-3a	US East Coast MSLP Gradient: Observation vs 20c3m GCMs
C-3b	Aus East Coast MSLP Gradient: Observation vs 20c3m GCMs
C-4a	US East Coast Abs Wind: Observation vs 20th Century Reanalysis GCMs
C-4b	Aus East Coast Westward Wind: Observation vs 20th Century Reanalysis GCMs
C-4c	US East Coast Abs Wind: Observation vs 20c3m GCMs
C-4d	Aus East Coast Westward Wind: Observation vs 20c3m GCMs



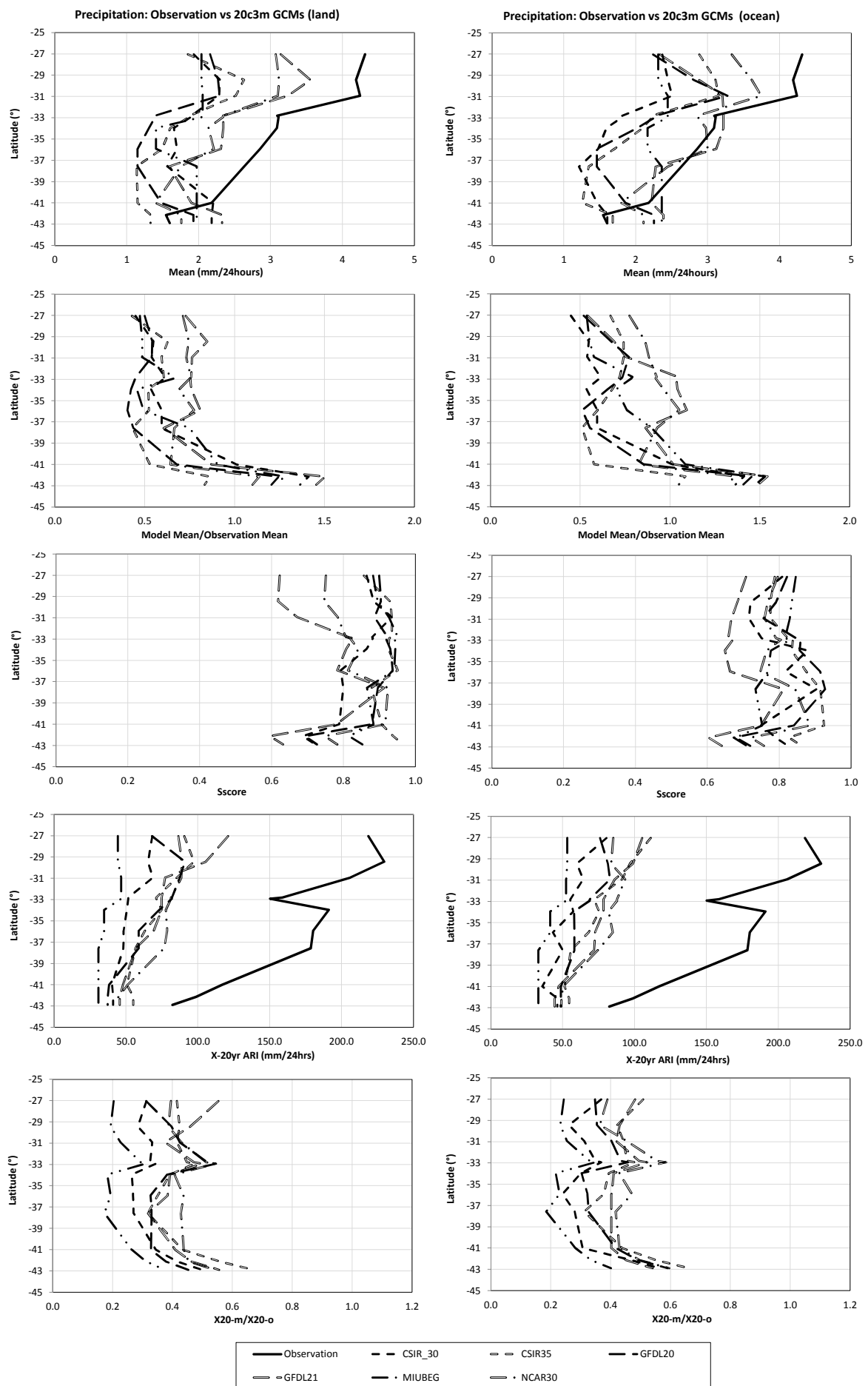
US East Coast Precipitation: Observation vs 20th Century Reanalysis GCMs



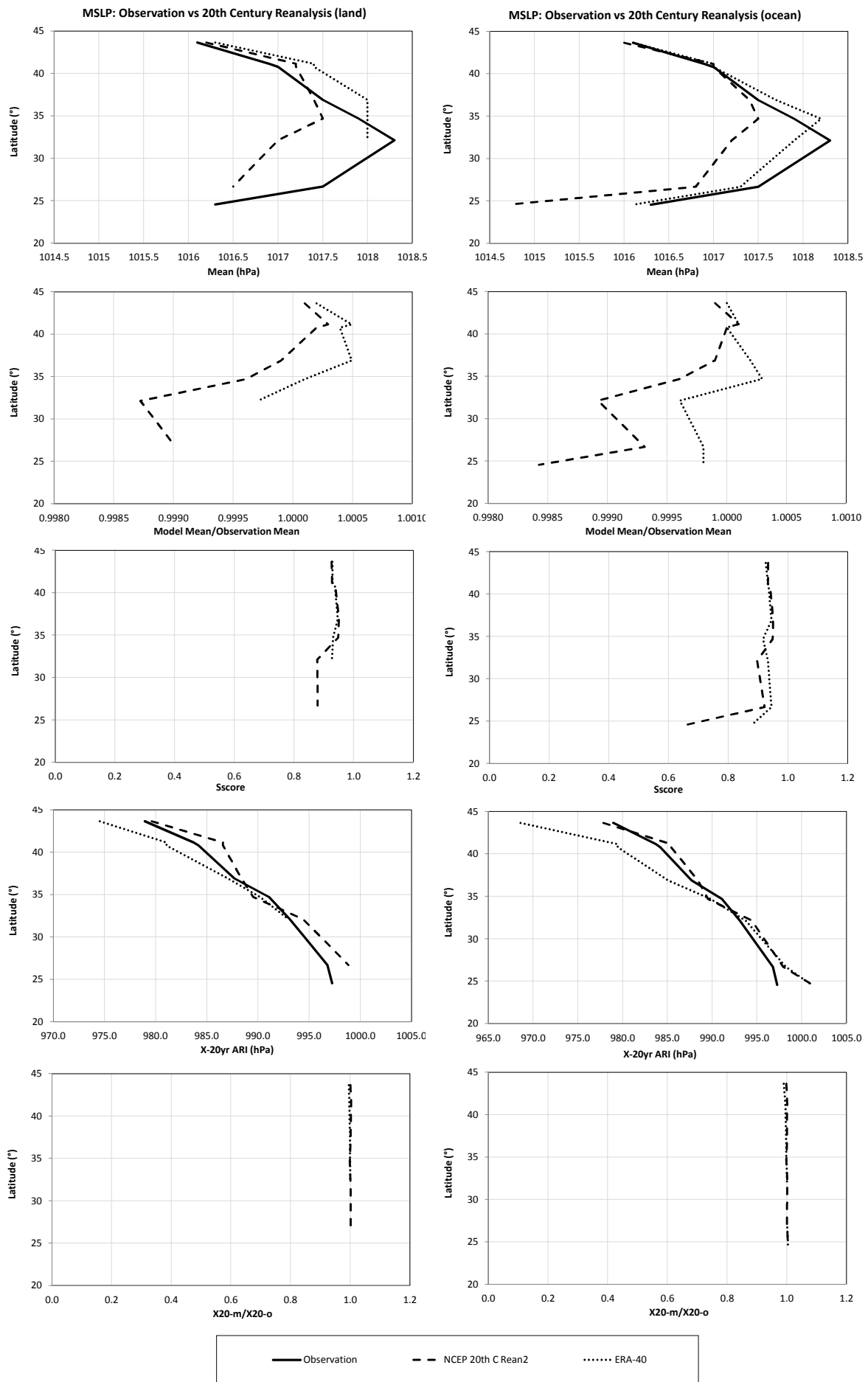
Aus East Coast Precipitation: Observation vs 20th Century Reanalysis GCMs



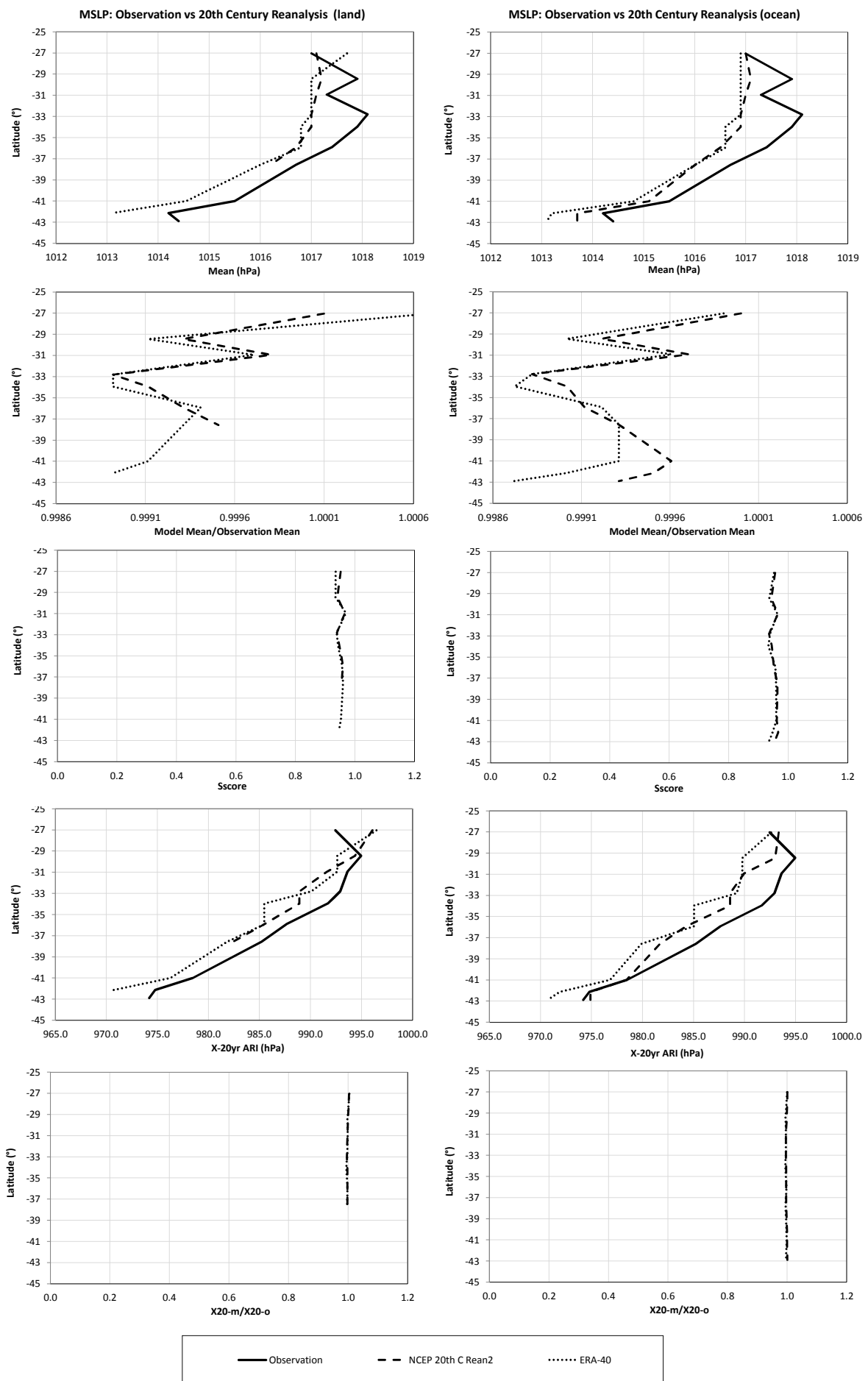
US East Coast Precipitation: Observation vs 20c3m GCMs



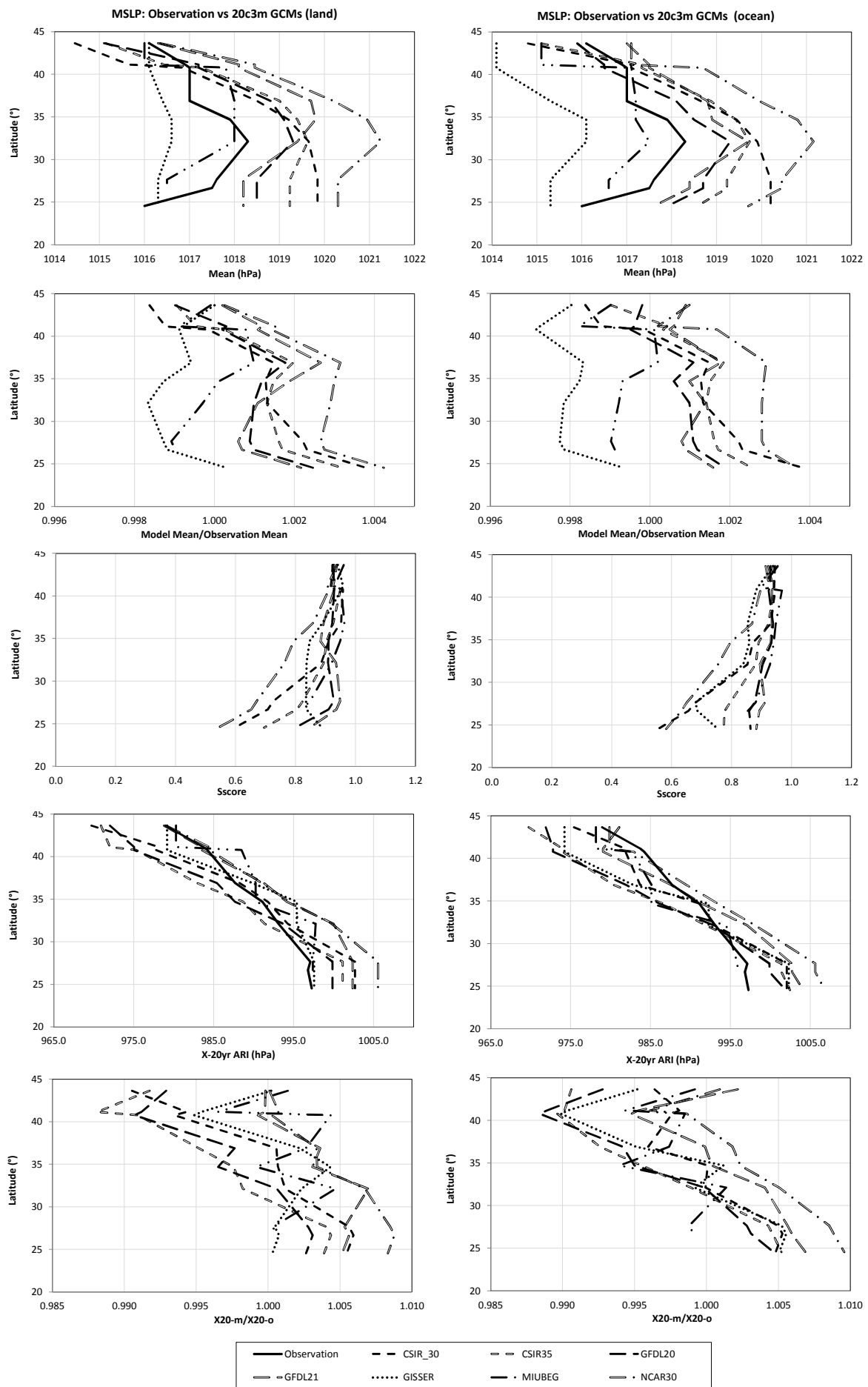
Aus East Coast Precipitation: Observation vs 20c3m GCMs



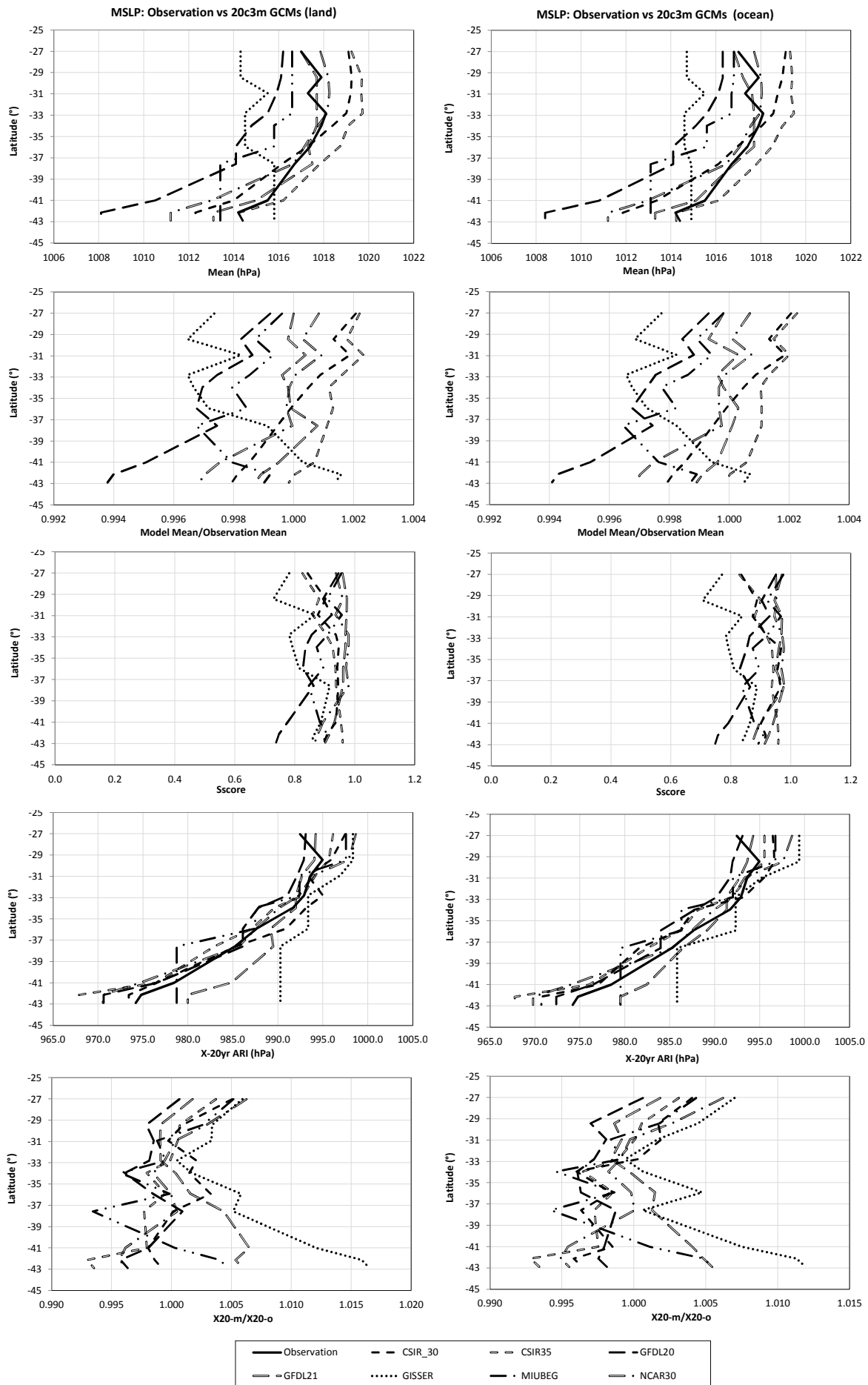
US East Coast MSLP: Observation vs 20th Century Reanalysis GCMs



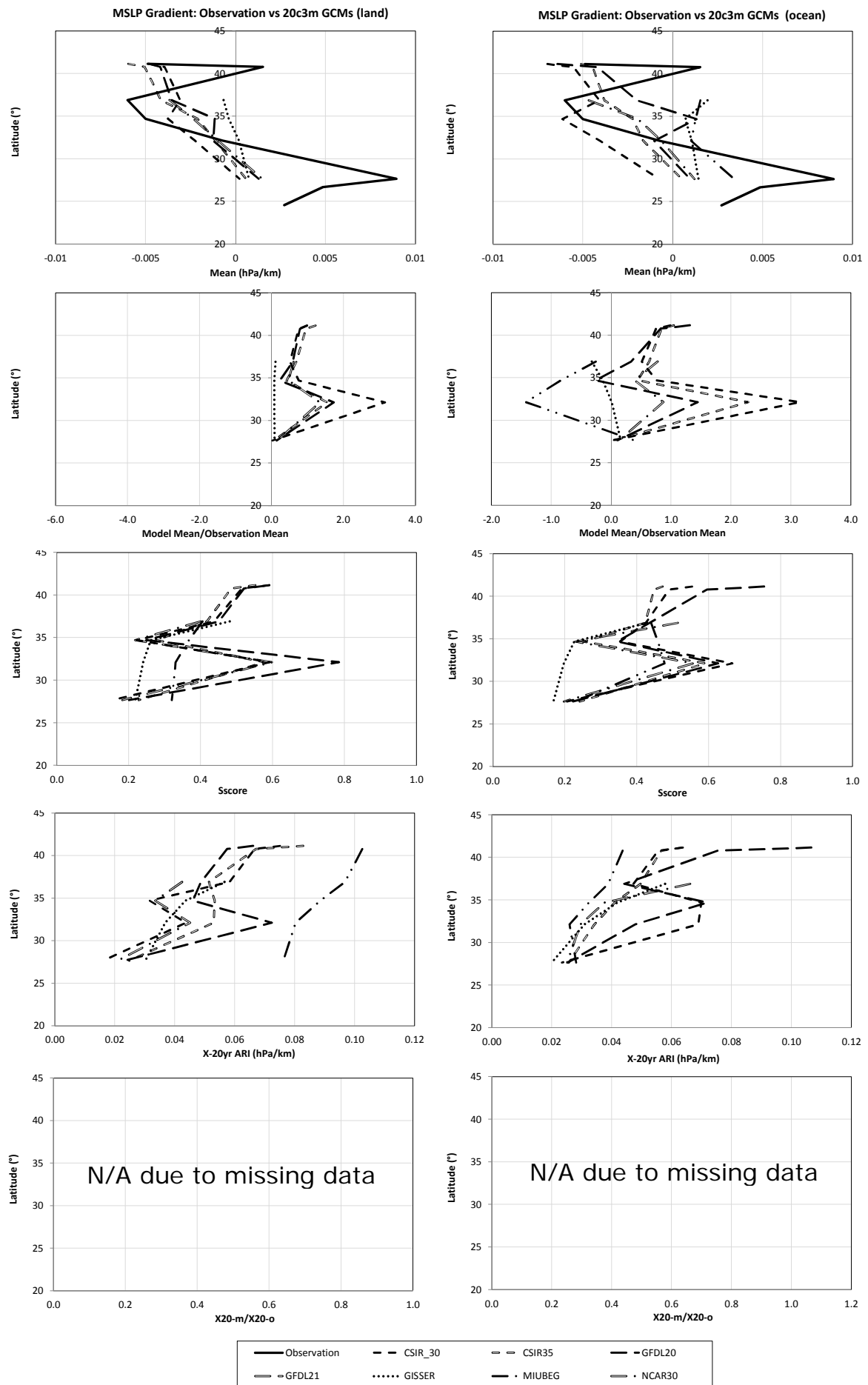
Aus East Coast MSLP: Observation vs 20th Century Reanalysis GCMs



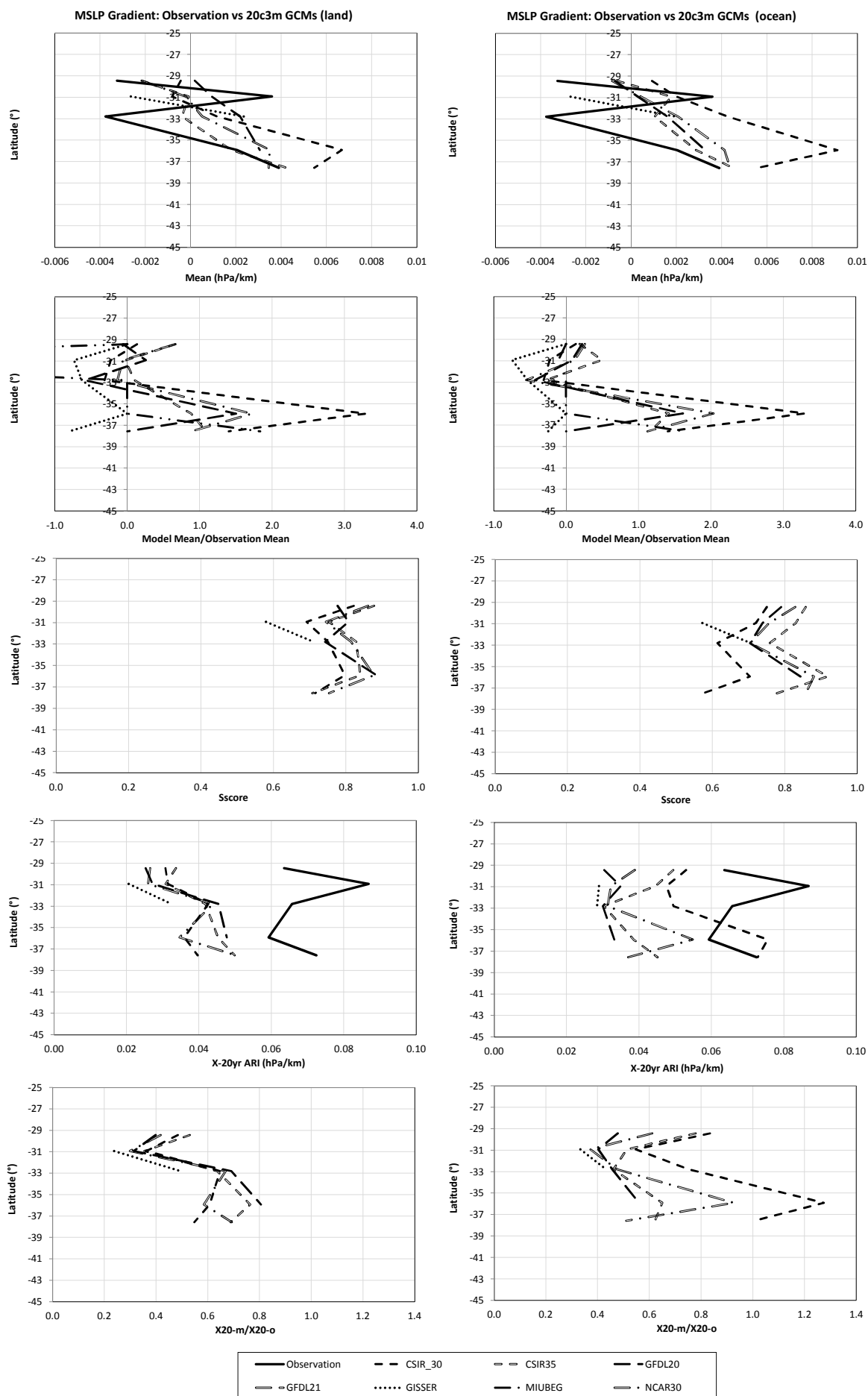
US East Coast MSLP: Observation vs 20c3m GCMs



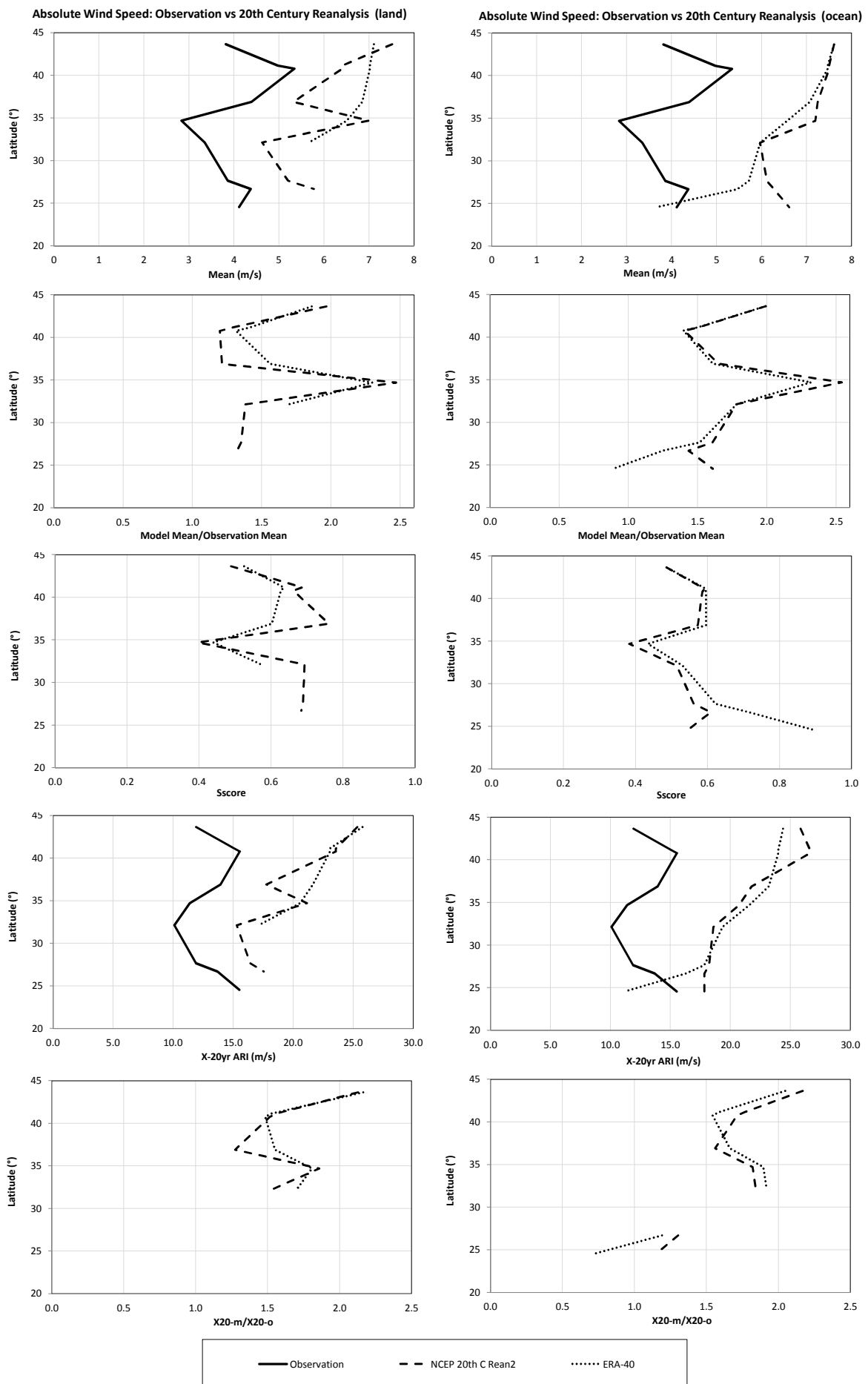
Aus East Coast MSLP: Observation vs 20c3m GCMs



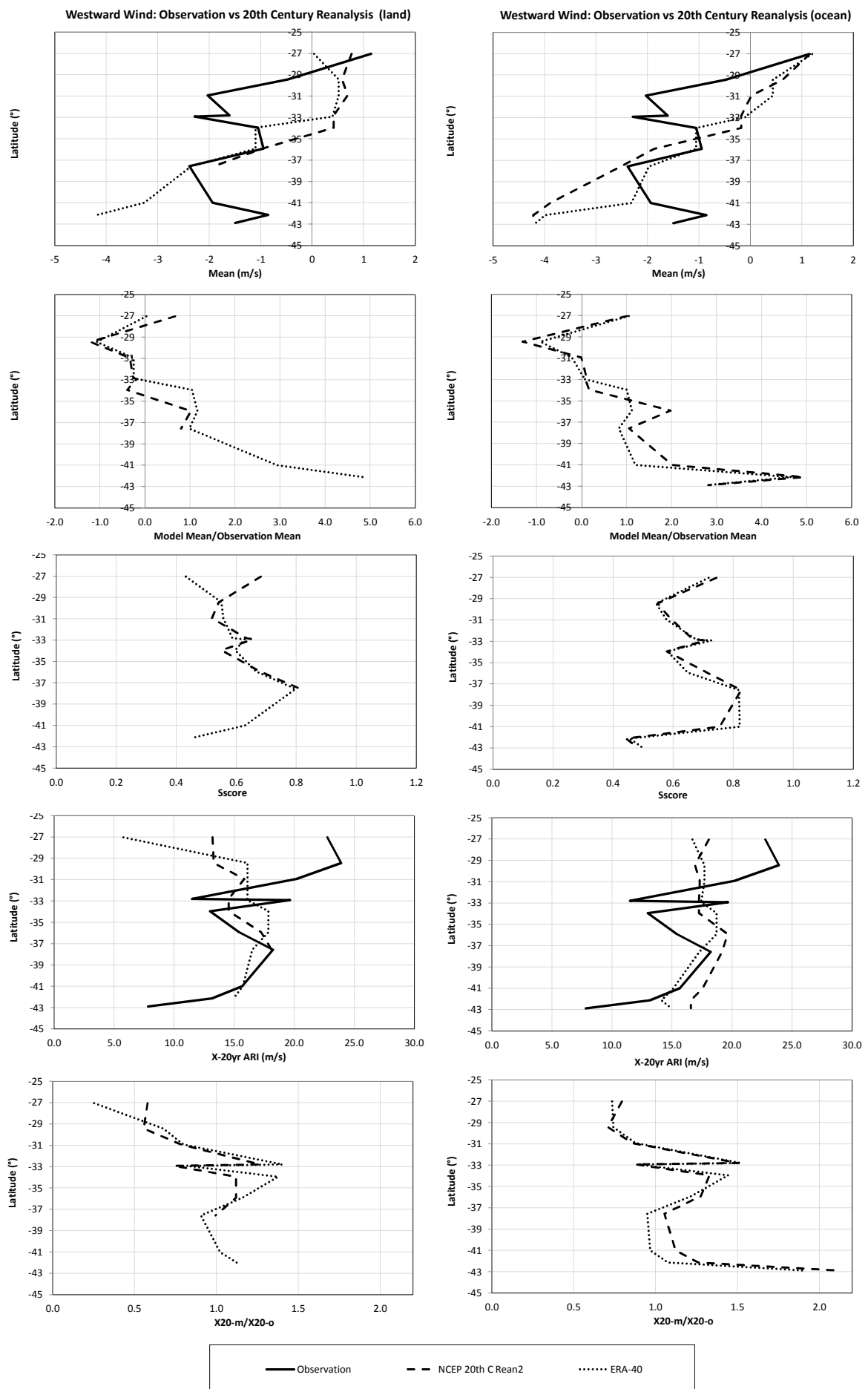
US East Coast MSLP Gradient: Observation vs 20c3m GCMs



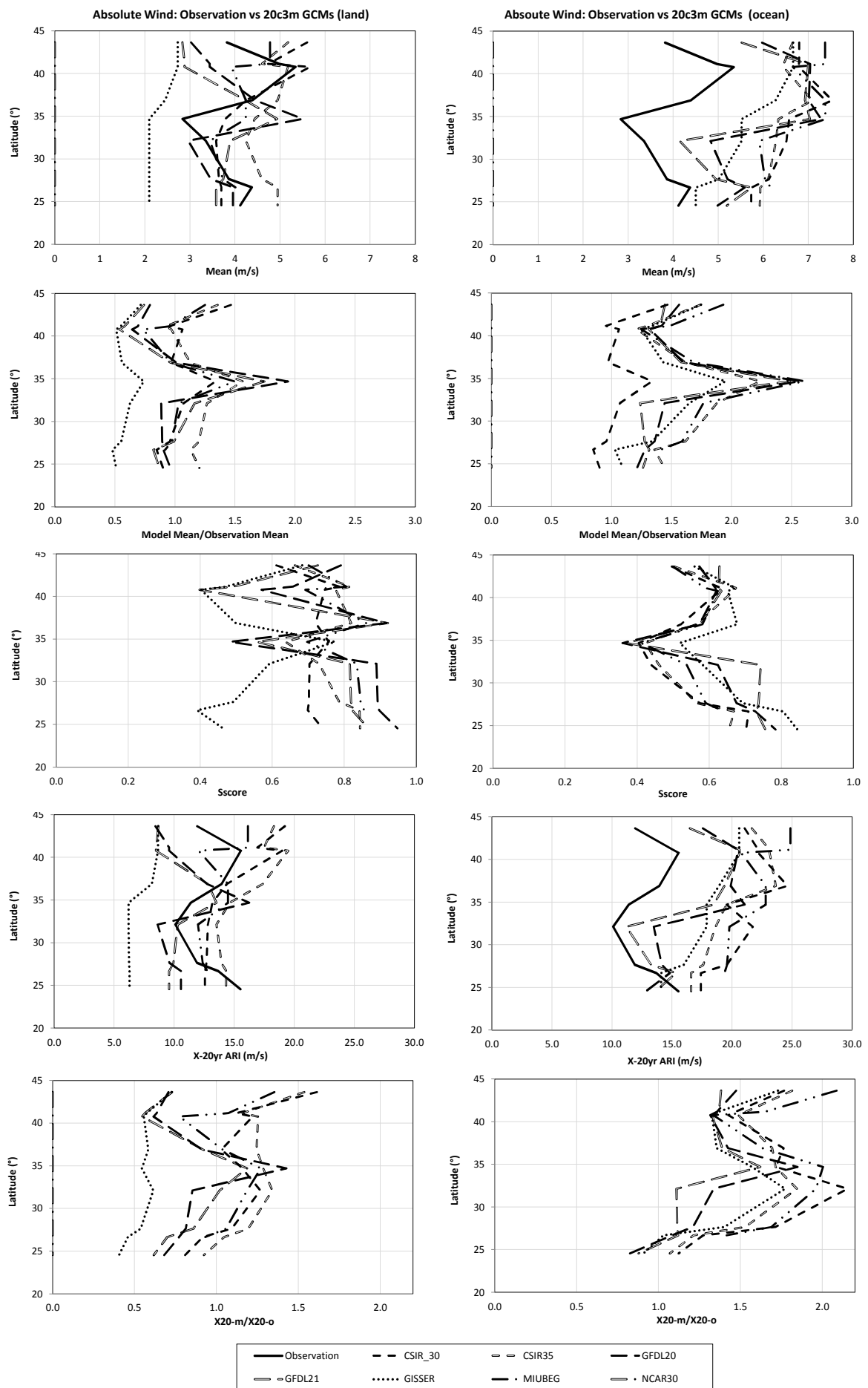
Aus East Coast MSLP Gradient: Observation vs 20c3m GCMs



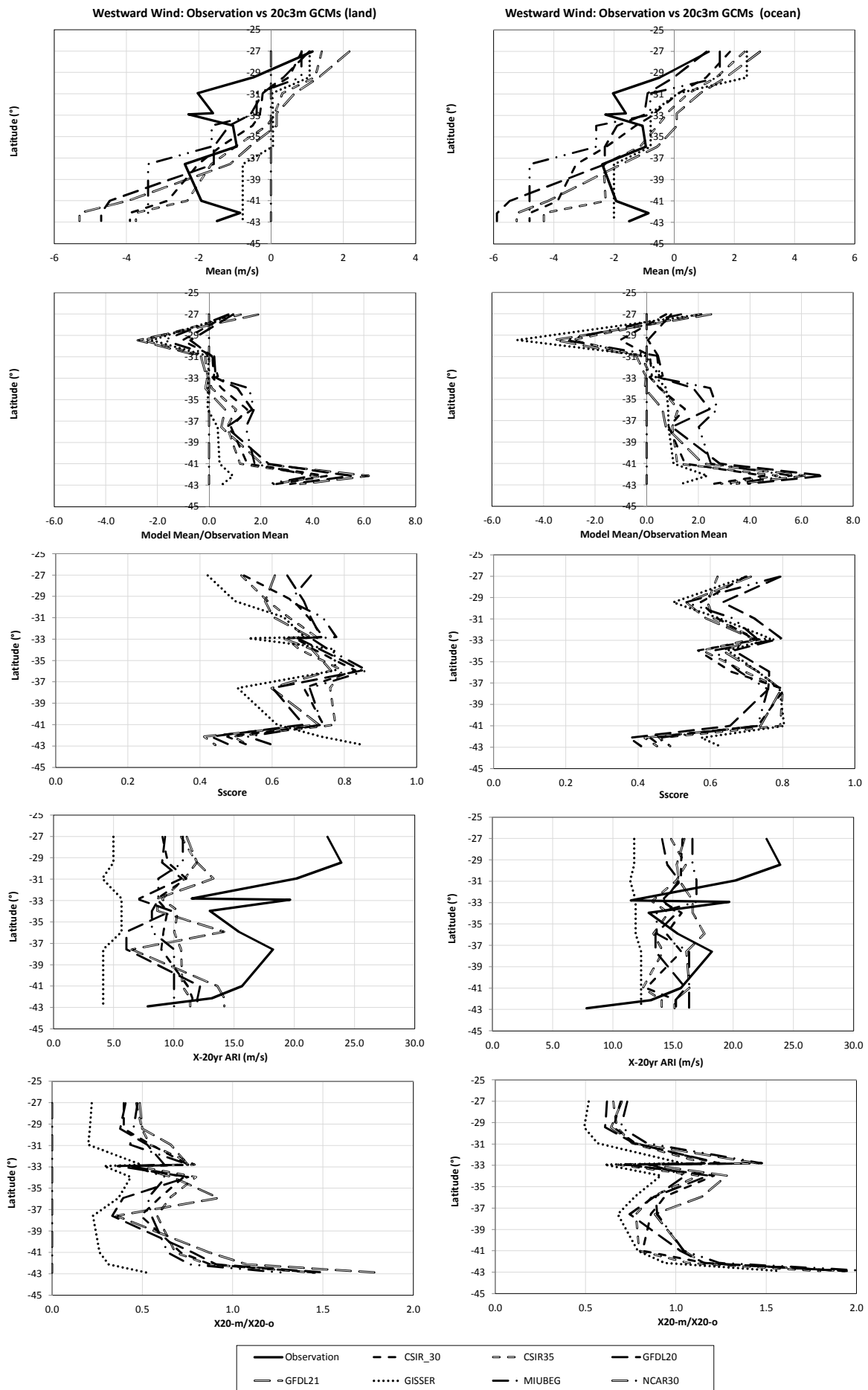
US East Coast Abs Wind: Observation vs 20th Century Reanalysis GCMs



Aus East Coast Westward Wind: Observation vs 20th Century Reanalysis GCMs



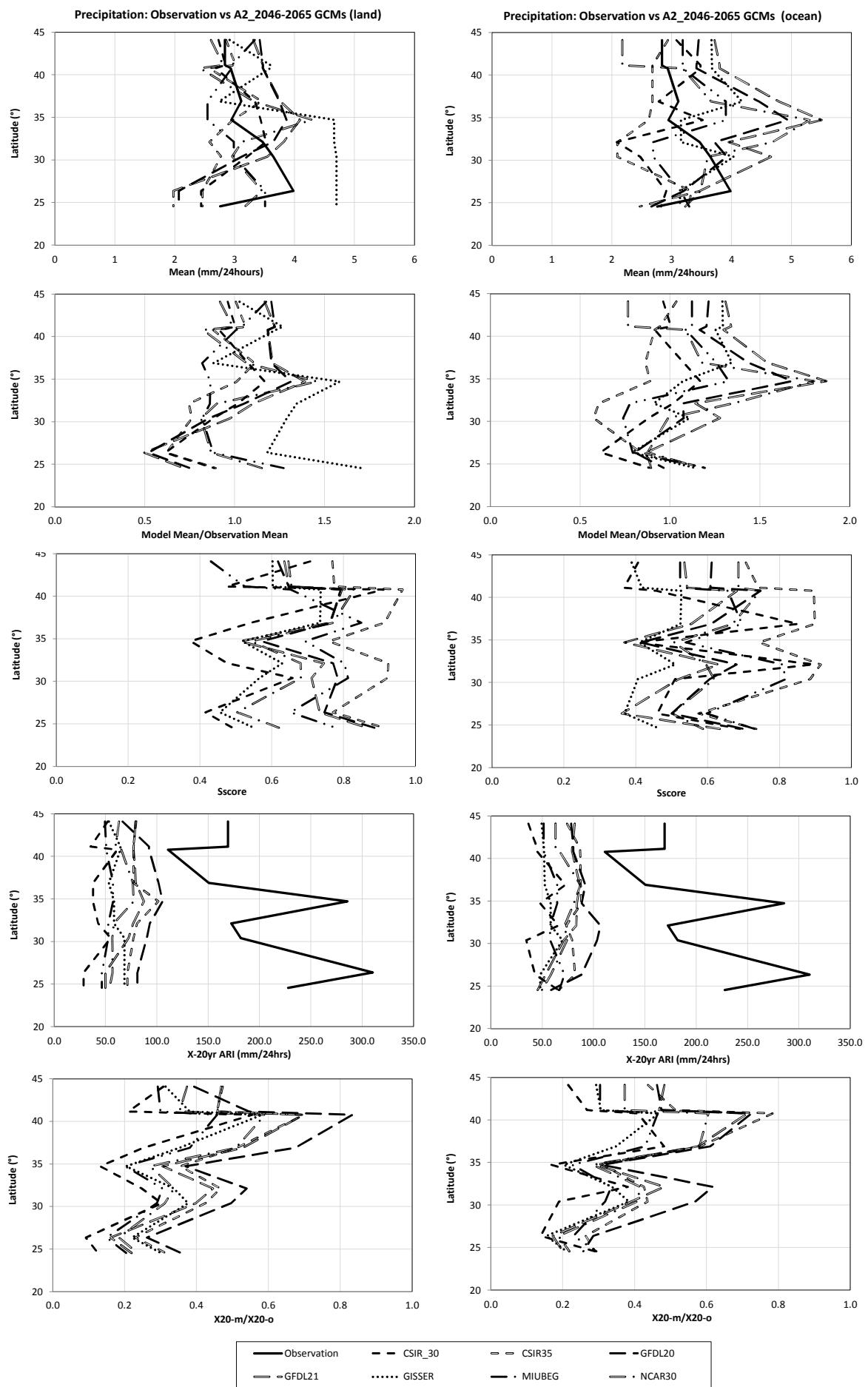
US East Coast Abs Wind: Observation vs 20c3m GCMs



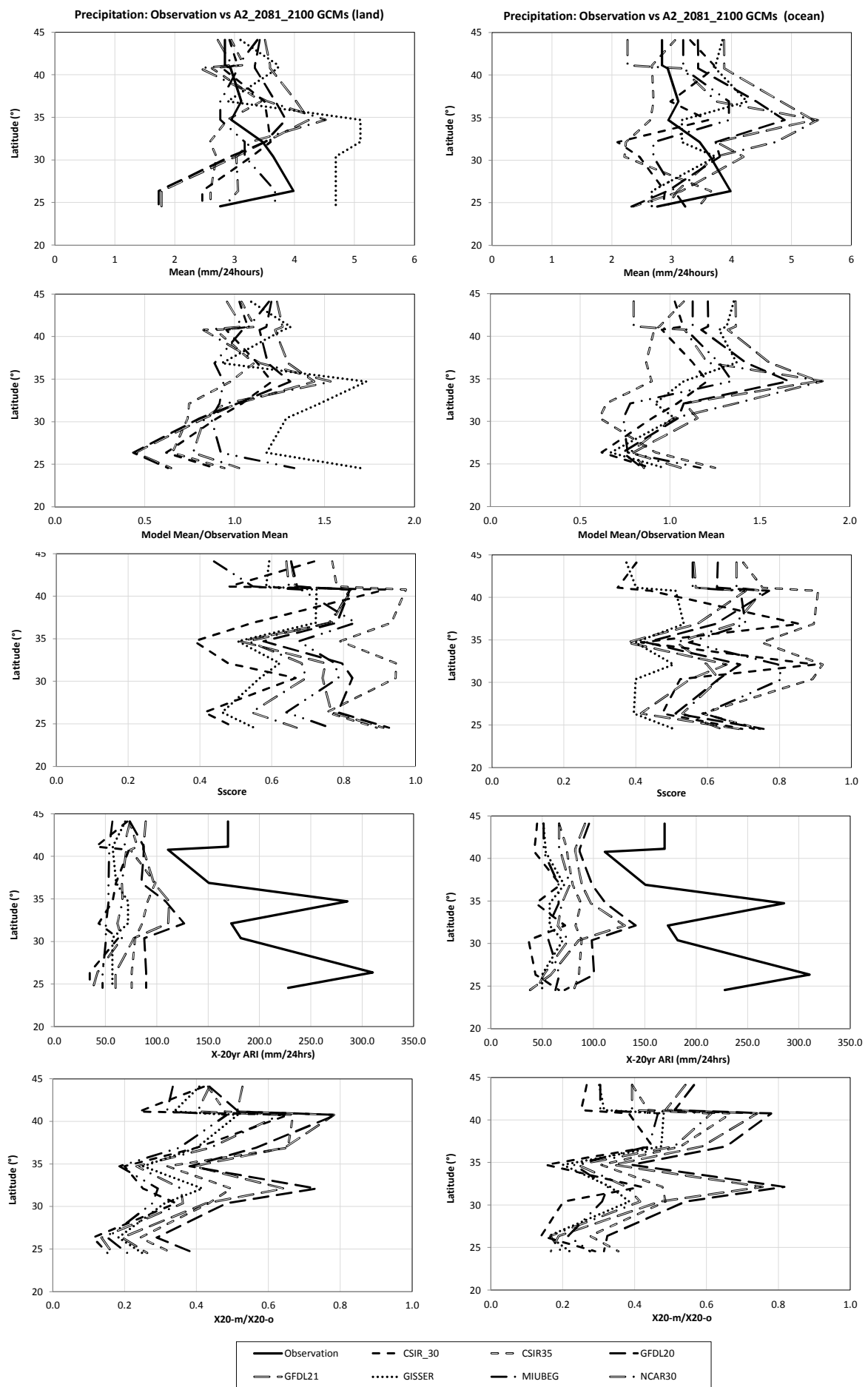
Aus East Coast Westward Wind: Observation vs 20c3m GCMs

Appendix D 21st Century A2 Scenario Results

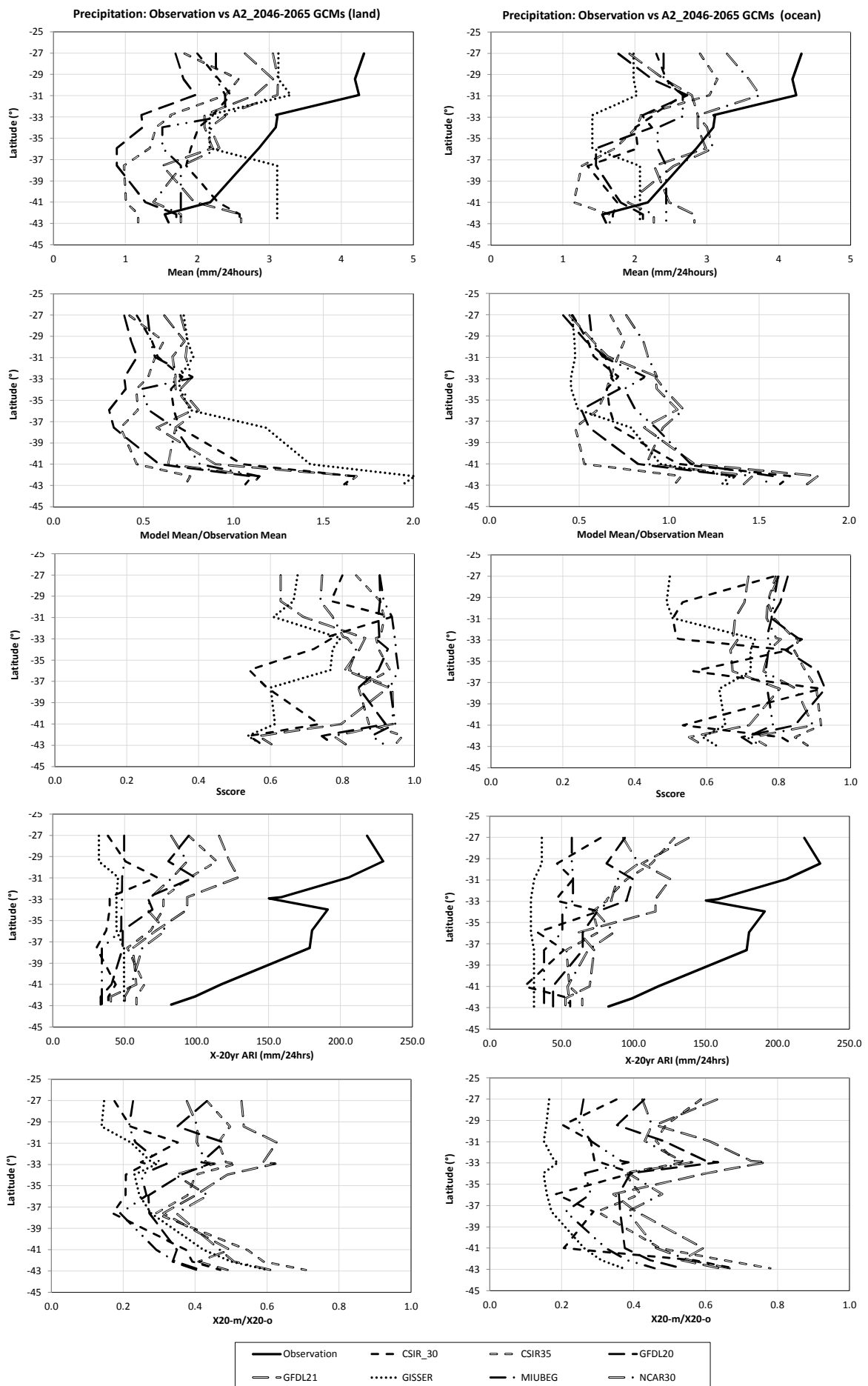
Figure Number	Figure Name
D-1a	US East Coast Precipitation: Observation vs A2 2046-2065 GCMs
D-1b	US East Coast Precipitation: Observation vs A2 2081-2100 GCMs
D-1c	Aus East Coast Precipitation: Observation vs A2 2046-2065 GCMs
D-1d	Aus East Coast Precipitation: Observation vs A2 2081-2100 GCMs
D-2a	US East Coast MSLP: Observation vs A2 2046-2065 GCMs
D-2b	US East Coast MSLP: Observation vs A2 2081-2100 GCMs
D-2c	Aus East Coast MSLP: Observation vs A2 2046-2065 GCMs
D-2d	Aus East Coast MSLP: Observation vs A2 2081-2100 GCMs
D-3a	US East Coast MSLP Gradient: Observation vs A2 2046-2065 GCMs
D-3b	US East Coast MSLP Gradient: Observation vs A2 2081-2100 GCMs
D-3c	Aus East Coast MSLP Gradient: Observation vs A2 2046-2065 GCMs
D-3d	Aus East Coast MSLP Gradient: Observation vs A2 2081-2100 GCMs
D-4a	US East Coast Abs Wind: Observation vs A2 2046-2065 GCMs
D-4b	US East Coast Abs Wind: Observation vs A2 2081-2100 GCMs
D-4c	Aus East Coast Westward Wind: Observation vs A2 2046-2065 GCMs
D-4d	Aus East Coast Westward Wind: Observation vs A2 2081-2100 GCMs



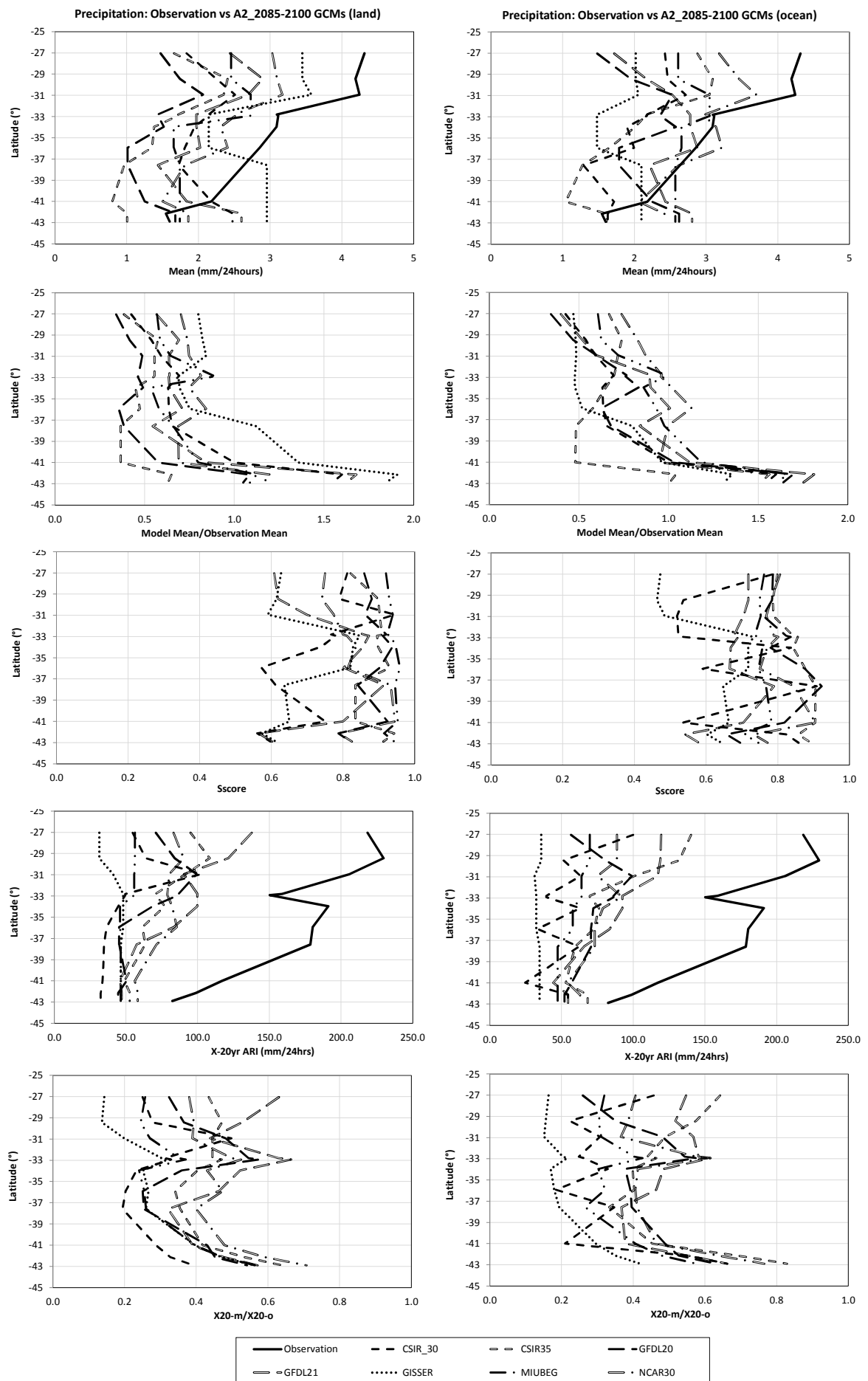
US East Coast Precipitation: Observation vs A2 2046-2065 GCMs



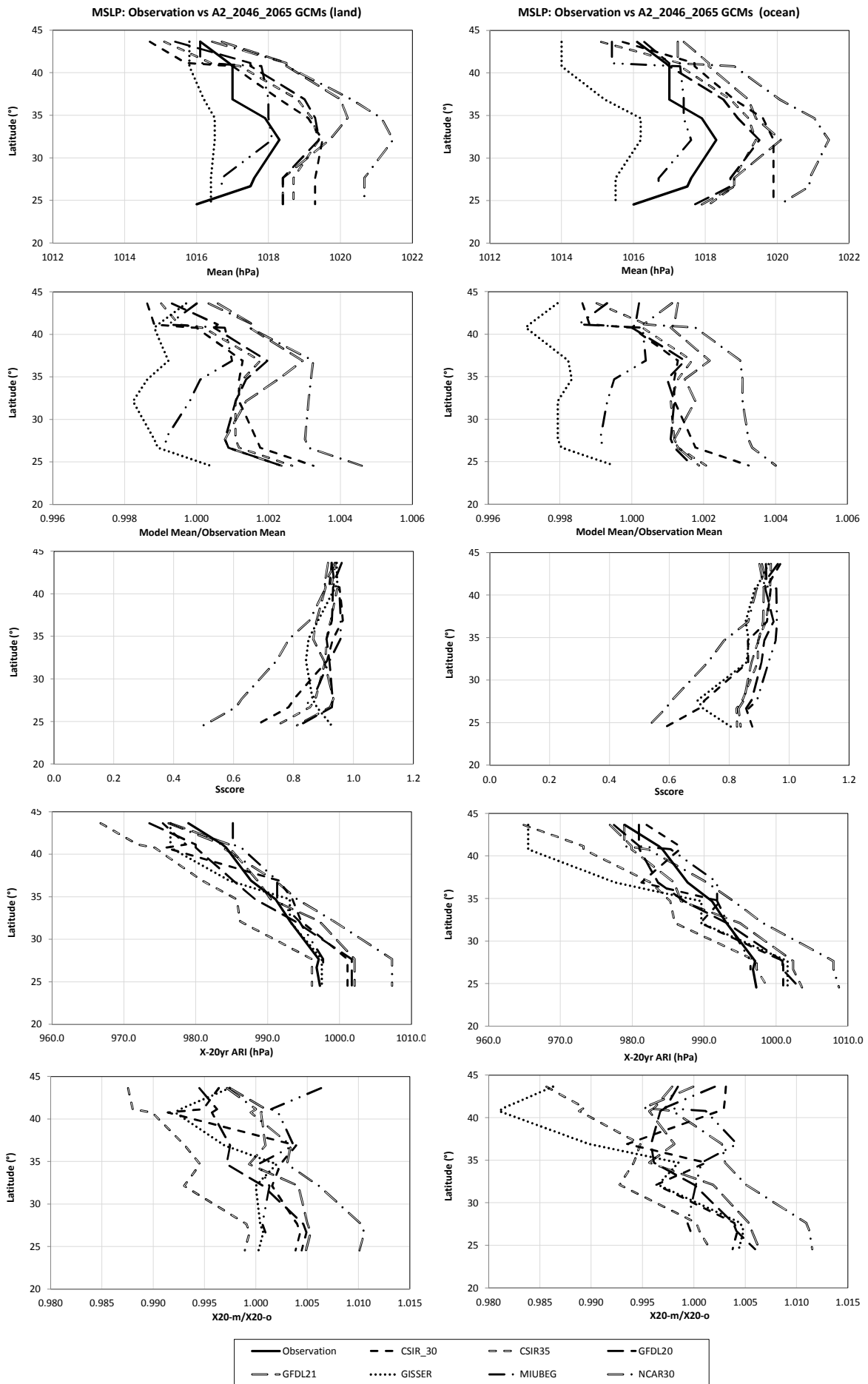
US East Coast Precipitation: Observation vs A2 2081-2100 GCMs



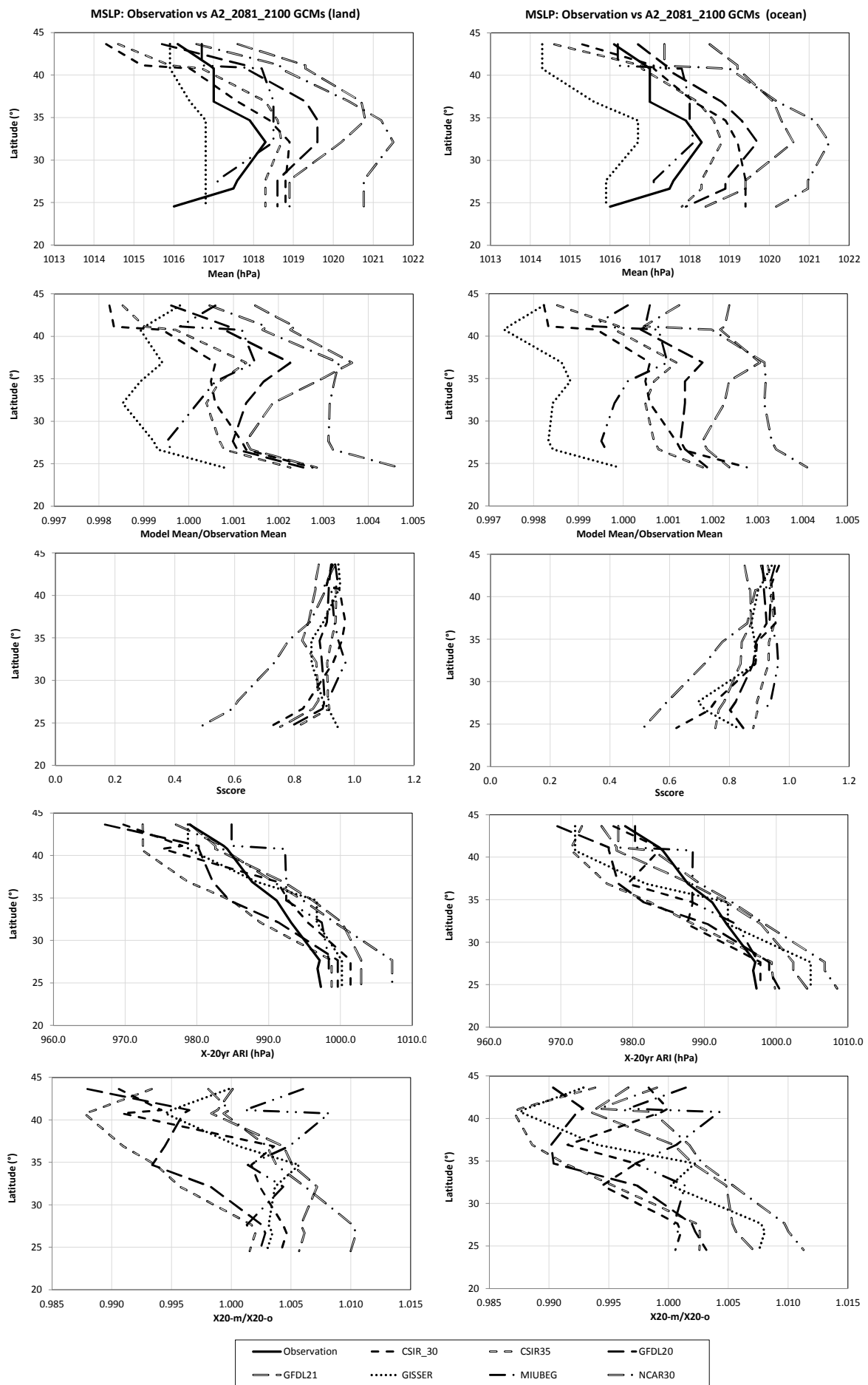
Aus East Coast Precipitation: Observation vs A2 2046-2065 GCMs



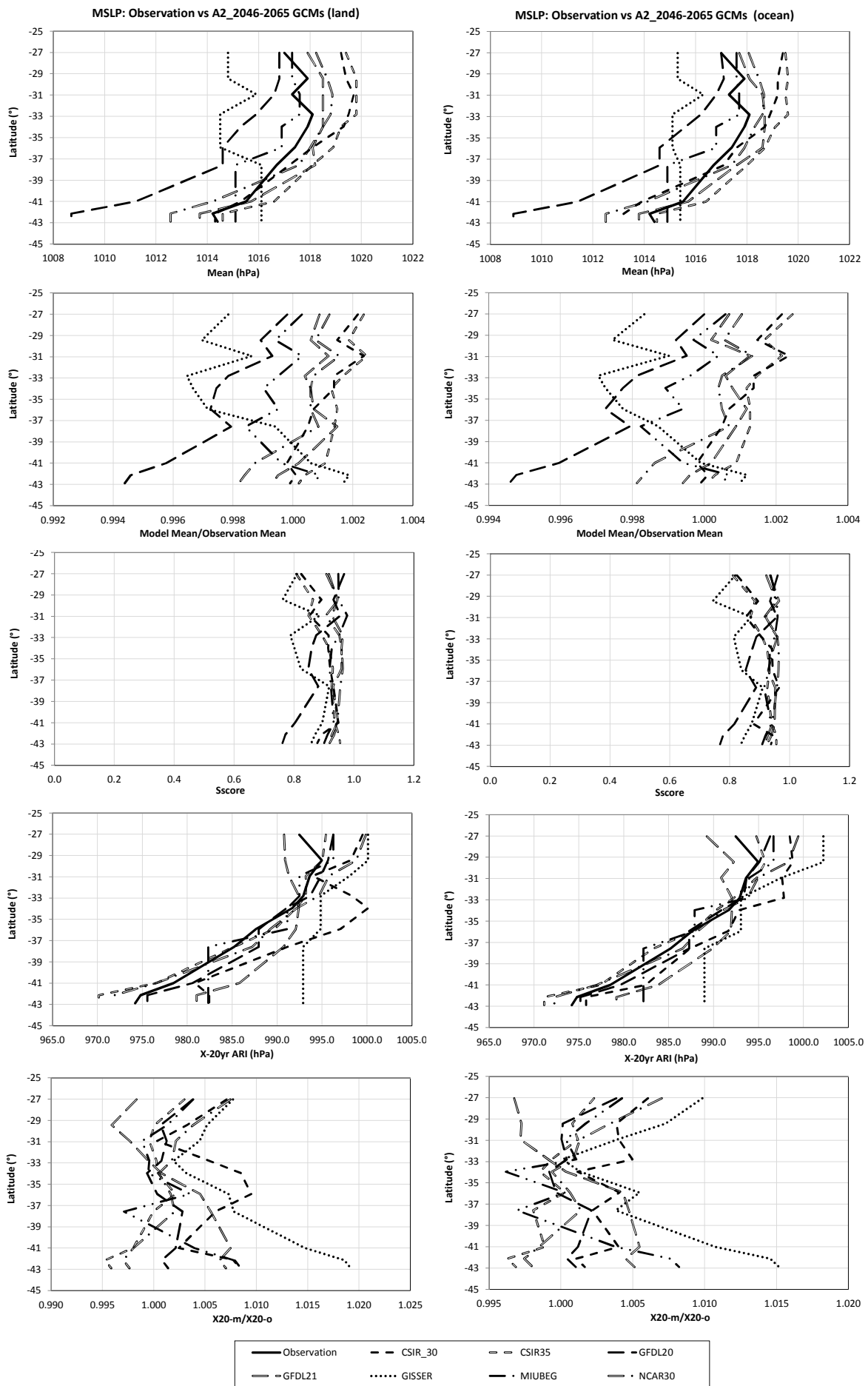
Aus East Coast Precipitation: Observation vs A2 2081-2100 GCMs



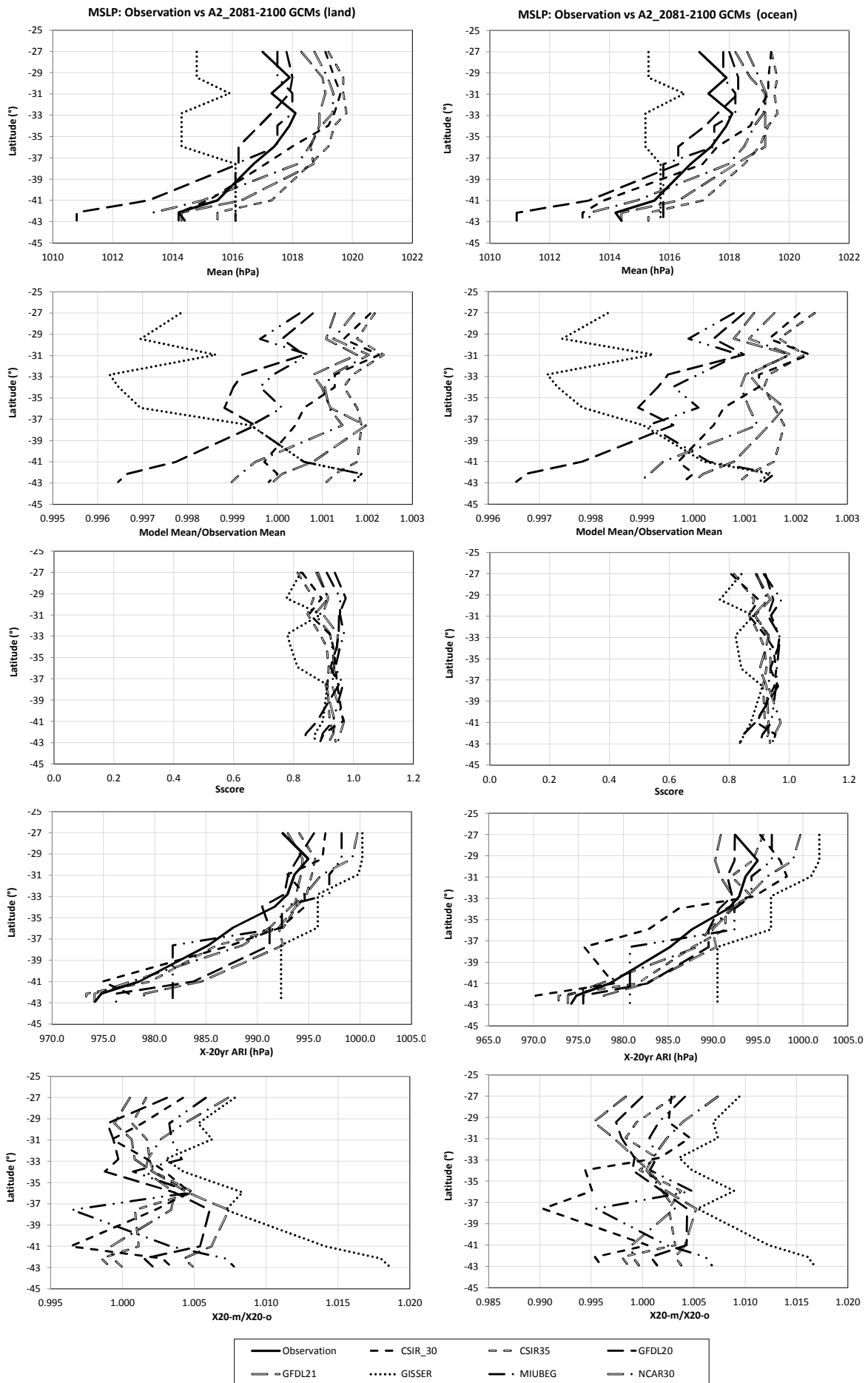
US East Coast MSLP: Observation vs A2 2046-2065 GCMs



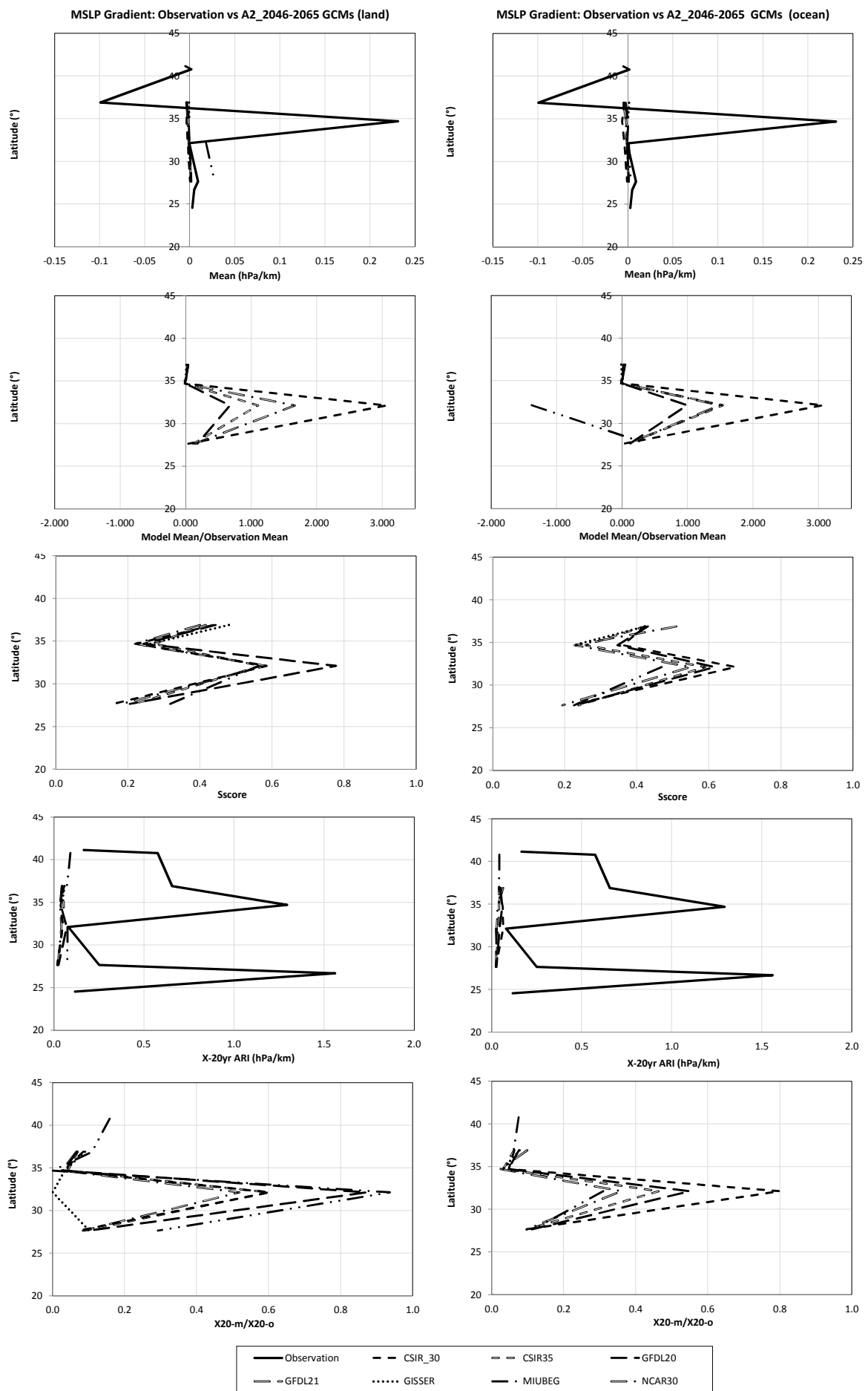
US East Coast MSLP: Observation vs A2 2081-2100 GCMs



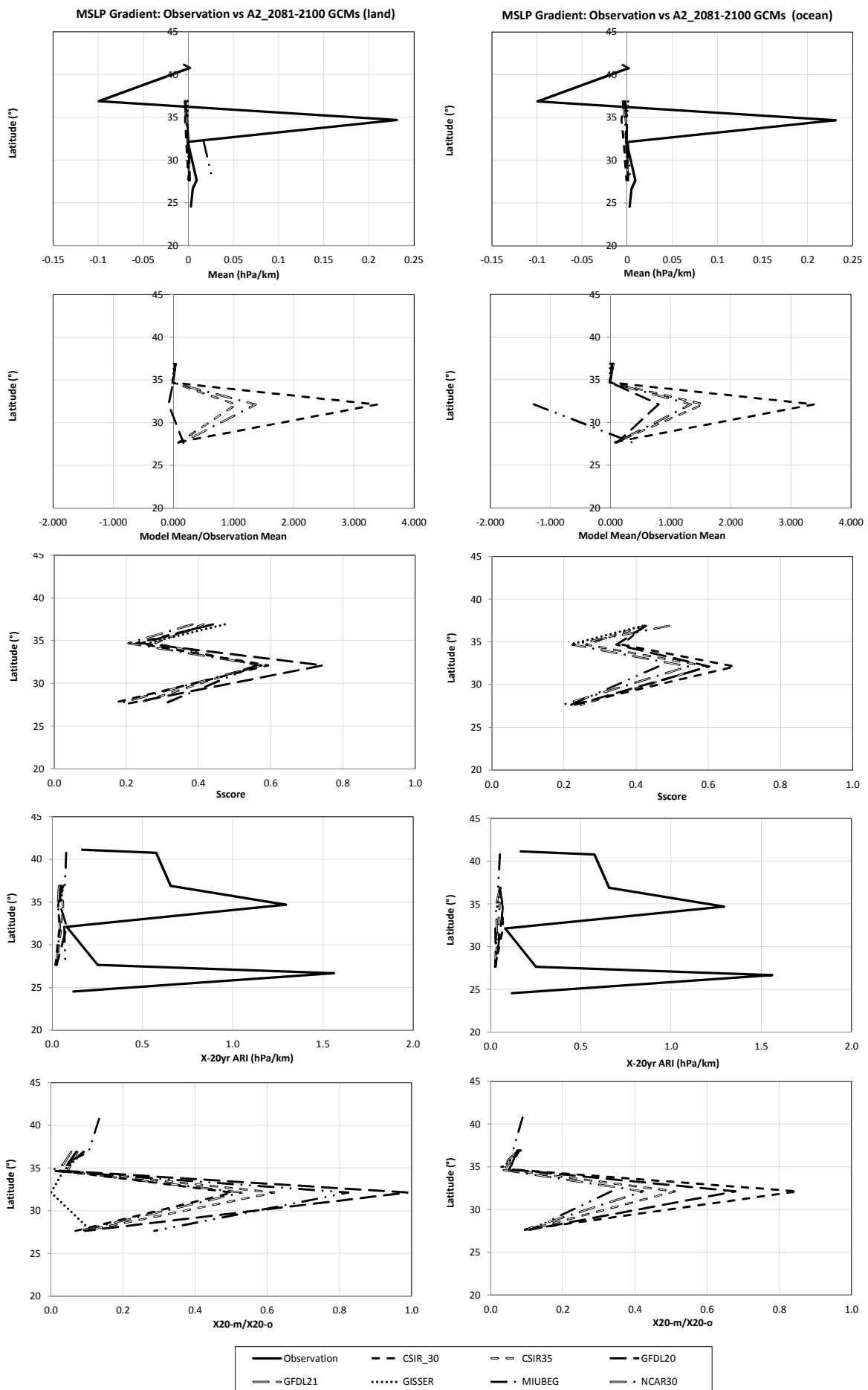
Aus East Coast MSLP: Observation vs A2 2046-2065 GCMs



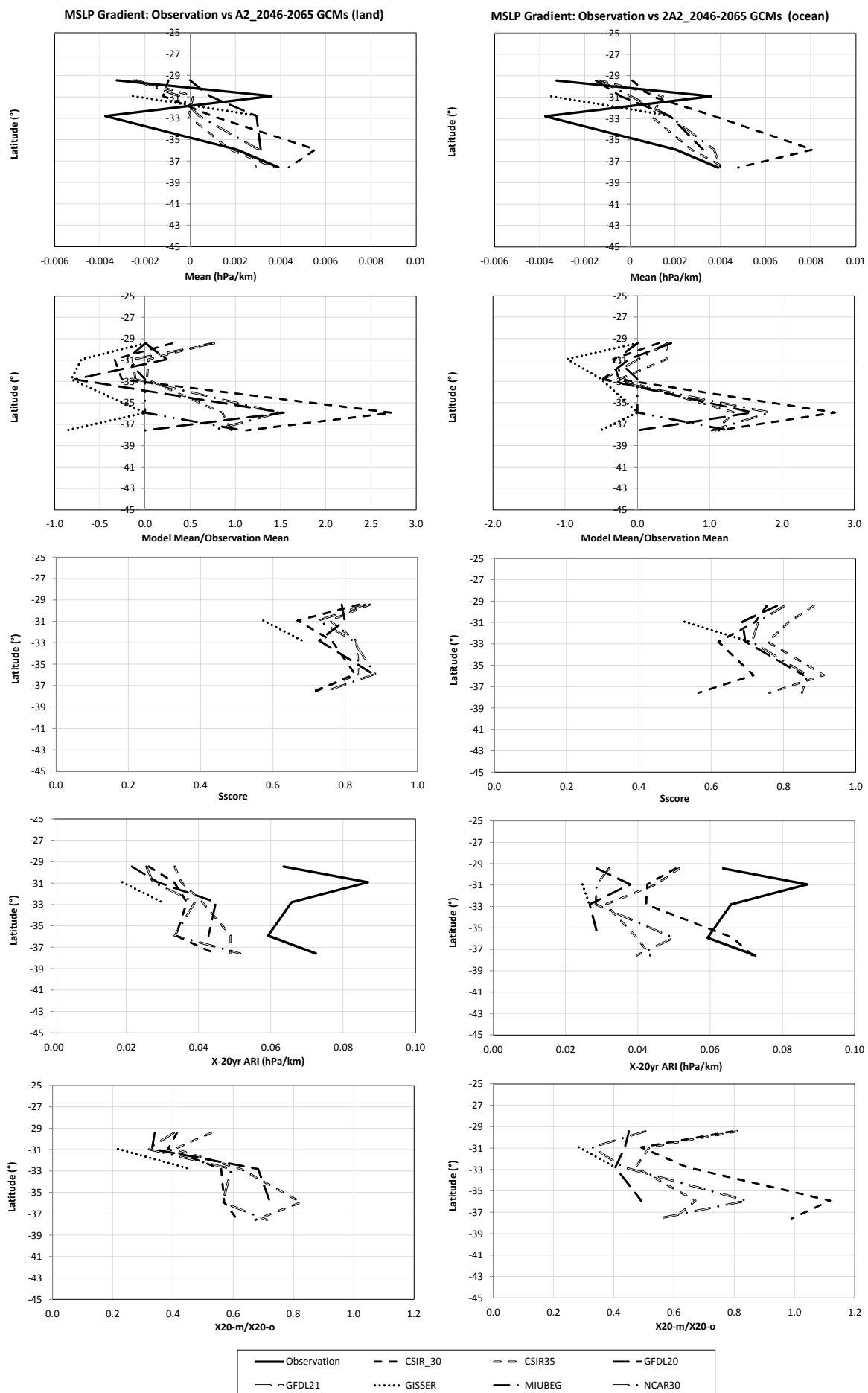
Aus East Coast MSLP: Observation vs A2 2081-2100 GCMs



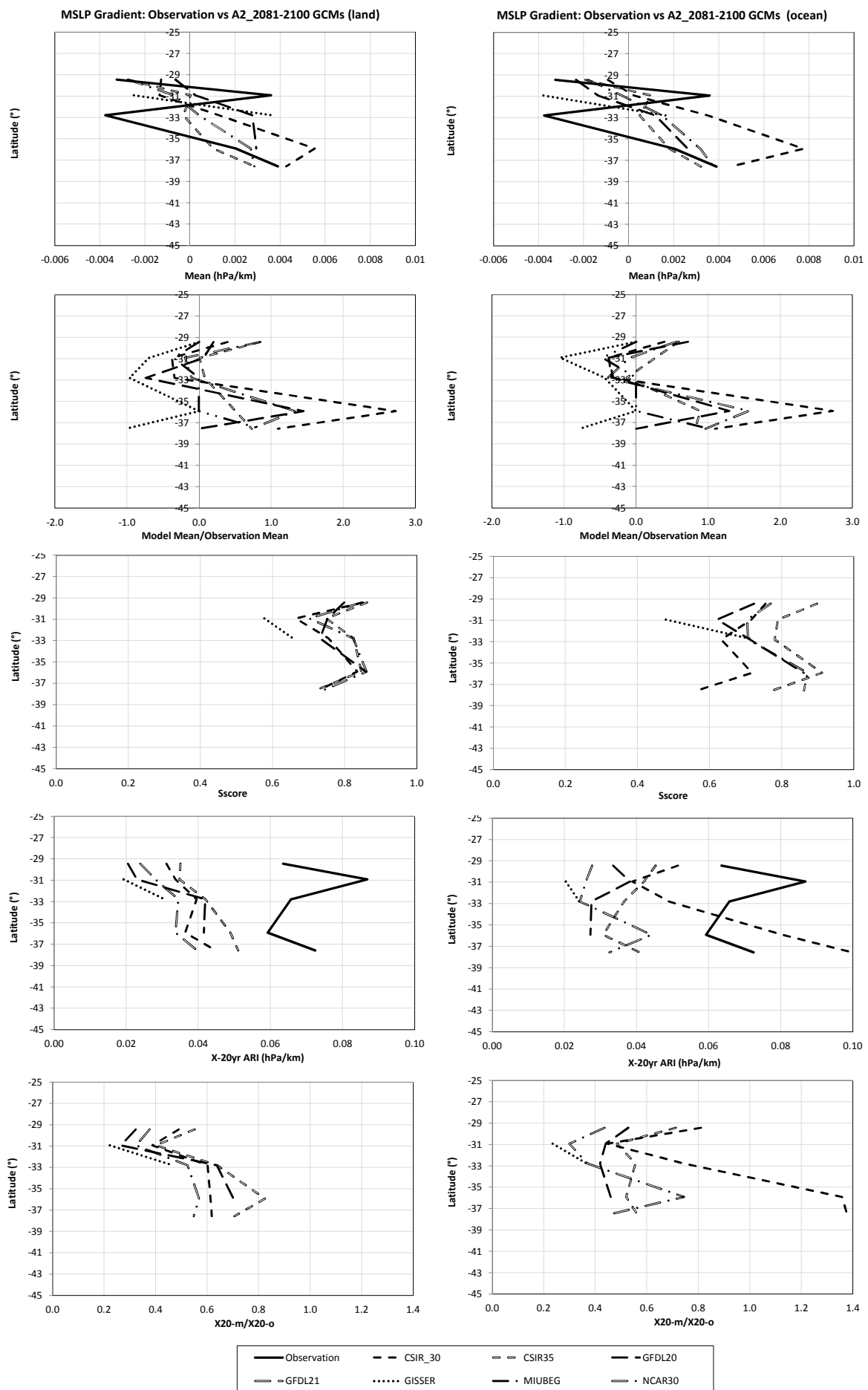
US East Coast MSLP Gradient: Observation vs A2 2046-2065 GCMs



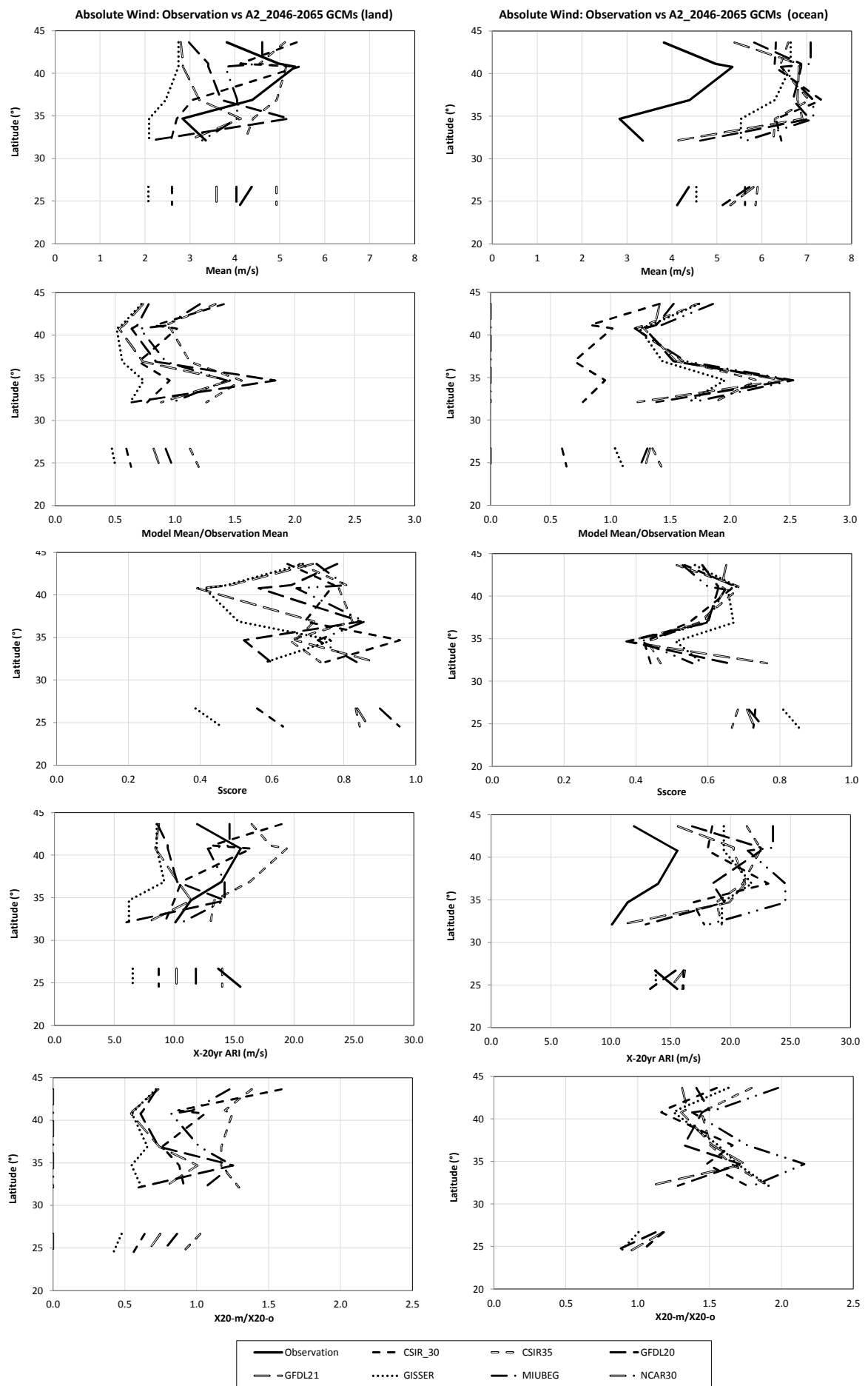
US East Coast MSLP Gradient: Observation vs A2 2081-2100 GCMs



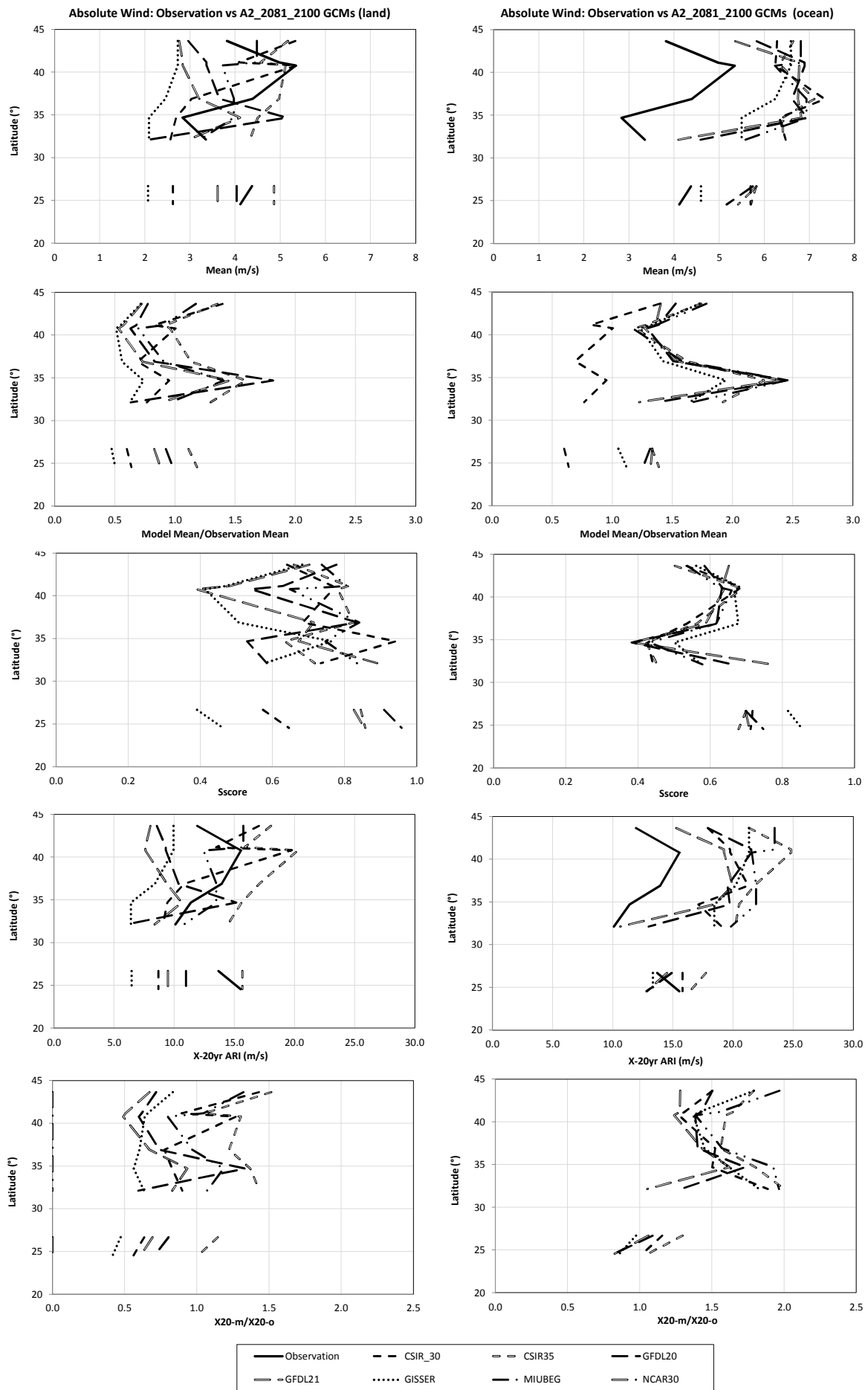
Aus East Coast MSLP Gradient: Observation vs A2 2046-2065 GCMs



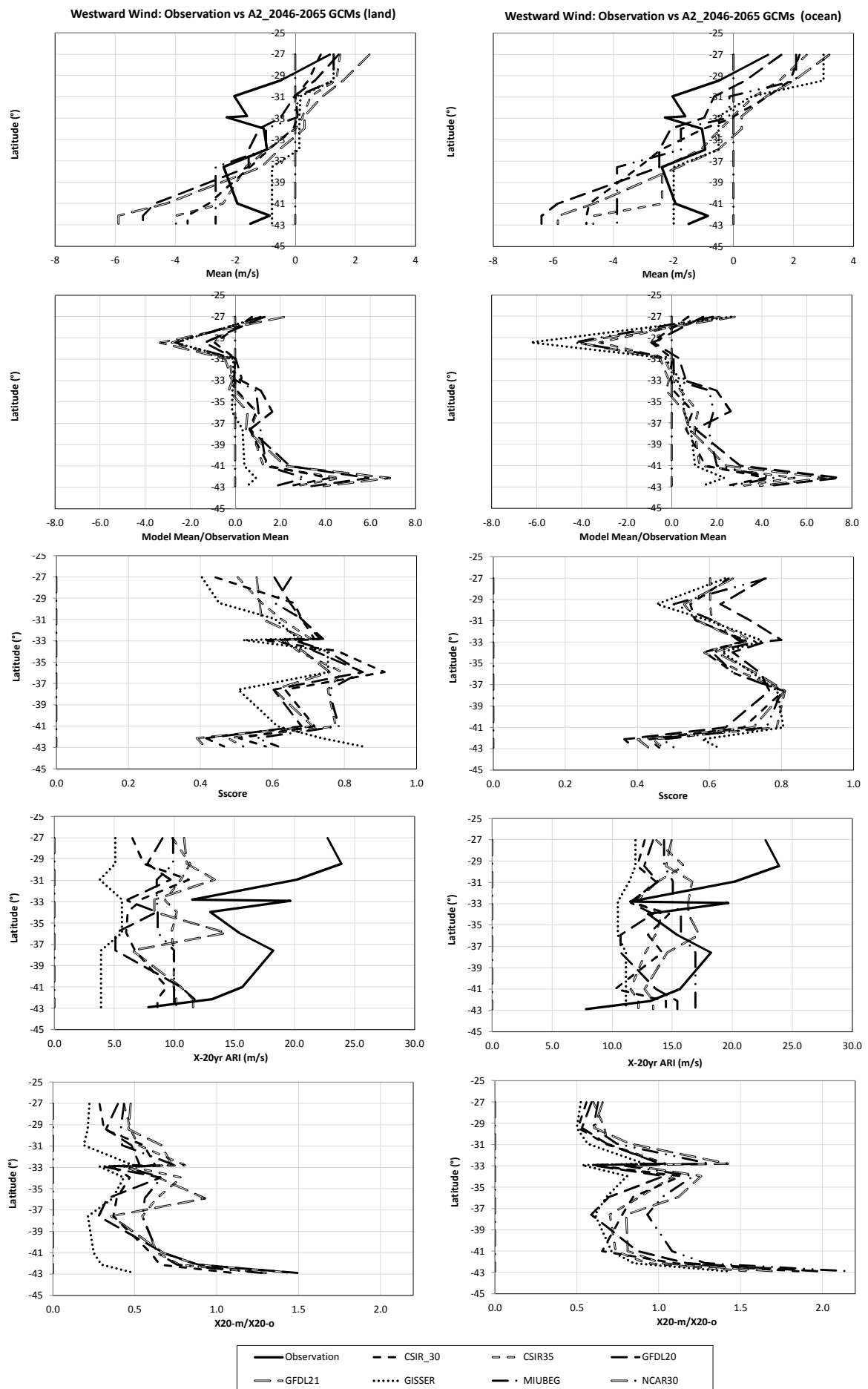
Aus East Coast MSLP Gradient: Observation vs A2 2081-2100 GCMs



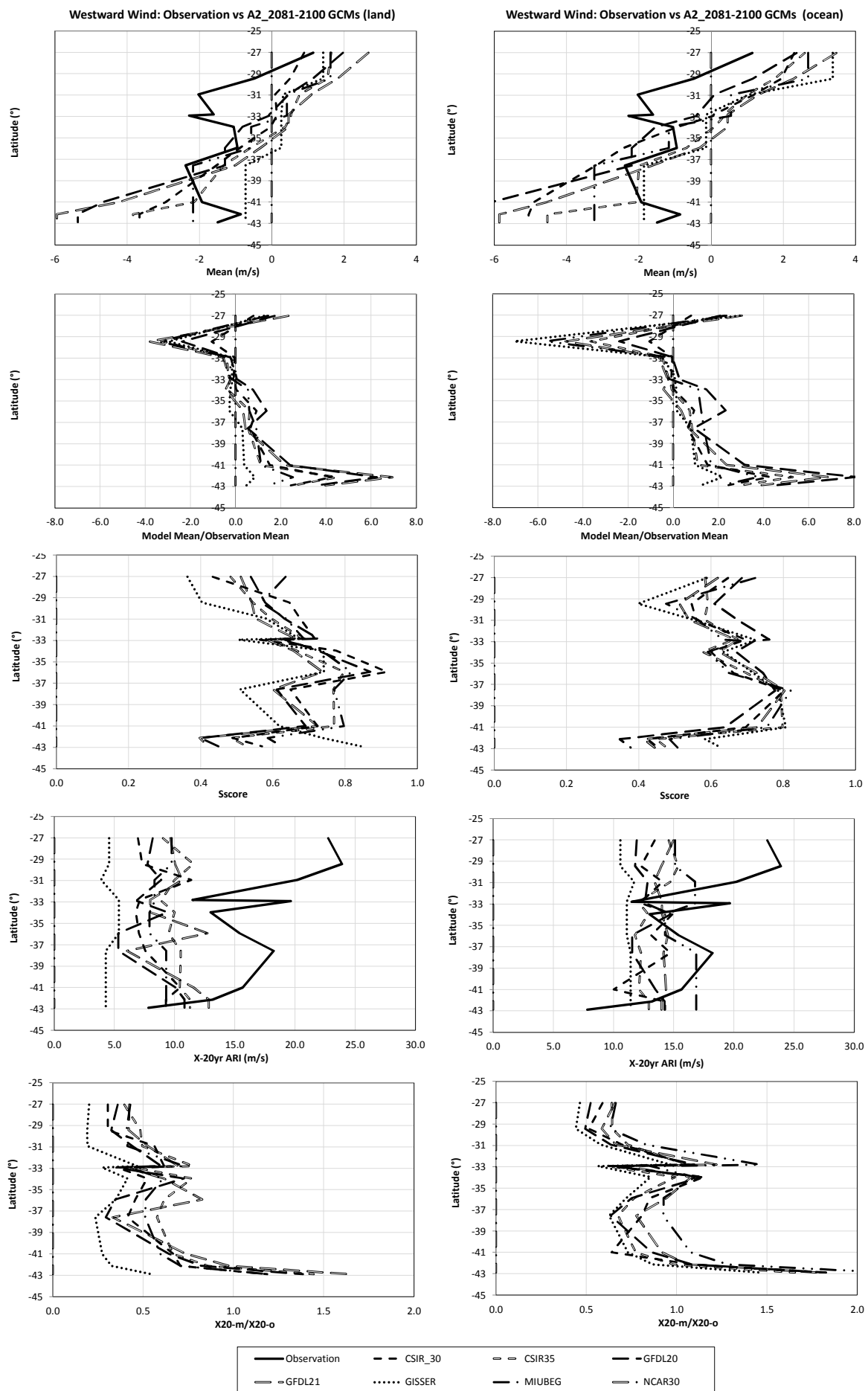
US East Coast Abs Wind: Observation vs A2 2046-2065 GCMs



US East Coast Abs Wind: Observation vs A2 2046-2065 GCMs



Aus East Coast Westward Wind: Observation vs A2 2046-2065 GCMs



Aus East Coast Westward Wind: Observation vs A2 2081-2100 GCMs